UNIVERSITY OF CALIFORNIA, MERCED

The Role of Inflammation and Antibiotics in the Development of Post-Traumatic Osteoarthritis in Mice

A dissertation submitted in partial satisfaction of the requirements for the degree Doctor of Philosophy

in

Quantitative and Systems Biology

by

Melanie Esperanza Andrea Mendez

Committee in charge:
Dr. Katrina K. Hoyer, Chair
Dr. Jennifer O. Manilay
Dr. Clarissa Nobile
Dr. Gabriela G. Loots

2019

Signature Page

The Dissertation of Melanie Esperanza Andrea Mendez is approved, and it is acceptable in quality and form for publication on microfilm and electronically:

Clarissa Nobile

Jennifer O. Manilay

Gabriela G. Loots

Katrina K. Hoyer

Date

University of California, Merced

2019

Dedication

To my mom and dad. I love you. Thank you.

Table of Contents

List of Abbreviations

AB – Antibiotic
AC – Articular cartilage
ACL – Anterior Cruciate Ligament
ADAMNTS – A Desintegrin and Metalloproteinase Thrombospondin-Like Motifs
BV/TV – Subchondral Bone Volume
CACTC – Cyclic Articular Cartilage Tibial Compression
CON – Contralateral
ECM – Extracellular Matrix
IATPF – Intra-Articular Tibial Plateau Fracture
IHC – Immunohistochemistry
IL-1 – Interkeukin-1
IL-1Rα - Interleukin-1 Receptor Alpha
IL-13 – Interkeukin-13
IL-4 – Interkeukin-4
IL-6 – Interkeukin-6
IL-6(-/-) – Interleukin-6 Knockout Gene Mice
IL-9 – Interkeukin-9
INJ – Injured
LCL – Lateral Collateral Ligament
LLNL – Lawrence Livermore National Laboratory
LPS – Lipopolysaccharides
M1 – Macrophages Type 1
M2 – Macrophages Type 2
MAMP – Microbial Associated Molecular Pattern
MCL – Medial Collateral Ligament
MMPs – Matrix Metalloproteinase
MRL/MpJ – Murphy Roths Large
NSAIDs – Non-steroidal anti-inflammatory drugs
OA – Osteoarthritis PTOA – Post-Traumatic Osteoarthritis
OB – Osteoblast
OC – Osteoclast
OCY – Ostecytes
Op.V – Osteophyte Volume
PCL – Posterior Cruciate Ligament
RA – Rheumatoid Arthritis
RANKL – Receptor Activator of Nuclear Factor Kappa-B Ligand
RNASeq – RNA Sequencing
Tb.N – Trabecular Number
Tb.Sp – Trabecular Spacing
Tb.Th – Trabecular Thickness
TC – Tibial Compression
TCL – Tibial Collateral Ligament
TLR – Toll-Like Receptor
TLR4 – Toll-Like Receptor 4

TNF-α – Tumor Necrosis Factor Alpha

TRAP – Tartrate-Resistant Acid Phosphatase

UCD – University of California, Davis

UCM – University of California, Merced

UNIN – Uninjured

USA – United States of America

μCT – Micro-Computed Tomography

List of Figures

List of Tables

Acknowledgements

This study received funding from LDRD 16-ERD-007. This work was conducted under the auspices of the USDOE by LLNL (DE-AC52-07NA27344). I would like to acknowledge the Eugene Cota Robles Fellowship for providing partial financial support.

I would like to acknowledge Dr. Gabriela G. Loots, the best mentor that I could have ever had. Her support, guidance, patience, and understanding are what made the four years I have spent in her lab both the hardest and most rewarding ever. She leads by example and has made me a better scientist and a better person just by allowing me to be in her lab. Words cannot express my gratitude for everything she has done for me. She is iconic and beyond reproach. I am thankful that I was fortunate enough to have her as my mentor.

I would like to acknowledge present and former members of the Loots lab. Deepa K. Murugesh for helping me with animal husbandry and technical assistance. Dr. Aimy Sebastian, Nicholas Hum, and Jillian McCool for technical support and personal support. Dr. Kelly A. Martin, Dr. Naiomy Rios-Arce, Dr. Sean Gilmore, and Cesar Morfin for their encouragement. Dr. Cristal Yee and Dr. Jiun Chang for mentorship during their time at the lab.

I would like to acknowledge the scientist at LLNL, UCM, and UCD for their help. I would like to especially thank my collaborator Dr. Blaine A. Christiansen for his incredible mentorship and motivation. I would like to thank Dr. Dina Weilhmer, Dr. Nicole Colette, and Dr. Dave Gravano for helping me with specialized techniques. I would like to thank Dr. Allison W. Hsia for technical assistance and Dr. Armaun Emami for giving me a place to stay while working at UCD.

I would like to acknowledge Dr. Sun H. Peck, Dr. Claire Roberts, and Dr. Megan Moore Weivoda for helping me navigate graduate school and explaining the steps that will follow. I would like to acknowledge Dr. Vanessa Granados for being the person who introduced me to science and Dr. Gary Villa because he was the person who told me I could be a scientist and sometimes you need someone else to tell you what you are capable of. As a first-generation PhD, I am beyond grateful for their help, support, and words of encouragement. I would have been lost and not even here without them.

I would like to acknowledge my family and friends. My parents for their love and support through this entire journey. My mom, Lilia E. Castellanos, for loving me more than anyone has ever loved anyone ever. She spent months every year for hours each day listening to my committee meeting presentations over and over. My mami helped me understand how to be a better science communicator by just listening to me speak and asking earnest questions. She has never doubted me and has always reminded me that if I work hard and listen, I can achieve anything. My dad, Edgar L. Mendez, for always being an inspiration of what hard work, honesty, and determination can do. Because of my papi I now understand that impossibly high expectations were what pushed me to be my absolute best. My little brother Juan Diego Mendez, for coming to see me and lifting my spirits when I really needed it. My tia madrina Berta Castellanos who cooked me food, sent me care packages, and gave me a place to sleep when I came to this country to pursue my dreams. My cousin Dr. Berta A. Castellanos who has been my laughing partner since I was 3 months and 22 days old. My cousins B. Victoria Castellanos and Jorge A. Castellanos for being the best cousins and doing the cross-country journey with me so I would not feel alone and scared. Estela Calel for her love and support my entire life. My dad’s wife Ana Carlota Leonardo for always being kind to me and sending me awesome snacks.

I would like to acknowledge the rest of my gigantic family most especially my tio Jorge A. “Tuco” Castellanos, tia Blanca Solares-Castellanos, tia Bety Solares, cousin Katerin Solares, auntie Egma Mendez, cousin Dolly Cabrera, cousin Naty Cabrera, my French parents Stephen Reuge and Cathrine Reuge, my American mom Melissa Gould, my best friend Savanna Lightfoot and the Lightfoot family, and Sasha and Chris Gruber for being there with support, love, and words of encouragement during these past years. My friends Lauren Casonhua, Dr. Stephen Wilson, Noelle Anderson, Cristie Donham Clement, Dr. Robert Poston, Dr. Kristen Valentine for listening to my talks, giving me notes, and hearing me break down. The Wilson family for having me each year so I would not spend Thanksgiving alone. Finally, my significant other Shae Herron, for being the calming force through the last push to get my doctorate. Thank you to all of you and so many more friends and family. I love you.

Curriculum Vitae

2019	Doctor of Philosophy in Quantitative and Systems Biology (QSB) University of California, Merced with Lawrence Livermore National Laboratory (LLNL) affiliation
2015	Master of Science in Tumor Biology Georgetown University Washington, DC
2014	Bachelor of Science in Biological Science Lynn University Boca Raton, FL

Relevant Project Experience/Involvement

2015-Present	The Role of Inflammation and the Gut Microbiome on the Development of Post-Traumatic Osteoarthritis (Thesis)
2018-Present	Mechanisms of Systemic Bone Loss Following Femur Fracture in Mice (PI: Blaine Christiansen, NIH 1R01AR071459, University of California, Davis)
2016-2019	Characterizing Host-Pathogen Immunity-Gut-Brain Interactions (PI: GG Loots, ER-LDRD-16-007, LLNL)
2016-2017	The Role of the Inflammatory Response in Bone and Cartilage Changes Following Non-Invasive Injury (PI: Blaine Christiansen, NIH/NIAMS AR062603, University of California, Davis)

2016-2017	Evaluating Efficacy of Novel Therapeutics for Mitigating Post-Traumatic Osteoarthritis (PI: GG Loots, DOD OR130220, LLNL)
2015	Mechanisms of Inhibiting Bone Formation Through Antagonism (PI: GG Loots, R01 DK075730, LLNL)

Honors and Awards

2019	Quantitative and Systems Biology Department Travel Award, University of California, Merced
2018	Annual Meeting Diversity Poster Competition Award, American Society for Bone and Mineral Research Annual Meeting
2017	Quantitative and Systems Biology Summer Fellowship, University of California, Merced
2015	Relocation Award, University of California, Merced
2015	Graduation Commencement Speaker, Georgetown University
2012-2014	Dean's List, Lynn University
2013	Order of Omega, Lynn University

Publications

Yee CS, Manilay JO, Chang JC, Hum NR, Murugesh DK, Bajwa J, **Mendez ME**, Economides AN, Horan DJ, Robling AG, Loots GG. (2018) Conditional Deletion of *Sost* in MSC-derivedlineages Identifies Specific Cell type Contributions to

Bone Mass and B Cell Development. *J Bone Miner Res*. May 11. Doi: 10.1002/jbmr.3467

Sebastian A, Chang JC, **Mendez ME**, Murugesh DK, Hatsell S, Economides AN, Christiansen BA, Loots GG. (2018). Comparative Transcriptomics Identifies Novel Genes and Pathways Involved in Post-Traumatic Osteoarthritis Development and Progression. *Int J Mol Sci*. Sep 7;19(9). Pii: E2657. Doi: 10.3390/ijms 19092657

Conference Poster and Talk Presentations

Mendez ME, Murugesh DK, McCool JL, Hsia AW, Christiansen BA, Loots GG. LPS Induced Inflammation Days Prior to Injury Increases the Severity of Post-Traumatic Osteoarthritis on C57Bl/6J Mice Models. American Society for Bone and Mineral Research Annual Meeting. Orlando, FL. September 2019.

***Mendez ME**, Murugesh DK, Hsia AW, Christiansen BA, Loots GG. Effects of Long-Term Antibiotic Treatment and LPS Induced Inflammation Pre-Injury on ACL Rupture Mouse Models of Post-Traumatic Osteoarthritis. Orthopeadic Research Society Annual Meeting. Austin, TX. February 2019. Poster and Talk.

Hsia AW, Cunningham HC, Emani AJ, **Mendez ME**, Loots GG, Christiansen BA. The Effect of Temporary Unloading on Post-Traumatic Osteoarthritis Development Following Knee Injury in Mice. Orthopeadic Research Society Annual Meeting. Austin, TX. February 2019.

Mendez ME, Murugesh DK, Kuhn EA, McCool JL, Hsia AW, Christiansen BA, Loots GG. Chronic Antibiotic Use Decreases the Severity of Post-Traumatic

Osteoarthritis in STR/ort Mice. American Society of Bone and Mineral Research Annual Meeting. Montreal, Canada. October 2018.

Mendez ME, Murugesh DK, Hsia AW, Christiansen BA, Loots GG. LPS Induced Inflammation Increases the Severity of Post-Traumatic Osteoarthritis on MRL/MpJ Mice. American Society of Bone and Mineral Research Annual Meeting, Montreal, Canada. October 2018.

Mendez ME, Murugesh DK, Hsia AW, Christiansen BA, Loots GG. Effects of LPS Induced Inflammation Pre-Injury on ACL Rupture Mouse Models of Post-Traumatic Osteoarthritis. Orthopedic Research Society Annual Meeting. New Orleans, LA. March 2018.

Teaching/Mentorship Experience

2019	Teaching Assistant: BIO 003: To Know Ourselves: Molecular Basis of Health and Disease, UC Merced. Instructor of Record: Professor Evin Doscher
2019	Teaching Assistant: BIO 003: To Know Ourselves: Molecular Basis of Health and Disease, UC Merced. Instructor of Record: Dr. Liza Gomez-Daglio
2019	Teaching Assistant: BIO 003: To Know Ourselves: Molecular Basis of Health and Disease, UC Merced. Instructor of Record: Dr. Nicholas Arthur
2018	NSF I-CORP BIO-Entrepreneurship Workshop Faculty, BIO 2018, Boston, MA. Supervisor: Dr. Marc Sedam.

2016	Teaching Assistant: BIO 003: To Know Ourselves: Molecular Basis of Health and Disease, UC Merced. Instructor of Record: Dr. Chistiane Touma
2015	Teaching Assistant: BIO 120L: General Microbiology Laboratory, UC Merced. Instructor of Record: Dr. Marcos Garcia-Ojeda.
2013-2014	Biology and Algebra High School Teacher, Elev8 Sports Institute, Boca Raton, FL.

Professional Affiliations

2017-Present	American Society of Bone and Mineral Research (ASBMR)
2017-Present	Orthopedics Research Society (ORS)
2017-Present	NSF I-CORP

Abstract

The Role of Inflammation and Antibiotics in the Development of Post-Traumatic Osteoarthritis in Mice

by

Melanie Esperanza Andrea Mendez

Doctor of Philosophy

University of California, Merced, 2019

Dr. Gabriela G. Loots, Advisor
Dr. Katrina K. Hoyer, Chair
Dr. Jennifer O. Manilay
Dr. Clarissa Nobile

Osteoarthritis (OA) is a painful and debilitating disease. There is no treatment for OA other than an expensive full joint replacement surgery that requires an extensive recovery period. Approximately 50% of people who suffer a severe articular injury will develop a form of OA as early as 8 years after injury, which is a secondary form of OA called post-traumatic osteoarthritis (PTOA). PTOA develops from a severe joint injury, like an anterior cruciate ligament (ACL) tear. I want to identify external factors that could be contributing to either a resolution or a progression to the disease. It has been suggested that the progression towards PTOA is led by a continuous activation of inflammatory pathways, which led to questions about which factors affecting the body prior to injury could be changing the PTOA phenotype. The normal gut microbiome aids in immunoregulation by continuously activating an inflammatory cascade helping naïve immune cells mature. However, if there is a bacterial infection, there will be an increase in the levels of inflammation and an increase in mature immune cells to fight the infection. I want to account for patients who are suffering from systemic inflammation after acute bacterial related inflammation. In addition, knowing that in 2015 the CDC reported 269 million antibiotic prescriptions, I want to account for people treated for bacterial infections. Specifically, long term antibiotic treatment will affect PTOA outcome. I will induce inflammation and disrupt the gut microbiome prior to injury separately and later together to study the PTOA phenotype. I will use a non-invasive injury model which will temporarily displace the tibia and produce an ACL rupture. Last, in order to account for different PTOA susceptibilities, I will use three mice models of both sexes that vary from resistant to PTOA to highly susceptible. The contribution of this research will give a better understanding of the role of inflammation and the gut microbiome in the initial inflammation stage and the PTOA outcome after articular injury.

Osteoarthritis (OA) is a disease characterized by the progressive degradation of articular cartilage. The treatment for OA is limited to stabilization of the joint, pain management, and ultimately full joint replacement surgery. The primary form of OA is caused by normal wear and tear or genetics. Post-

traumatic osteoarthritis (PTOA) is the secondary form of OA develops in ~50% of people severe articular injury like a tibial plateau fracture, a meniscal tear, or an anterior cruciate ligament (ACL) rupture. PTOA can take as little as 8 years and up to 20 years to develop.

It has been suggested that elevated levels of inflammation after injury could increase the risk of developing PTOA and the severity. We wanted to use bacterial related inflammation, given how common *E. coli* and other bacterial infections are today. We aim to look at how residual effects from a sudden increase in inflammation could affect injury outcome. Lipopolysaccharides (LPS) are microbial associated molecular patterns (MAMPS) released by gram-negative bacteria to activate toll-like receptors (TLR), specifically TLR4. LPS is released normally by the gut microbiome, and acts as a transcription factor for immune cell maturation. During a gram-negative bacteria infection there is an increase in LPS. LPS spikes in the short-term cause a fever and pain. Long term increases in circulating LPS cause persistent elevated levels of inflammatory chemokines and cytokines, as well as lower bone volume and a larger spleen. This project examines how a spike in MAMPs induced inflammation days prior to injury will increase the severity of PTOA. This will allow us to provide new insight that could help personalize medicine and create therapeutic treatments specifically for people more vulnerable.

In contrast, we wanted to examine how removing part of the MAMP activation by using chronic antibiotic treatment could change the injury progression. There are over 270 million prescriptions of antibiotics each year in the United States, and it is important to know how this would affect it PTOA outcome. There is conflicting data as to how the gut microbiome affects bone, seeming to be dependent on age, housing type, and treatment. We will be using ampicillin and neomycin, which target mainly gram-negative bacteria for six weeks prior to injury. Antibiotic treatment will end the day of injury and we will examine the joints six weeks later. We found that the bone phenotype is worsen by antibiotic treatment while the cartilage staining is stronger on antibiotic treated

joints. Last, we did a combination of antibiotic treatment an LPS induced inflammation. We found that it restores the phenotype closet to VEH.

Chapter 1: Introduction

Bone, Cartilage, and Joint Background

The human skeleton provides support, creates movement, allows for protection of vital organs, aids in the production of blood cells, and provides storage of minerals and fats[1–6]. Long bones like the femur and tibia are composed of a main shaft called diaphysis that contains compact bone and the medullary cavity which is filled with yellow marrow and stores fat. At each long bone end there is the epiphyses, that contains trabecular bone and red marrow, where blood cells are made, and where the joints articulate[7,8].

Synovial joints (**Fig 1**) are the juncture of two long bones that are connected by ligaments to muscles to facilitate articulated movements, like in the case of the knee[9]. The synovial joint is composed of the meniscus, articular cartilage, subchondral bone, and the synovial membrane[10,11] (**Fig 1**). The meniscus makes up most of the synovial joint, since it allows for movement. The meniscus is composed of fibrocartilage, a thicker cartilage[12,13]. The cells of the fibrocartilage like all cartilage, are chondrocytes[14–19]. Fibrocartilage allows the meniscus to withstand high levels of pressure and tension that come from load bearing and shock[20,21]. Fibrocartilage is mainly composed of water, type I collagen, and proteoglycans. It has type II, III, V, and VI collagen[22].

Articular cartilage (AC) (**Fig 1**) surrounds the ends of bones within synovial joints. AC is composed of hyaline cartilage that covers the epiphyses and allows for synovial joint movement[23]. AC is a gel-like matrix that has elastic and collagenous fibers[24]. The cells of the AC are called chondrocytes. The AC matrix is made of mainly water, followed by type II collagen and proteoglycans. It is divided into three zones: superficial, middle, and deep layer[25,26]. There is a layer of thin calcified cartilage between the deep layer and bone that serves as a transitional barrier. AC has no innervation or blood supply; it relies on

neighboring tissues and synovial fluid for nutrients and waste release[27]. That is the reason AC is slow to heal and if damaged may never properly heal.

The bone (**Fig 1**) is made of mineralized tissue mainly composed of type I collagen. Mineralized bone is composed of three kinds of cells: osteoclasts (OC), osteoblasts (OB), and osteocytes (OCY). OCs are bone resorbing cells that break down the bone matrix during bone remodeling[28]. OBs are bone forming cells that secrete organic matrix of bone and promote calcification. Once OBs are surrounded by a calcified matrix, they differentiate into OCYs, the most abundant cell type within mineralized bone which functions to transduce mechanical forces into molecular signals to help maintain the structure of the bone[29–31]. The bone is vascular and innervated which allows for it to heal when injured. Fractured bones heal very efficiently in young and healthy individuals, but the process slows as a function of age and is less effective in people suffering from bone thinning conditions such as osteoporosis and osteopenia[32,33]. Severe orthopedic trauma can also damage surrounding soft tissues and may impact the cartilage in compound fracture or intraarticular fracture events[34].

The knee is the largest joint in the body and is essential for allowing horizontal movement like walking and running and vertical movement such as jumping or climbing[20]. The knee is a hinge synovial joint made of the articulations between the femur and the tibia, where the patella acts as the hinge[35] (**Fig 1**). The inside of the knee contains synovial fluid which maintains lubrication[36,37]. As previously mentioned, articular cartilage cushions the end of the bones and reduces friction, allowing for easy and smooth movement[38]. The menisci are connective tissue that serve to protect the joint integrity from higher impact activities such as running or jumping. Blood supply to the knee is provided by the femoral and popliteal arteries. Ligaments are present outside and inside of the joint to control movement in order to maintain articular stability. The knee is stabilized by four main ligaments: the anterior cruciate ligament (ACL), the posterior cruciate ligament (PCL), the medial (tibial) collateral ligament (MCL),

and the lateral (fibular) collateral ligament (LCL)[39]. Tendons are present outside of the knee in order to allow for flexion or extension of the joint.

The cruciate ligaments are strong rounded bands of connective tissue and collagenous fibers that extend from the intercondyloid notch of the femur towards the head of the tibia. They are named by the position on the tibia and together they form an “x”. These ligaments prevent excessive forward or backward movement of the tibia in relationship to the femur during flexion and extension. The ACL extends from the lateral femoral condyle to the intercondyloid eminence of the tibia[40]. The ACL is the most commonly injured ligament in the knee. In the USA alone over 100,000 ACL ruptures happen every year[41]. The PCL starts in the anterolateral part of the medial femoral condyle in the intercondylar notch and moves to the extraarticular part of the posterior tibial plateau[42]. The PCL can be up to twice as thick and have twice the strength of the ACL. It is not as commonly injured as the ACL, but when injured, the most common causes are motor vehicle injures by hitting the dashboard or falling forward onto a flex knee.

The collateral ligaments are located on the outside of the knee[43]. The collateral ligaments are flat bands of connective tissue that go from the femur towards the fibula or the tibia depending on which ligament it is. The role of the collateral ligaments is to provide valgus stability to the knee joint. The MCL starts at the medial epicondyle of the femur and extends to the medial condyle of the tibia. The MCL is less commonly injured than the ACL and PCL. The MCL is most commonly injured during sports, mainly skiing which makes up over half of the MCL injures[44]. MCL is usually injured in conjunction with other knee structures like the ACL and the medial meniscus. The LCL moves down and back from the lateral epicondyle of the femur to the head of the fibula. The LCL is less susceptible to injury due to its position and flexibility compared to the other ligaments[45].

The synovium (**Fig 1**) produces synovial fluid which is composed primarily of lubricin and hyaluronic acid that lubricates and nourishes the joint[46]. The cells producing the synovial fluid components are fibroblast. Additionally, there are

macrophages present in the synovial fluid that are usually dormant but active during stages of inflammation[47]. Inflammation of the synovium is called synovitis, during synovitis there is an increase in the levels of catabolic enzymes like disintegrin, metalloproteinase thrombospondin-like motifs (ADAMTS), collagenases, matrix metalloproteinases (MMPs) and of inflammatory cytokines like interleukins 1 (IL-1), 4 (IL-4), 6 (IL-6), 9 (IL-9), 13 (IL-13), and tumor necrosis factor alpha (TNF-α)[48–53]. A prolonged increase in any of these inflammatory markers is likely to increase the degradation of collagens, which can cause articular cartilage and meniscus degeneration[54].

Osteoarthritis Disease

Osteoarthritis (OA) is a painful and debilitating disease that involves the whole articular joint[55]. The disease happens when the joint undergoes anatomical changes characterized by chronic and progressive degeneration of articular cartilage and bone erosion[56]. These changes reduce the joint space and cause osteophyte formation. The most common locations for OA development are the hip and the knee joints. OA is the most common mobility limiting disease, affecting over 30 million people in the United States of America (USA). Over 40% of individuals suffering from OA are over the age of 65[57]. Given that the aging population is increasing in the USA, it is expected that the incidence of OA will steadily increase[57,58,58]. OA treatments are limited, and mainly treat the symptoms of OA, not the underlying disease. OA treatment includes pain management, but full joint replacement represents the only option when excessive pain persists. Joint replacement surgery is expensive and has a long recovery period[59]. The financial burden associated with OA in the USA is over $150 million, annually. Full recovery after surgery, ranges from six months to a year, but may be even longer in the elderly. This can have an impact on the financial stability and quality of life of those recovering from OA-related surgeries[60].

Treatment during early stage OA includes pain-management in the form of pharmaceuticals, physical therapy, weight management, moderate exercise, or a combination[61,62]. Due to pain, stiffness, and swelling, OA patients with limited mobility may require pharmacological treatments, especially in the later stages of OA[63]. The most common pharmacological treatment are non-steroidal anti-inflammatory drugs (NSAIDs)[64]. NSAIDs are taken during the early symptoms of OA and along with exercise and weight management can help prolong the time between diagnosis and surgery[65]. The caveats of NSAIDs are gastrointestinal complications and accidental overdoses.

Pharmacological treatments other than NSAIDs include intra-articular supplements of hyaluronates, chondroitin, and glucosamine sulfate[66]. Hyaluronates help the joint by providing proper lubrication and maintaining viscoelasticity in the joint. Chondroitin and glucosamine decrease joint space narrowing, which treats the illness and not just the symptoms[67].

OA is divided into two main types: primary and secondary[68]. The primary form of OA is mainly due to normal wear and tear but can also be caused by genetic predisposition. Physically active individuals like athletes and members of the military are at higher risk of developing primary OA due to the increased levels of physical activity[69]. Additionally, individuals who have multiple sites of osteoarthritis are more susceptible to systemic and genetic OA. The secondary form of OA is post-traumatic OA (PTOA), which develops in approximately half of patients who have suffered a severe articular injury, like an anterior cruciate ligament (ACL) rupture, tibial plateau fracture, or meniscal tear[55]. PTOA develops as early as eight years and as late as over twenty years post injury.

OA is a prevalent disease that will become more common as our population ages[57]. It is important to note that in the USA there is a large number of younger individuals without access to healthcare and therefore could potentially be suffering from OA. The older population has access to federally funded healthcare that the younger population does not benefit from, and

therefore more individuals may be suffering from undiagnosed OA than current statistics reflect.

Post-Traumatic Osteoarthritis Disease

PTOA accounts for about 12% of all OA cases and affects ~50% of people who have suffered a severe articular injury, as previously described[70]. PTOA symptomatic phase is seen mainly in people below the age of 45. This suggest that the majority of the injuries happened during the early 20s to late teen years. That means that the cases of PTOA will continue to increase as the aging population of injured military veterans, extreme sport athletes, vehicle injury victims, etcetera have increased during the 21st century. It is not currently known why half of the patients go into spontaneous resolution, but factors like repeated injury, chronic inflammation, and genetic pre-disposition can contribute to the development of PTOA[71].

PTOA development (**Fig 2**) is initiated by a traumatic joint injury event. Right after the injury, it proceeds to the immediate phase, acute phase, asymptomatic phase, and lastly, the chronic phase[72]. The immediate phase happens seconds after injury and includes cell necrosis, collagen rupture, swelling of the cartilage, hemarthrosis, and loss of glycosaminoglycan. Hours after the injury, during the acute phase there will be apoptosis, leukocyte infiltration, matrix degradation, deficient lubrication, and secretion of inflammatory mediators like IL-1, IL-4, IL-6, IL-9, IL-13, IL-1β, and TNF-α[73,74]. About half of severe articular trauma patients will have a spontaneous resolution, and half will go on to an asymptomatic phase that can last as long as 20 years before it moves to the symptomatic, chronic phase.

PTOA and primary OA exhibit the same clinical manifestations during the chronic phase, the only difference is how they arrived to this point. Both PTOA and primary OA display degradation of cartilage and narrowing of the joint space that causes the joint to become stiff, swollen, and painful. The joint will have

limited mobility and may also develop ectopic calcifications called osteophytes. Joints with increased lateral subluxation may have elevated levels of osteophytes.

PTOA and OA severity are measured by the level of cartilage erosion, bone resorption, and osteophyte volume. Quantifiable clinical parameters in the joint that correlate with OA symptoms include mineralization of soft tissues like the meniscus, thickening of the synovium, and cellular infiltration. Additionally, the macrophages that are usually inactive and circulating in the joint will become activated and their numbers will increase[75].

Mouse Models of Osteoarthritis

OA can be studied in many animal models including but not limited to rat, rabbit, horse, dog, sheep and mouse[76]. Mouse models of osteoarthritis are common due to cost, the length of the experiment, and the similarity between disease development in mice and humans. In mouse models the knee is the most commonly used site of study[77]. Skeletal growth and disease progression of mice is faster than most other models, which makes it a convenient model to study PTOA. This study focused on mouse models of osteoarthritis only.

Available mouse models include inbred mouse strains or genetically modified mice that spontaneously develop OA and can be used to study primary forms of OA. An example of a spontaneous OA mouse model is STR/ort inbred strain which has elevated circulating pro-inflammatory cytokines and chemokines levels, and develops synovitis[78]. STR/ort adult mice show a progressive degradation of articular cartilage in all joints including the knee, elbow, and temporomandibular joint. C57Bl/6J mice show a reduction in cartilage as a function of age, which is consistent with loss of cartilage thickness in older humans however they are not considered a spontaneously developing OA model, but are used as a representation of ‘normal’ joint morphology. Spontaneous models of OA are helpful due to the similarity they have to what

happens in humans, exhibiting elevated levels of inflammatory cytokines and moderate loss of cartilage that can affect the joints[71]. This makes them a helpful model to understand non-injury driven OA.

An example of a genetically modified model would be the interleukin-6 knockout mice (IL-$6^{-/-}$)[79]. This mouse model has a decrease in proteoglycan synthesis and a reduction in mineral bone density when compared to C57Bl/6J mice, exhibiting more severe OA than IL-$6^{+/+}$ littermate controls. Genetically modified models provide tools to study the specific gene role during disease, however it is not naturally occurring in most humans, unless the mutation corresponds to a mapped quantitative trait locus (QTL) in patients with increased susceptibility to OA[80].

Secondary OA models include invasive and non-invasive models. Invasive models can be induced chemically or surgically. Chemically induced OA models include delivery of monoiodoacetate and collagenase directly into the joint. Monoiodoacetate causes joint inflammation and chondrotoxicity[81]. In these animals, OA is observed approximately six weeks after the injection. Collagenase injections produce joint inflammation and collagen breakdown and cause OA phenotypes approximately 3 weeks after injury. These models are helpful to study degradation of particular tissues but not the progression of OA since it is very different than naturally occurring OA in humans.

Surgical models include meniscectomy, destabilization of the medial meniscus, medial meniscal tear, and ACL transection[76]. All these models allow for rapid disease progression and study of the development of PTOA. Surgical models have been widely used to study OA disease progression. They require surgery training and due to their invasive nature, are open to the risk of infection. Surgical models are not the best approach to studying the effects of inflammation given that the surgery itself will cause additional inflammation that has to be carefully controlled through the use of sham surgery groups.

Until recently, the study of PTOA has exclusively utilized surgical models, establishing them as the gold standard in the field. In 2012, our collaborator, Dr.

Blaine Christiansen at UC Davis reported the first account of a single-mechanical load applied to the knee joint as an effective and highly reproducible means of creating a non-invasive injury model of OA[77]. Since, other, non-invasive injury models of PTOA have emerged that are generated by load-applying instruments to perform highly reproducible injuries. Our group published one of the first comprehensive transcriptomic profile of non-invasive PTOA model, and highlighted molecular differences and similarities to the surgical models[82]. Non-invasive injury models require a small level of training, if properly done perfectly replicate the injury, and are significantly faster to perform than PTOA inducing surgery. A drawback of the non-invasive models is the initial equipment cost. The last 5 years has seen a great increase in the number of investigators utilizing non-invasive models causing higher demand for the instrument and lowering their purchase cost, however it still remains a much higher up-front cost than surgery.

Non-invasive models include intra-articular tibial plateau fracture (IATPF), cyclic articular cartilage tibial compression (CACTC), and tibial compression overload (TC)[77,83,84]. IATPF flexes the knee into a triangular cradle where an indenter provides a set force of impact causing a closed fracture. This model shows PTOA development after a high energy impact that is similar to a car accident. IATPF looks at changes that happen in highly traumatic injuries involving fracture. This is a good model to study acute injuries, but not chronic injuries or low energy impact. CACTC applies a cycle of loads over a specific period of time. CACTC does not produce a single injury but contributes to progressive degeneration of the cartilage due to the chronic overuse of the joint. This model would mimic overuse that may occur in a marathon runner, or other types of excessive movements. TC uses a single load that ruptures the anterior cruciate ligament (ACL)[85].

Previous studies have shown that the inbred mouse strains *C57Bl/6J*, *C3H/HeJ*, *STR/ort*, and *MRL/MpJ* all have varying susceptibilities to the

development of PTOA on male mice, in the absence of trauma[86–89]. It has not been studied how the injury affect PTOA progression in female mice.

C57Bl/6J male mice have been previously shown to be susceptible to PTOA and are the primary model used to study disease progression, and all other strains are compared to *C57Bl/6J* to evaluate deviations in PTOA outcomes. *MRL/MpJ* male mice are resistant to PTOA due to their ability to repair damaged cartilage[87,88,90]. *STR/ort* male mice develop OA spontaneously and are highly susceptible to PTOA due to elevated levels of circulating pro-inflammatory cytokines and chemokines[78,91,92]. Male *C3H/HeJ* develop more severe PTOA than C57Bl/6J, but have never been compared to the two other strains, used at the same age as this study, and never been used in a tibial compression overload (TC) model[93]. *C3H/HeJ* mice have higher bone mass than C57Bl/6J and carry a mutation on toll-like receptor 4 (TLR4) that makes them less susceptible to gram-negative bacteria induced inflammation[94–97].

Tibial Compression Loading Model of Post-Traumatic Osteoarthritis

This project focuses on ACL ruptures, due to the high incidence of this type of injury in humans[41]. TC loading model is the only non-invasive models that focuses specifically on ACL rupture. The TC system has two custom-built loading platens (**Fig 3**). The top platform keeps the ankle flexed at approximately 30°, while the bottom one holds the knee bent. The load will move at 1mm/s that overextends the ligament in a single dynamic axial compressive load until the ACL ruptures at a force of 12-18N (**Fig 3**)[98]. The force however can vary among individual mice depending on their weight and bone mass of each mouse.

The non-invasive TC model closely resembles a real injury where the knee dislocates and ruptures the ACL in the process. This is a non-invasive injury that is ideal for studying early OA changes and effects to early treatment, unlike tibial plateau fracture models it has a lower impact. The TC model is not a good model to study long-term effects due to excessive osteophyte formation

that appears in order to help stabilize the joint, given that it does not have surgical re-stabilization of the joint. Higher volume of osteophyte growth rate in TC injury is the main difference between TC injury and clinical studies. Currently there is no published method established to stabilize the joint after the TC injury[99,100].

LPS Induced Inflammation Affects the Bone and the Development of PTOA

The body is constantly exposed to small doses of inflammation from sun exposure, the food we eat, and even from the bacteria living inside our intestinal tract. The gut microbiome releases microbial associated molecular patterns (MAMPs) that bind to toll-like receptors (TLR) which activate an inflammatory cascade that releases pro-inflammatory cytokines and chemokines[101]. These pro-inflammatory cytokines and chemokines will act as transcription factors for naïve immune cells to turn into mature immune cells[102]. This process is known as positive protective immune activation. The MAMP we will be focusing on is lipopolysaccharide (LPS) which is released by gram-negative bacteria and binds to TLR4[103] (**Fig 4**). In the case of LPS, the positive protective activation induces the inflammatory cascade that ends with the release of tumor necrosis factor alpha (TNFα), interferon-b (IFN-b), IL-1b, IL-6, IL-12, and stimulate naïve immune $CD4^+$ T cells to turn into mature T cells. IL-6, IL-1β, and TNF-α stimulate the naïve $CD4^+$ T cells to turn into T helper 17 cells. IL-1β and TNF-α stimulate the naïve $CD4^+$ T cells to turn into a T helper 2 cell [104–107]. A constant stimulation of the immune system by the gut microbiome allows to support different immune cell lineages.

Negative effects of inflammation come when it is not small but during elevated levels of systemic inflammation. Literature has suggested that an increase in circulating LPS causes a decrease in bone mass due to an increase in osteoclastogenesis, however if treated with calreticulin there will be an inhibition of osteoclastogenesis [108].The inflammatory cascade associated with

elevated levels of LPS increases levels of two pro-inflammatory cytokines like IL-6 and IL-1b, and TNF-α, which promote inflammation and osteoclastogenesis given that it is a promoter of the receptor activator of nuclear factor kappa-B ligand (RANKL) in bone marrow and stroma cells [109,110]. RANKL activates a number of osteoclast-specific genes through direct interaction with their promoters and with that promoting osteoclastogenesis[111]. The higher the levels of osteoclastogenesis, the lower the bone mass density will be[52].

The effects of inflammation on osteoclastogenesis have been seen on other types of inflammation inducing methods, not just during LPS induced inflammation. In rheumatoid arthritis (RA) inflammation has been shown to have an aggressive bone destruction phenotype mediated by osteoclasts[112]. One of the RA treatments includes TNF-α inhibitor in order to combat the rapid bone resorption that is one of the symptoms of this disease [112]. These studies confirm that the elevated presence of TNF-α for prolonged periods of time will cause the aggressive resorption of bone by osteoclasts[113].

Inflammation does not only affect bone mass density; studies have shown that bone repair after bone injury is impaired when mice are exposed to daily systemic injections of LPS[109]. After cortical defects were drilled in the femoral diaphysis the mice treated with daily LPS injections had less bone repaired than the untreated group[114]. The study found that there was impaired revascularization, decreased bone turnover by osteoblasts, and increased catabolic activity by macrophages and osteoclasts[109].

A number of studies have shown the link between LPS induced inflammation and the effect on bone[115]. The effects of localized LPS in the joint have been studied and have shown significant differences when compared to untreated joints[116]. Localized LPS injections in the joint cause synovitis in horses within an hour of the injection[117]. Intra-articular injections of LPS showed increased levels of IL-1b, IL-6, prostaglandin E2, TNF-α, and chondrocyte hypertrophy[118]. Due to the presence of chondrocyte hypertrophy it is evident that the constant exposure to LPS in the joint leads to progressive cartilage damage

that results in an accelerated progression to an exacerbated osteoarthritis phenotype. No study to date has examined how LPS affects the development of PTOA when paired with injury.

It is well documented that inflammation can contribute to a more severe PTOA phenotype. Studies *in vivo* have shown that mice that are believed to be resistant to the development of PTOA resolve inflammation faster than their control[86]. On the opposite side, it has been shown that systemic inflammation at the time of injury could lead to a more severe PTOA phenotype. Clinical studies have shown that the presence of pro-inflammatory cytokines IL-1, IL-6, IL-8, TNF-α, and the constant activation of inflammatory pathways correlate with a more severe PTOA phenotype after injury in patients[46,68,119]. In contrast, the presence of anti-inflammatory cytokines IL-10 and IL-1 receptor alpha (IL-1Rα) correlated with a faster resolution of inflammation and clinical manifestation of PTOA after injury[120].

The results have led to studies that suggested that targeting the early inflammatory response post-trauma, could decrease the probability of developing PTOA. This is supported by results from Shen *et al*, in which the authors stated that after an ACL transection, CD4+ T-cell deficient mice had reduced synovitis and cartilage erosion[121]. *Shen et al* proposed that this was due to a lower production of macrophage inflammatory protein-1γ. A reduction in inflammation and cartilage erosion on CD4+ T-cell deficient mice shows a link between the immune system and PTOA development. Studies have also shown that a depletion of macrophages in the synovium after injury reduce synovitis in obese mice and with that cartilage destruction, preventing PTOA[75]. Some studies have suggested that pro-inflammatory bacteria living in our gut could be partially responsible for the progression of PTOA and changing the gut biome composition could help reverse some OA phenotypes .

All these studies have looked at how persistent inflammation or a spike in inflammation at the time of injury changes the PTOA phenotype. There have been no studies that examined how residual inflammation from a spike prior to

injury affect the outcome of PTOA. Narrowing down the possibility of developing PTOA to the time of injury does not allow us to see the whole system. Studies are required to look at how the residual effects of a spike in inflammation will affect the development of PTOA, so we can better understand how we can block the PTOA contributing factors.

Changes to the Gut Microbiome Affect Bone and the Development of PTOA

The cells of the gut microbiome outnumber the cells in our body by a factor of ten[123]. The gut microbiome enters a state of dynamic stability around the age of three[124]. The gut microbiome is incredibly resilient, studies have shown that fluctuation during travel abroad or illness will not cause significant changes to the gut microbiome. The gut microbiome has a symbiotic relationship with the host. The gut microbiome contributes to fighting pathogens, synthesizing proteins, nutrient extraction, immunoregulation, and more[125].

Dysbiosis or microbial imbalance has been shown to have effects throughout the entire body. Dysbiosis can result in obesity[61], inflammatory bowel disease [126], metabolic changes [127], malnutrition [101], cardiovascular disease [128], and more[129,130]. The gut microbiome has been shown to be changed in cohorts of RA patients that are not under treatment; they were able to see that there was an enrichment in gram-positive bacteria while the gram-negative bacteria was depleted when RA patients were untreated[131]. The balance returned back to normal once treatment resumed. The suggestion that dysbiosis is linked to RA is made by other studies that looked at how the gut microbiome is affected by the disease[132]. Another study has shown that there is a link between the presence of certain bacteria like *Prevotella copri* and RA[133].

The gut microbiome has an indirect effect on bone through synthesizing vitamin D and MAMPs. There is conflicting evidence as to exactly what the gut microbiome does to influence bone metabolism. Some studies reported that germ-free female *C57Bl/6J* mice between 7 and 9 weeks of age had a

substantial increase in trabecular and cortical bone volume that was suggested could be possibly linked to the decrease in $CD4^+$ T cells and $CD11b^+$/GR1 osteoclast precursors in the bone marrow[134]. In the same study they saw that after the repopulation of the gut microbiome the $CD4^+$ T cells volume increased and there was subsequent bone loss. These findings were confirmed in a study about osteoporosis with germ-free female *C57Bl/6J* mice that were 20 weeks old. The authors observed an increase in cortical thickness but no changes in the trabecular thickness of these mice[135]. Studies in female C57Bl/6J at 7 weeks using low-dose antibiotics saw the bone mass density increase but at 11 weeks there were no difference; this study proposed that the changes to the bone might be transient and not long-term[136]. Studies in male and female *C57Bl/6J* mice exposed to low dose antibiotics since birth showed an increase in bone mineral density at 20 weeks of age[127]. The majority of published studies showed that an increase in bone occurs when the gut biome is depleted, however no study to date has examined how changes in the gut biome modulate responses to orthopedic trauma.

A few recent studies looked at how the gut microbiome might affect OA but one study was conducted in the context of a high fat diet and obesity. Obesity is highly correlated with OA development due to the high load the joints are subjected to during movement[69]. Treatment with clodronate-loaded liposomes on the synovial joints depletes macrophages in the synovium, lessening the number of pro-inflammatory macrophages, reducing synovitis, and slowing down cartilage degradation[75]. The second OA and obesity study showed that treatment with oligofructose supplements could target the microbiota, reduce inflammation, and protect against OA in obese mice[122].

The CDC reported that there were 793 antibiotics prescriptions dispensed per 1000 people in the United States in 2017[137]. That means that modifications to the gut microbiome due to antibiotic use is highly prevalent. People experience different kinds of gut dysbiosis but the connection between antibiotics use and PTOA has not yet been examined. Development of PTOA takes decades and

looking into how modifications to the gut microbiome can affect the outcome after injury is key in order to find methods to treat populations at risk.

Significance and Hypothesis

The purpose of this project is to discover changes between males and females in the development of PTOA after injury, and how systemic modifying factors could potentially hinder or aid in joint injury resolution, specifically how external factors can modify the acute phase. The cause of OA might be different between primary or secondary, but the illness and treatments could be the same. We must find ways to better identify potential OA patients and treat them before they undergo expensive surgeries.

This project looked at how the residual effects of a gram-negative-like bacterial infection would change the injury in both males and females. During a gram-negative infection levels of LPS spike, which at high concentrations have been linked to fever, systemic inflammation, and loss of bone mineral density. The associated malaise prevents patients from performing daily activities, however when activity resumes, we must determine how residual inflammation may significantly elevate the risk for developing PTOA, in the event a traumatic injury occurs.

The second part of this project used a chronic antibiotics treatment regimen to induce a state of gut dysbiosis, similar to what may happen in the intestinal tract of many individuals being treated for a chronic middle ear infection, malaria, or even teenagers suffering from acne, prior to injury. Chronic antibiotic use modifies the gut microbiome and indirectly affect osteoclastogenesis, gene expression, and immune response, all of which can modulate aspects of PTOA development.

I hypothesize that LPS induced inflammation and gut dysbiosis will modify the PTOA phenotype of *C57Bl/6J* injured mice by increasing the levels of bone resorption through gene expression changes and macrophage activity within the

joint. PTOA phenotype severity will be exacerbated in female injured joints compared to male injured joints.

Figures

Figure 1 Synovial Joint Structure

Knee as an example of the synovial joint showing the anatomical structures and circulating cells.

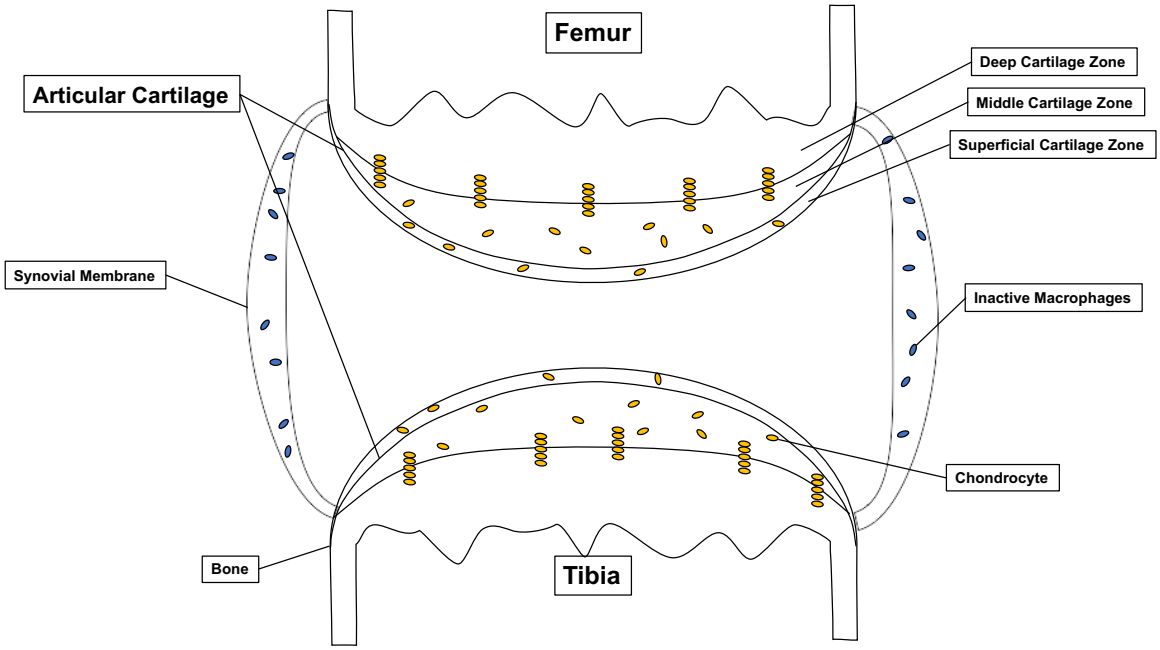

Figure 2 Injury Progression to PTOA

Representation of injury followed by the immediate phase and acute phase. These phases are followed by either a spontaneous resolution or a chronic phase that can develop over 20 years after the initial injury.

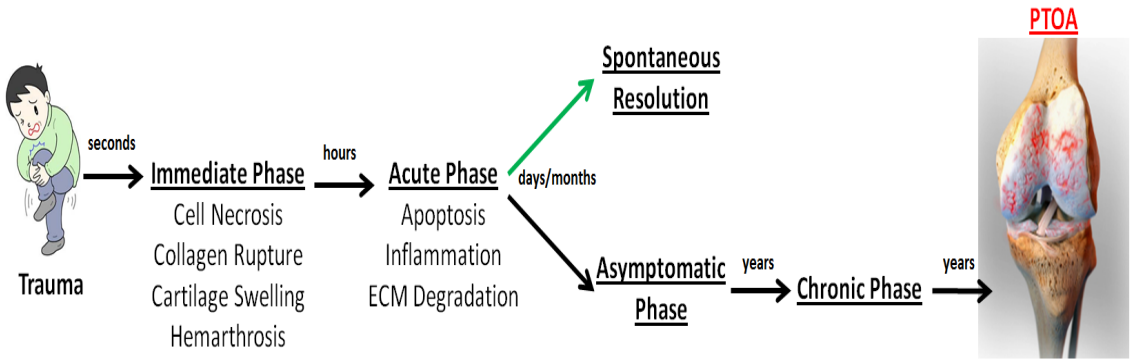

Figure 3 Tibial Compression Loading

Non-invasive knee injury model used for mice 10 weeks of age, that were injured using a non-invasive single-dynamic tibial compression load (1mm/s) until ACL rupture (~12N).

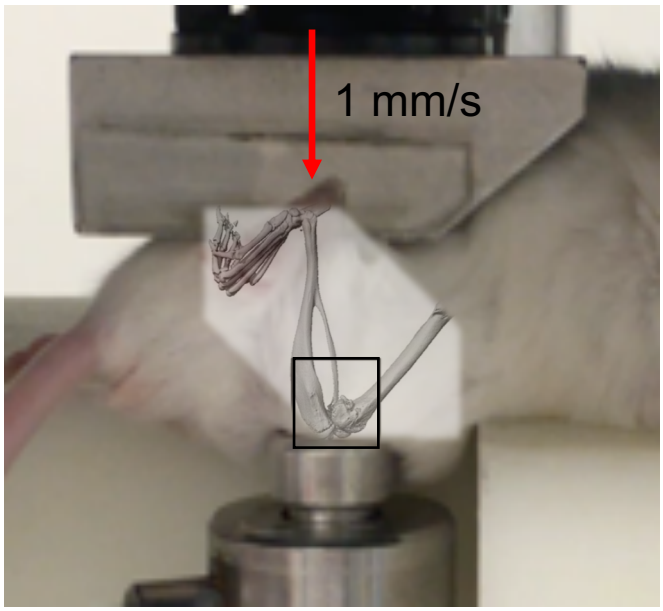

Figure 4 LPS Binding to Toll-Like Receptor 4 Pathway

Signaling involved in the activation of the TLR4 receptor by commensals that aid immunoregulation. Gram-negative bacteria stimulate immune cell activation via LPS, activating transcription factors downstream of TRL4.

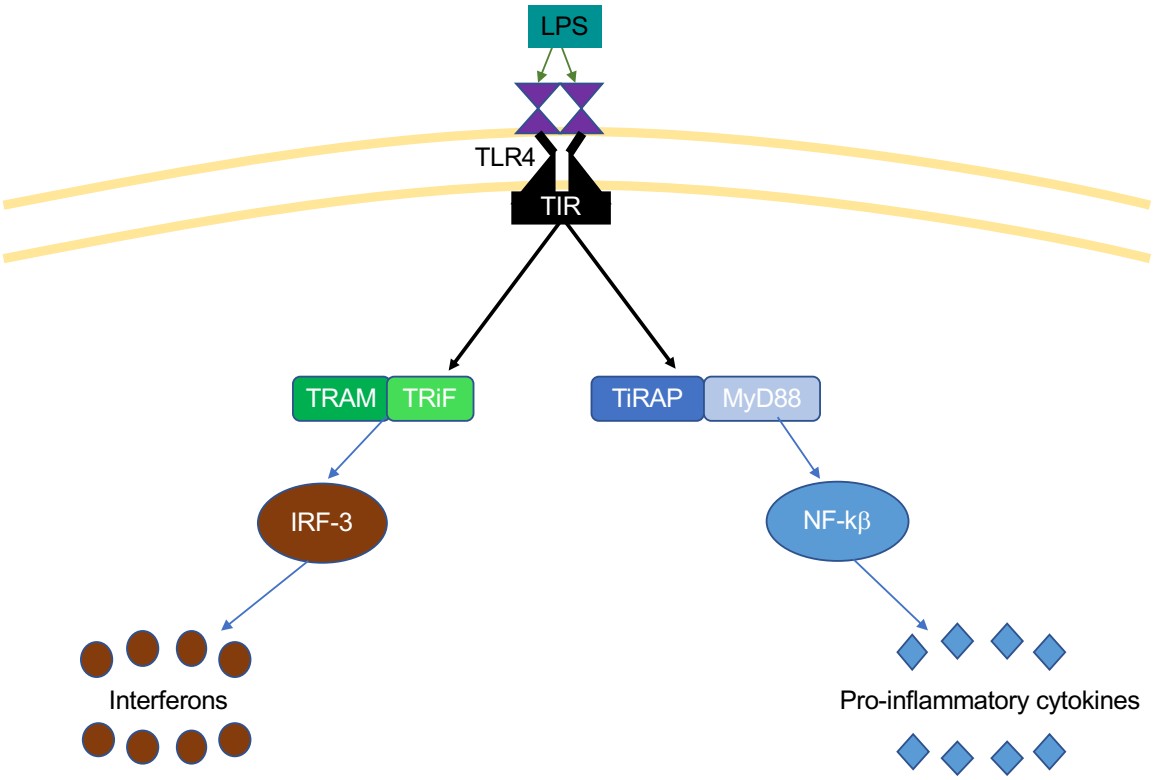

Chapter 2: Comparing the Severity of Post-Traumatic Osteoarthritis on *MRL/MpJ*, *C57Bl/6J*, *C3H/HeJ,* and *STR/ort* Mouse Models

Introduction

Post-traumatic osteoarthritis (PTOA) is a secondary form of OA that develops between a decade or two in approximately half of the people who have suffered a severe articular injury[82,138]. Inflammation, severity of injury, genetic predisposition, and repeat of injury have been suggested as factors that might contribute to the progression of PTOA[71,139,140]. Previous studies have shown that the inbred mice strains *MRL/MpJ, C57Bl/6J*, *C3H/HeJ,* and *STR/ort* all have varying susceptibilities to the development of PTOA in male mice, using different types of injury models. However, female mice have not yet been investigated to determine whether injury affects PTOA progression differently, in females.

C57Bl/6J male mice have been previously shown to be susceptible to PTOA and are used as controls. Murphy Roths Large (*MRL/MpJ)* males are resistant to PTOA after intraarticular fracture[88], destabilization of the medial meniscus[87], and tibial compression overload[86]. *MRL/MpJ* have been suggested to be resistant to PTOA due to their ability to resolve inflammation faster than male *C57Bl/6J* post-injury and the ability repair damaged cartilage, these two factors makes them virtually resistant to PTOA. This model may correspond to the ~50% of patients who go on to spontaneously resolve the injury and never develop PTOA. *C3H/HeJ* mice have higher bone mass and a defect on toll-like receptor 4 (TLR4) making them insensitive to gram-negative released endotoxin[97]. The higher bone mass phenotype could be a contributing factor to the development of PTOA, but the contribution of bone mass to cartilage function still remains unclear. *STR/ort* male mice develop OA spontaneously due to elevated levels of circulating pro-inflammatory cytokines and chemokines. Additionally, *STR/ort* have altered articular cartilage chondrocytes with lower succinate dehydrogenase and lactate activities, with changes in the monoamine

oxidase on the articular cartilage that later presents OA[89]. *STR/ort* represents the population that is genetically predisposed to developing PTOA or have constantly activated inflammatory pathways.

Studying mice with varying susceptibilities to PTOA due to their individual characteristics is comparable to humans due to the variability of genetic predisposition and other related factors like inflammatory diseases. Additionally, we must take into account that half of the population is female, and the majority of studies to date have focused on male mice with the assumption that disease progression would be independent of sex. This model will allow us to describe sex-related changes to PTOA progression and better understand how susceptibility to the disease changes in females compared to males.

Materials and Methods

Experimental Animals and ACL Injury Model. *C57Bl/6J* and *C3H/HeJ* mice were purchased (Jackson Laboratory, Bar Harbor, ME, USA; Stock No: 000664, 000659) at 4 weeks of age and kept under normal cage conditions. *STR/ort* and *MRL/MpJ* strains were bred in house. Cohorts of mice (n=4 for female *STR/ort* and *MRL/MpJ*, n=5 male *STR/ort*, male *MRL/MpJ*, and female *C3H/HeJ*, n=10 male *C3H/HeJ*, male *C57Bl/6J*, and female *C57Bl/6J*) included male and female groups. At 10 weeks of age, both groups received a non-invasive single dynamic tibial compressive load for an ACL rupture using an electromagnetic material testing machine (ElectroForce32000, TA Instruments, New Castle, DE, USA) as previously described [54]. Animals returned to normal cage activity until samples were collected at 16 weeks of age. All animal work was conducted in accordance to the Institutional Animal Care and Use Committees at Lawrence Livermore National Laboratory and the University of California, Davis in AAALAC-accredited facilities.

Micro-Computed Tomography. Samples were collected 6-weeks post injury for female and male *C57Bl/6J*, *MRL/MpJ*, *C3H/HeJ,* and *STR/ort* injured, contralateral, and uninjured joints. Samples were dissected and fixed for 72 hours at 4°C using 10% neutral buffer formalin. Samples were stored in 70% EtOH at 4°C until scanned. Whole knees were scanned using a SCANO μCT 35 (Bassersdorf, Switzerland) according to the rodent bone structure analysis guidelines (X-ray tube potential = 55kVp, intensity = 114 μA, 10 μm isotropic nominal voxel size, integration time = 900 ms). Trabecular bone in the distal femoral epiphysis was analyzed manually drawing contours on 2D transverse slides. The distal femoral epiphysis was designated as the region of trabecular bone enclosed by the growth plate and subchondral cortical bone plate. We quantified trabecular bone volume per total volume (BV/TV), trabecular thickness (Tb.Th), trabecular number (Tb.N), and trabecular spacing (Tb.Sp). Osteophyte volume in injured and contralateral joints was quantified by drawing contours around all heterotopic mineralized tissue attached to the distal femur and proximal tibia as well as the whole fabellae, menisci, and patella as previously described[141]. Total mineralized osteophyte volume was then determined as the volumetric difference in mineralized tissue between injured and uninjured joints.

Micro-Computed Tomography Statistics. Statistical analysis was performed using two-way ANOVA and Student's T-test with a two-tailed distribution, with two-sample equal variance (homoscedastic test)[142,143]. For all tests, $p<0.0042$ was considered statistically significant, after a Bonferroni correction. *C3H/HeJ* female samples were not scanned.

Histological Assessment of Articular Cartilage and Joint Degeneration. *C57Bl/6J*, *MRL/MpJ*, *C3H/HeJ* and *STR/ort* injured, contralateral, and uninjured joints were dissected 6 weeks post injury, free of soft tissue, fixed, dehydrated, paraffin embedded and sectioned as previously described[144,82]. The cartilage was visualized in sagittal 6μm paraffin serial using Safranin-O (0.1%, Sigma;

S8884) and Fast Green (0.05%, Sigma; F7252) as previously described[144,82]. OA severity was evaluated at 6 weeks post injury on sagittal sections using a modified osteoarthritis research society international (OARSI) scoring scale as previously described[145]. Starting from the synovium membrane to the articular cartilage, for each region, cartilage scoring began ~0.4 mm out from the start of synovium. Blinded slides were evaluated by seven scientists (six with and one without expertise in OA) utilizing a modified (sagittal) OARSI scoring parameters due to the severity of the phenotype due to TC loading (**Fig. 1**). Modified scoring scores (0) for intact cartilage staining with strong red staining on the femoral condyle and tibia, (1) minor fibrillation without cartilage loss, (2) clefts below the superficial zone, (3) cartilage thinning on the femoral condyle and tibia, (4) lack of staining on the femoral condyle and tibia, (5) staining present on 90% of the entire femoral condyle with tibial resorption, (6) staining present on over 80% of the femoral condyle with tibial resorption, (7) staining present on 75% of the femoral condyle with tibial resorption, (8) staining present on over 50% of the femora condyle with tibial resorption, (9), staining present in 25% of the femoral condyle with tibial resorption, (10) staining present in less than 10% of the femoral condyle with tibial resorption (**Fig. 1**).

Results

Evaluating the Progression of PTOA Development in the Cartilage on *MRL/MpJ*, *C57Bl/6J*, *C3H/HeJ* and *STR/ort* on Male and Female Mice

Using a tibia compression PTOA mouse model, we examined what changes the inbred mouse strain would have on the OA outcome, in male and female mice. *MRL/MpJ, C57Bl/6J, C3H/HeJ* and *STR/ort* mice were examined on the medial side in sagittal sections of the joint histologically 6 weeks post injury. Uninjured contralateral male and female *MRL/MpJ* and *C57Bl/6J* showed no cartilage erosion and strong staining and no significant changes on the OARSI scores (**Fig. 2A, C, E, G**). Uninjured contralateral male and female *C3H/HeJ* and

STR/ort showed less cartilage staining but no cartilage erosion throughout the joint (**Fig. 2I, K, M, O**). Female *C3H/HeJ* and *STR/ort* had significantly higher OARSI scores than the corresponding male of each strain due to a thinner articular cartilage layer. *C3H/HeJ* contralateral female showed significantly higher OARSI scores than all other uninjured contralateral groups (**Fig. 2K, Q**). All injured samples had significantly higher OARSI scores than the corresponding contralateral joints (**Fig. 2Q**). Uninjured samples showed statistically significant changes when compared to the injured corresponding group, except for *MRL/MpJ* males strain which showed no significant differences between the uninjured and injured. All *p*-values are listed in Table 1.

Injured *C57Bl/6J* males had more cartilage erosion than injured *C57Bl/6J* females on the medial side (**Fig. 2B, D**). The femoral condyle of the females showed thinner cartilage (**Fig. 2b, d; arrow asterisk**). *C57Bl/6J* injured showed a hyperplastic synovium suggesting more elevated levels of inflammation than the male counterpart of the meniscus compared to the injured *C57Bl/6J* male (**Fig. 2 bb, dd; asterisk**). Female injured *C57Bl/6J* had a significantly higher OARSI score than the male counterpart (**Fig. 2Q**).

In injured *MRL/MpJ* males we observed strong cartilage staining and found the cartilage to be intact relative to the *C57Bl/6J* injured males (**Fig. 2B, F**). Injured *MRL/MpJ* males had cartilage staining throughout the entire femoral condyle, giving it a significantly lower OARSI score than the injured *C57Bl/6J* males. However, the femoral condyle had a thinner cartilage layer than the injured *C57Bl/6J* males that had thicker cartilage layer, but with fainter staining, and less uniformity throughout (**Fig 2b, f; arrow, asterisk**). Injured female *MRL/MpJ* showed no cartilage erosion but had significantly less staining on the femoral condyle, suggesting that the injury had a more dramatic effect on females than males (**Fig. 2f, h; arrow, asterisk**). Injured *MRL/MpJ* males had less cellular infiltration compared to the *C57Bl/6J* injured males and *MRL/MpJ* injured females (**Fig. 2bb, ff, hh; asterisk**). Injured *MRL/MpJ* females had

thicker cartilage on the femoral condyle (**Fig. 2d, h; arrow, asterisk**) and less cellular synovium than the injured *C57Bl/6J* females (**Fig. 2dd, hh; asterisk**).

Injured *C3H/HeJ* male mice had less cartilage than their *C57Bl/6J* counterpart (**Fig 2B, J**). Injured *C3H/HeJ* females were similar to males while having increased cartilage erosion, the female and male *C3H/HeJ* injured samples were significantly different (**Fig. 2J, L**). The femoral condyle of the male and female *C3H/HeJ* injured joints showed thinner cartilage than the corresponding *C57Bl/6J* groups, *C3H/HeJ* injured samples had significantly higher OARSI scores than the corresponding *C57Bl/6J* and *MRL/MpJ* (**Fig. 2b, d, j, l; arrow, asterisk**). There was synovitis in the joint of the males due to an increase in cellularization of the injured male *C3H/HeJ* compared to the injured male *C57Bl/6J* and injured male *MRL/MpJ* (**Fig. 2bb, jj; asterisk**). The female *C3H/HeJ* has decreased cellular infiltration compared to male *C3H/HeJ* and female *C57Bl/6J* (**Fig. 2dd, jj, ii; asterisk**).

Injured *STR/ort* male mice had the most severe phenotype from all the male mice examined. *STR/ort* male injured mice had a significantly higher OARSI score than the injured male *MRL/MpJ*, injured male *C57Bl/6J*, and injured male *C3H/HeJ*, due to the large amount of cartilage erosion and loss of staining (**Fig. 2B, F, J, N**). Injured *STR/ort* mice show thicker cartilage on the femoral condyle than the injured *STR/ort* female mice but a thinner when compared to the male strains (**Fig. 2b, f, j, m, p; arrow, asterisk**). There was no significant difference between the injured male and female *STR/ort* when comparing OARSI scores. This could be due to the fact that the injured female *STR/ort* mice showed increased staining on the anterior tibial condyle than the male injured *STR/ort* and increased cellular infiltration which indicate that the systematic inflammation they are suffering from has a large effect on cartilage erosion (**Fig. 2nn, pp; asterisk**).

There is a distinct phenotype present after TC as early as 6 weeks post-injury, in each strain, and some are sex specific. *C57Bl/6J* and *MRL/MpJ* did not show differences between sexes on the uninjured contralateral leg. *C3H/HeJ* and

STR/ort females had decrease staining that was statistically significant on uninjured contralateral joints.*C57Bl/6J*, *MRL/MpJ*, and *C3H/HeJ* showed a significantly more severe PTOA phenotype in injured female joints than in males. *STR/ort* injured joints did not have significant changes to the severity of PTOA when males and females were compared.

Evaluating the Femoral Epiphysis Bone Changes and Osteophyte Volume During the Progression to PTOA Development on *MRL*/*MpJ*, *C57Bl*/*6J*, and *STR*/*ort* in Male and Female Mice

Using μCT we examined the changes caused to the femoral epiphysis six weeks after ACL rupture using strains of varying PTOA susceptibilities (**Fig. 3**). Femoral epiphysis subchondral bone volume (BV/TV) analysis showed significantly lower BV/TV on the injured joints of each strain compared to the corresponding contralateral (**Fig. 3A**). Results for *MRL/MpJ, C57Bl/6J*, and *STR/ort* males are consistent with our previously published data[86]; results for females and for *C3H/HeJ* follow the trend presented previously. Percentage comparisons for those not presented in this result section are found on Table 1.

To understand how injury changes between strains with different susceptibilities and sexes we analyzed the differences between injured samples. Injured female *C57Bl/6J*, *MRL/MpJ*, and *STR/ort* presented ~5.2% lower, ~5.7% lower, and ~7.2% higher BV/TV than the corresponding male (**Fig 3A**). *C57Bl/6J* and *MRL/MpJ* injured female to male comparisons were statistically significant (**Fig. 3A**). Results from this shows that there will a higher amount of subchondral bone loss after injury in the baseline and PTOA resistant strains when comparing females than males.

Injured *C57Bl/6J* females BV/TV was not significantly different than injured *MRL/MpJ* females. Injured *C57Bl/6J* and *MRL/MpJ* females had significantly lower BV/TV when compared to the injured *STR/ort* females. *STR/ort* mice have a higher bone mass than the *C57Bl/6J* and *MRL/MpJ*. There were no significant differences between the injured male *C57Bl/6J* when compared to the injured

MRL/MpJ male and injured *C3H/HeJ* male. *C57Bl/6J* injured male exhibited a significantly lower BV/TV than the injured *STR/ort* male. Male injured *MRL/MpJ* did not have significant differences when compared to the injured male *C3H/HeJ* using the Bonferroni correction. Male injured *STR/ort* had significantly higher BV/TV than the injured *C3H/HeJ* and *MRL/MpJ* males (**Fig 3A**).

Trabecular number (Tb.N) was significantly lower in *C57Bl/6J* and *MLR/MpJ* injured females by ~22.1% and ~20.1% than the corresponding male. *STR/ort* injured females and males had virtually the same Tb.N (**Fig. 3B**). There was no significant difference in the *C57Bl/6J* injured female compared to the female injured *MRL/MpJ* and female injured *STR/ort*.

There are no difference between the Tb.N of *MRL/MpJ* injured females compared to the *STR/ort* injured females. *C57Bl/6J* male injured had a significant difference when comparing the Tb.N to the male injured *C3H/HeJ*. *C57Bl/6J* male injured did not present any significant difference when comparing the Tb.N to the male injured *MRL/MpJ* and *STR/ort*. *MRL/MpJ* injured males exhibited a significantly higher Tb.N than the male injured *C3H/HeJ*. *STR/ort* injured males did not show significant differences comparing the Tb.N to injured male *MRL/MpJ* and *C3H/HeJ* (**Fig 3B**).

Trabecular thickness (Tb.Th) was higher on injured *C57Bl/6J, MRL/MpJ*, and *STR/ort* females by ~3.3%, ~1.2%, and ~25.9% than the corresponding injured males; *STR/ort* was the only statistically significant (**Fig. 3C**). *C57Bl/6J* injured females were not statistically significantly different than the injured female *MRL/MpJ*. *STR/ort* injured females had a significantly higher Tb.Th than the female injured *C57Bl/6J* and *MRL/MpJ*.

Injured *C57Bl/6J* males presented significantly lower Tb.Th than *C3H/HeJ* and *STR/ort* injured males. Injured males *MRL/MpJ* were not significantly different than the *C57Bl/6J*. *MRL/MpJ* injured males showed significantly lower Tb.Th than the male injured *C3H/HeJ* and *STR/ort*. *STR/ort* injured males were not significantly different than the *C3H/HeJ* injured males.

Trabecular spacing (Tb.Sp) was larger in female injured *C57Bl/6J, MRL/MpJ*, and *STR/ort* by ~23.7%, 23.3%, and ~7.5% than the corresponding injured males. Comparisons of female to male were statistically significant for the *C57Bl/6J* and *MRL/MpJ*. There were no differences between the injured females when comparing the different strains. *C3H/HeJ* injured males presented a significantly higher Tb.Sp than the *C57Bl/6J, MRL/MpJ*, and *STR/ort* injured males. There were no other significant differences between strains when comparing the injured male.

Osteophyte volume (Op.V) analysis represents the quantity of ectopic bone growth outside of the joint. *C57Bl/6J* females had ~26% less Op.V than *C57Bl/6J*. *MRL/MpJ* females had ~34.6% lower Op.V than *MRL/MpJ* males. *STR/ort* females had ~9.6% larger Op.V than the male *STR/ort* (**Fig 4**). *C57Bl/6J* females had significantly more Op.V than the *MRL/MpJ* females by ~56.1%. They had ~15.1% less Op.V than the *STR/ort* females. *MRL/MpJ* females had ~62.8% significantly less Op.V than the *STR/ort* females. *C57Bl/6J* males had significantly higher Op.V than *MRL/MpJ* males by ~50.3%, ~25.5% more than *C3H/HeJ* males that was not significant, and ~21.2% lower Op.V than the *STR/ort* males which was not significant. *MRL/MpJ* males had ~33.3% and ~37% less Op.V than the *C3H/HeJ* male *and STR/ort* male; neither were significant. *C3H/HeJ* males had ~5.5% lower Op.V than the male *STR/ort* which was not significant.

Discussion

C57Bl/6J, *MRL/MpJ*, *C3H/HeJ*, and *STR/ort* strains susceptibility differences have not been studied to assess the development of PTOA after a non-invasive injury that ruptures the ACL. Most importantly, females have not been rigorously included in prior PTOA studies to evaluate sex specific contributions to PTOA development. We also analyzed an earlier timepoint than those in prior publications in order to capture subtle differences at earlier time points that may delineate the progression of the disease, in different strains. We also added the

C3H/HeJ strain to this comparison to the three strains that we have previously described at 12 weeks post injury, in males only[86]. By adding the *C3H/HeJ* strain we provided additional support for the hypothesis that higher bone mass could negatively impact PTOA by contributing to a higher level of cartilage degeneration, post injury. *C3H/HeJ* strain showed higher bone mass and OARSI scores that were similar to the *STR/ort* strain which has historically been used to study OA, as a highly susceptible strain of OA. While our data suggests that higher bone mass negatively effects the ability for joints to spontaneous resolve an articular injury, the possibility that toll-like receptor 4 mutation in this strain directly contributes to this phenotype remains a possibility that warrants further investigation.

Our study analyzed the severity of PTOA on females which represents the first rigorous account of sex differences in a non-invasive model of PTOA. It has been previously hypothesized that PTOA development may progress in a similar fashion, in males and females, however, this study highlights significant differences in the severity of PTOA between males and females, of the same strain. Female cohorts of *C57Bl/6J*, *MRL/MpJ*, and *C3H/HeJ* displayed a more severe PTOA cartilage phenotype than the males of the same strain. Data indicated a significant increase in cartilage loss, supported by an increase in the OARSI scores for the females. The STR/ort strain was the only strain that did not show any statistically significant differences between sexes. In contrast, the *MRL/MpJ* strain was the only strain where no statistically significant difference were found between the injured and uninjured males. Since only *MRL/MpJ* males have been examined in prior studies, our finding that female *MRL/MpJ* have a significantly higher OARSI score when compared to the uninjured female MRL/MpJ, suggests that females are mildly susceptible to PTOA, in the TC injury model. This indicates that resistance to PTOA could be sex dependent, and future molecular characterization of this strain should include both sexes, as separate cohorts.

Bone analysis was performed on males and females of *C57Bl/6J*, *MRL/MpJ*, and *STR/ort*; it was also performed on male *C3H/HeJ* only, due to unforeseen technical challenges. Analysis showed that uninjured female *C57Bl/6J* had significantly lower BV/TV than their male counterparts; this was not the case for *MRL/MpJ* and *STR/ort* mice. *C57Bl/6J* and *MRL/MpJ* injured male mice had significantly higher BV/TV than the corresponding female group; there was no significant difference in *STR/ort* mice. This suggests that the *MRL/MpJ* females were affected more than males on both the cartilage and the bone phenotype. A limitation of this study is that we do not have the female *C3H/HeJ* data which would give insights into changes that could be sex linked on the bone phenotype. Given that PTOA is a cartilage disease the histological data provides compelling evidence that *C3H/HeJ* female mice are extremely susceptible to the disease, post injury. Another limitation has to do with the group numbers per mouse that are variable, these are dependent on breeding and females are necessary for breeding the *STR/ort* and *MRL/MpJ* strains which made it challenging to get as many mice as those that can be purchased due to the low breeding strains.

Our study uniquely looked at PTOA developmental changes on four strains that have not been compared previously, in the same non-invasive injury model of PTOA. Consistent with previous studies male mice showed *MRL/MpJ* to be resistant to PTOA, *STR/ort* mice and *C3H/HeJ* had higher OARSI scores than *C57Bl/6J* [78,86,87,93]. We show that the *C3H/HeJ* do not have a statistically significant difference comparing them to the *STR/ort* male mice, they have not been reported to have elevated levels of inflammatory cytokines, but they do have high bone mass, suggesting that the enhanced PTOA phenotypes in these strains may be mediated by different molecular mechanisms. As it was reported previously by our lab we need to start considering bone mass as being potentially correlated with high susceptibility to PTOA.

When examining the female mice our findings show a statistically significant difference between the injured male and female mice of every strain

except for *STR/ort*. The *STR/ort* strains show an almost total resorption of the cartilage on the injured femoral condyle, this leads both of the groups to have higher scores. The *MRL/MpJ* strain has been thought to be completely resistant to PTOA, we observed that the injured females have a significant loss of cartilage along with a hyperplastic synovium indicating cellular infiltration. *C3H/HeJ* female mice show lack of staining on the cartilage, suggesting spontaneous OA development. *C3H/HeJ* female injured joints had a significantly higher OARSI score than the *C3H/HeJ* males. Understanding that the PTOA phenotype becomes more severe in females than in males is the first step towards finding effective therapeutic techniques to prevent the development of PTOA after injury.

Tables

Table 1 Bone Analysis Percentage Comparison

Results from statistical analysis comparing groups by sex, injury type, and mice strains. Percentages were established by comparing the larger to the smaller of the values. Statistical significance was established when p <0.0042.

Comparison	BV/TV (%)	Tb.N (%)	Tb.Th (%)	Tb.Sp (%)
Injured C57Bl/6J Female to Male	16.4	22.1	3.3	23.7
Injured MRL/MpJ Female to Male	17.2	20.1	1.2	23.3
Injured STR/ort Male to Female	16.0	1.7	25.9	7.5
Injured Female C57Bl/6J to MRL/MpJ	4.6	0.5	3.8	0.2
Injured Female C57Bl/6J to STR/ort	41.7	10.2	42.0	5.7
Injured Female STR/ort to MRL/MpJ	38.9	9.8	44.2	5.6
Injured Male C57Bl/6J to MRL/MpJ	5.6	2.0	0.7	0.4
Injured Male C57Bl/6J to C3H/HeJ	9.3	29.3	18.1	29.7
Injured Male C57Bl/6J to STR/ort	17.1	14.6	24.4	12.5
Injured Male MRL/MpJ to C3H/HeJ	14.3	27.9	17.5	29.4
Injured Male STR/ort to MRL/MpJ	12.2	12.9	23.8	12.1
Injured Male STR/ort to C3H/HeJ	24.8	17.2	7.7	19.6

Figures

Figure 1 Modified OARSI Scoring for Non-Invasive Tibial Compression Loading

Scale has been modified in order to determine the severity of PTOA focusing on the femoral condyle cartilage staining. TC are known to cause rapid tibial resorption that will cause higher scores on the conventional OARSI scoring table.

0	Intact cartilage staining with strong red stain on the femoral condyle and tibia
1	Minor fibrillation without cartilage loss on femoral condyle and tibia
2	Clefts below the superficial zone on the femoral condyle and tibia
3	Cartilage Thinning on the femoral condyle and tibia
4	Lack of staining on part of the femoral condyle and tibia with no tibial resorption
5	Staining present in 90% of the femoral condyle with tibial resorption
6	Staining present in 80% of the femoral condyle with tibial resorption
7	Staining of cartilage present on 75% of the femoral condyle with tibial resorption
8	Staining of cartilage present on 50% of the femoral condyle with tibial resorption
9	Staining of cartilage present in 25% of the femoral condyle with tibial resorption
10	Staining of the cartilage present in 10% or less of the femoral condyle with tibial resorption

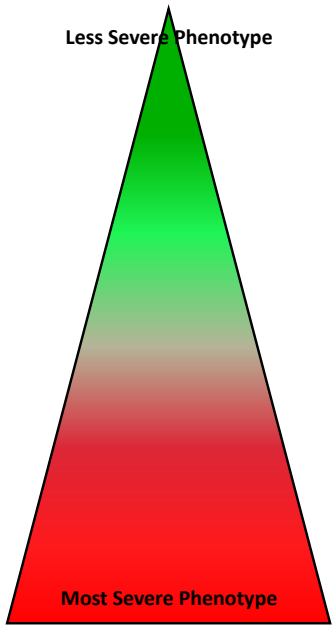

Figure 2 Histological Assessment of PTOA Severity Depending on Strains Post-Tibial Compression Injured Joints

(A-H) Histological assessment of contralateral and injured joints 6 weeks post-injury at 16 weeks of age using Safranin-O and Fast-Green staining. Joints were identified by sex, injured or contralateral, and strain. Images were taken in 5x magnification and 20x magnification. **(I)** OARSI scoring for histological samples separated by strain. *$p<0.05$.

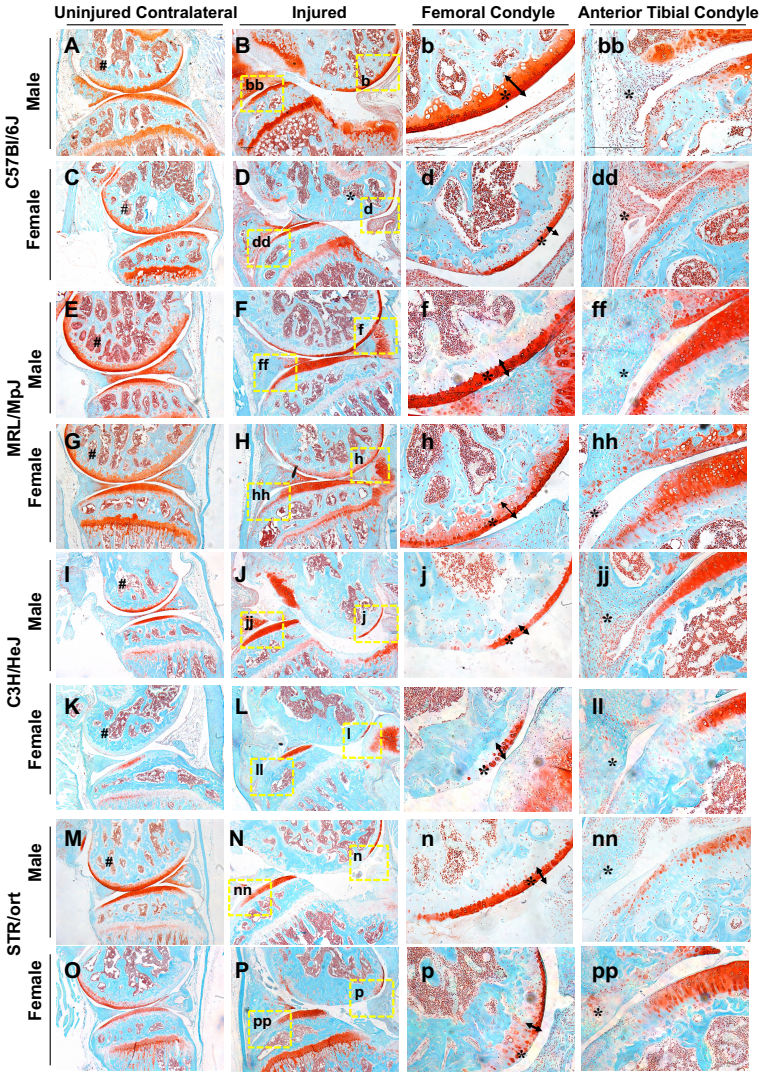
Uninjured Contralateral
Injured
Femoral Condyle
Anterior Tibial Condyle
C57Bl/6J
MRL/MpJ
C3H/HeJ
STR/ort
Male
Female
A
B
b
bb
C
D
d
dd
E
F
f
ff
G
H
h
hh
I
J
j
jj
K
L
l
ll
M
N
n
nn
O
P
p
pp
#
*

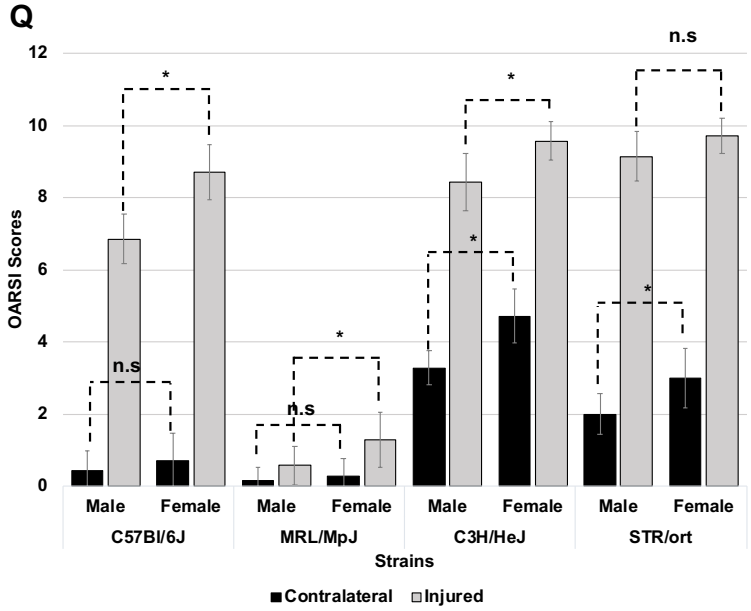
Q
OARSI Scores
12
10
8
6
4
2
0
n.s
*
Male
Female
C57Bl/6J
MRL/MpJ
C3H/HeJ
STR/ort
Strains
Contralateral
Injured

Figure 3 Bone Microstructure Assessment Using Micro-CTof Multiple Strains

(A) Subchondral bone volume (BV/TV) is the bone volume fraction which is the ratio of the segmented bone volume to the total volume of the region of interest. **(B)** Trabecular number (Tb.N) was measured using the average number of trabeculae per unit length. **(C)** Trabecular thickness (Tb.Th) was measured using the mean thickness of trabeculae, assessed using direct 3D methods. **(D)** Trabecular spacing (Tb.Sp) was measured using the mean distance between trabeculae, assessed using direct 3D methods[141]. All statistics were made using sex, injury type, and strain using two-way ANOVA and Student's T-Test. *p<0.0042.

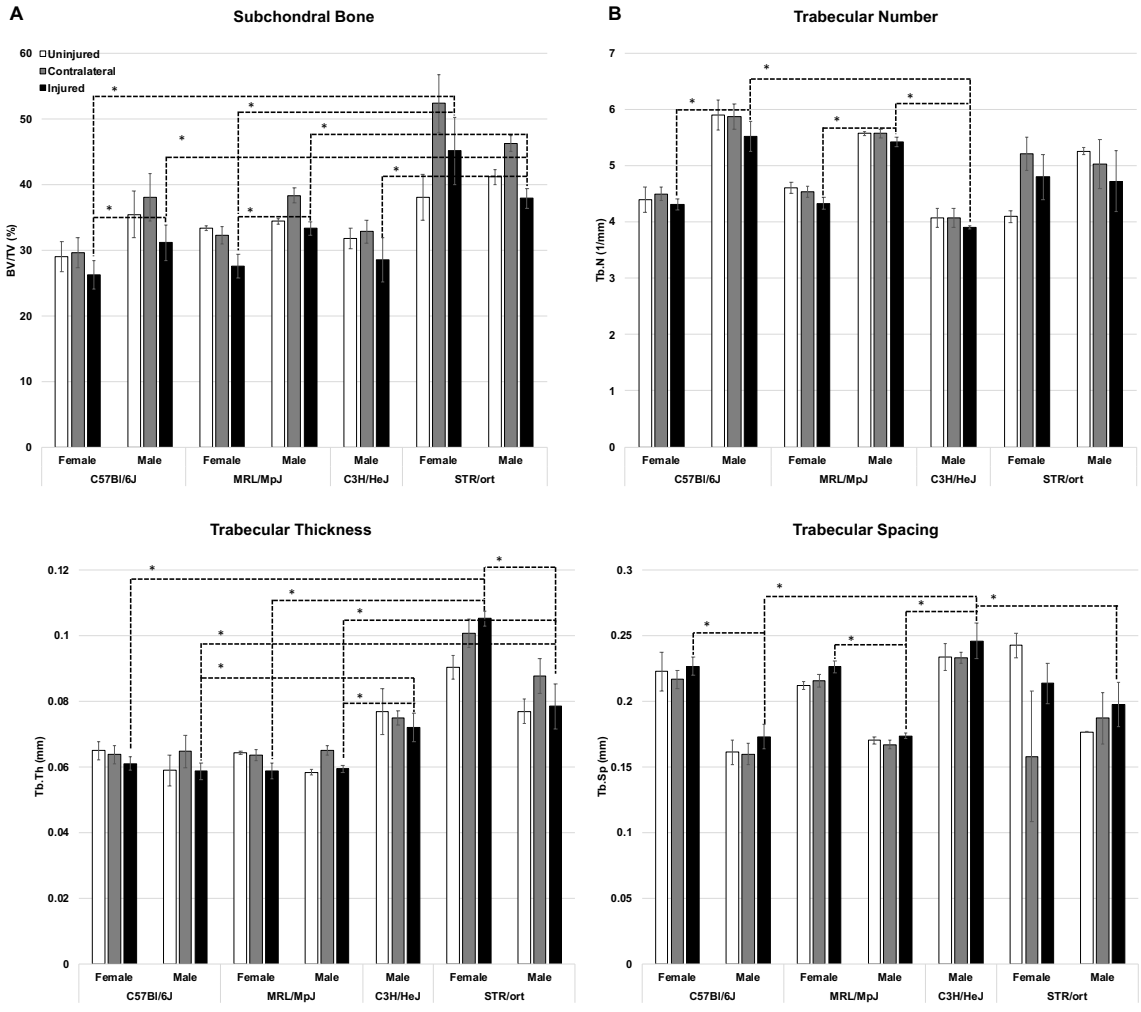

Figure 4 Osteophyte Representation Using Micro-Computed Tomography **(A)** Osteophyte volume was measured by quantification of ectopic bone around the injured joint compared to contralateral. All statistics were made using sex, injury type, and mouse strain using a combination of two-way ANOVA and Student's T-Test. *$p<0.0042$ **(B)** Micro-Computed tomography image of the joints of all groups using data gathered during **(A)**. Dark grey regions show osteophyte growth compared to the white. Contralateral shows the normal bone.

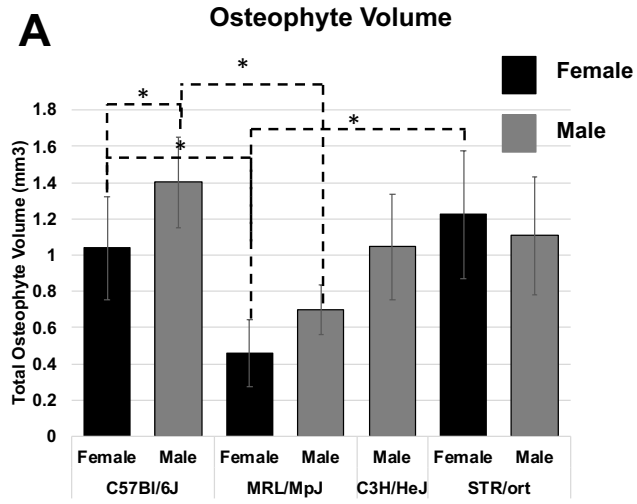
A
Osteophyte Volume
Female
Male
Total Osteophyte Volume (mm3)
1.8
1.6
1.4
1.2
1
0.8
0.6
0.4
0.2
0
Female
Male
Female
Male
Male
Female
Male
C57Bl/6J
MRL/MpJ
C3H/HeJ
STR/ort

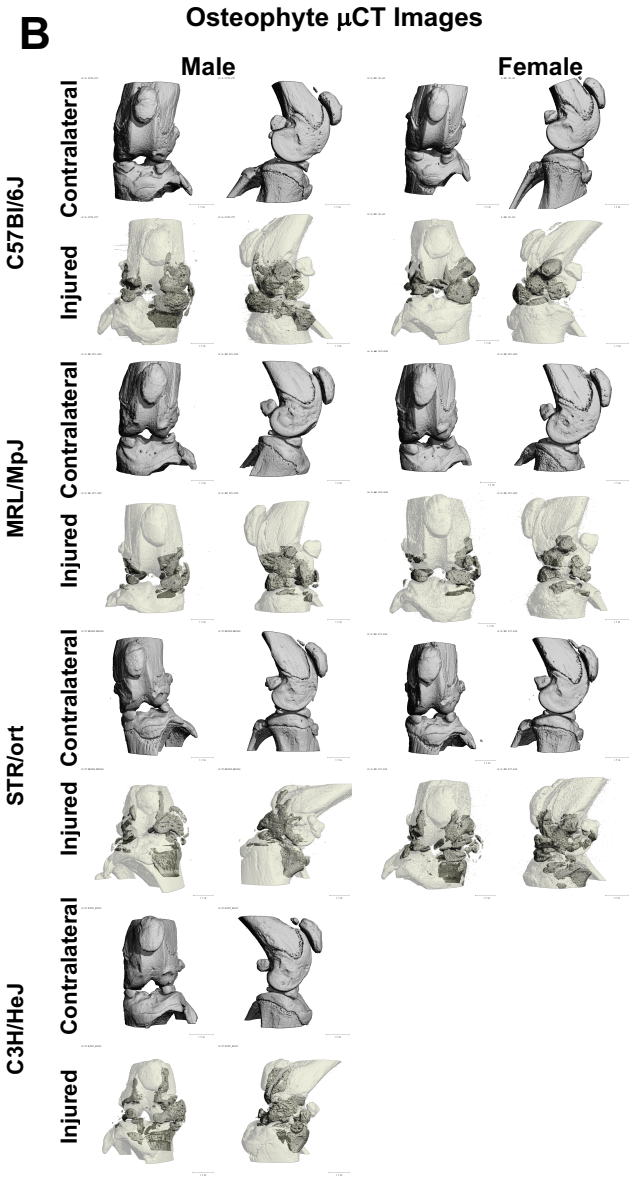
B
Osteophyte µCT Images
Male
Female
C57Bl/6J
MRL/MpJ
STR/ort
C3H/HeJ
Contralateral
Injured

Chapter 3: LPS induced Inflammation Prior to Injury Exacerbates the Development of Post-Traumatic Osteoarthritis on C57BL/6J Mice

Introduction

Post-traumatic osteoarthritis (PTOA) develops in approximately half of patients who have experienced a severe articular trauma like a tibial plateau fracture, meniscus tear, or an anterior cruciate ligament (ACL) rupture[55,70,146]. Within seconds of the traumatic event, cell necrosis, collagen rupture, swelling of the cartilage and synovium, hemarthrosis, and loss of glycosaminoglycans occur; events likely to contribute to PTOA initiation. The healing process initiates during the acute phase which is characterized by significant apoptosis, leukocyte infiltration, matrix degradation, loss of lubrication, and overexpression of inflammatory mediators[86,138]. For ~50% of these patients, the injury repairs and spontaneously resolves, but the rest persist in an asymptomatic phase that can last as little as 8 years and up to 20 years before entering the chronic phase that eventually leads to a PTOA diagnosis[86]. Although not currently classified as an inflammatory disease, some reports have described a state of elevated joint inflammation to strongly correlate with progression to the disease state[74]. Studies relating to inflammation and injury have not looked at how inflammation prior to injury affects PTOA development. A more detailed understanding of how elevated levels of inflammation prior to injury contributes to PTOA development could lead to the identification of prognostic inflammatory markers during the acute phase as well as the development of new therapeutic interventions for the prevention of PTOA unfavorable outcomes.

The endotoxin lipopolysaccharide (LPS) is secreted by gram-negative bacteria, such as *Escherichia coli*, and in healthy individuals LPS is released into circulation by the gut biome to provide a beneficial low-level immune activation[147]. During a gram-negative bacteria infection circulating LPS levels increase activating the immune system clear the bacteria, but this elevated

immune activation may negatively influence physiological processes sensitive to inflammation/cytokine levels. For example, mice with persistent high levels of circulating LPS have a significantly lower bone mass than mice with low levels of LPS[148–151]. Furthermore, focal LPS administration to joints induces synovitis in horses and has been used as a model to evaluate potential treatments for acute synovitis[115–118,152]. However, to date no study has investigated the effects of a single LPS injection a few days prior to joint injury on the outcomes of PTOA. Here we show that a single systemic inflammation-inducing dose of LPS administered 5 days prior to a non-invasive ACL tear is sufficient to modify outcomes by producing a more several PTOA phenotype[98]. Molecular characterization of the joint highlights downregulation of bone and cartilage matrix proteins during the acute phase and elevated presence of type 1 macrophages in the synovium six weeks after injury, suggesting that systemic inflammation when combined with ACL rupture will initiate synovitis suppressing cartilage and bone repair. This model will now allow us to evaluate therapeutics that can blunt inflammation at early stages of joint disease, and potentially block downstream cartilage degradation subsequent to injury.

Materials and Methods

Experimental Animals and ACL Injury Model. *C57Bl/6J* mice were purchased (Jackson Laboratory, Bar Harbor, ME, USA; Stock No: 000664) at 4 weeks of age and kept under normal cage conditions for six weeks. Five days prior to injury, at 10 weeks of age, cohorts of mice (N=10 per group) were separated into two groups for both males and females. 10-week-old LPS group received an LPS intraperitoneal injection (1mg/kg) in the abdominal area, while the vehicle (VEH) group received an injection of saline of equivalent volume. Both groups received a non-invasive single dynamic tibial compressive load for an ACL rupture using an electromagnetic material testing machine (ElectroForce32000, TA Instruments, New Castle, DE, USA) as previously described[76,82,144]. All animal

experimental procedures were completed in accordance with guidelines under the institutional animal care and use committees at Lawrence Livermore National Laboratory and University of California, Davis, under approved protocols by the IACUC committees and conforming to the NIH Guide for the care and use of laboratory animals.

Micro-Computed Tomography. Contralateral, injured and uninjured joints were collected 6-weeks post injury for female and male, VEH and LPS groups. Samples were dissected and fixed for 72 hours in a 4^{o}C using 10% neutral buffer formalin; samples were stored in 70% EtOH at 4^{o}C until scanned. Whole knees were scanned using a SCANO μCT 35 (Bassersdorf, Switzerland) according to the rodent bone structure analysis guidelines (X-ray tube potential = 55kVp, intensity = 114 μA, 10 μm isotropic nominal voxel size, integration time = 900 ms). Trabecular bone in the distal femoral epiphysis was analyzed manually drawing contours on 2D transverse slides. The distal femoral epiphysis was designated as the region of trabecular bone enclosed by the growth plate and subchondral cortical bone plate. We quantified trabecular bone volume per total volume (BV/TV), trabecular thickness (Tb.Th), trabecular number (Tb.N), and trabecular spacing (Tb.Sp)[141]. Osteophyte volume in injured and contralateral joints was quantified by drawing contours around all heterotropic mineralized tissue attached to the distal femur and proximal tibia as well as the whole fabellae, menisci, and patella. Total mineralized osteophyte volume was then determined as the volumetric difference in mineralized tissue between injured and uninjured joints. Statistical analysis was performed using two-way ANOVA and Student's T-test with a two-tailed distribution, with two-sample equal variance (homoscedastic test). For all tests, $p<0.01$ was considered statistically significant after Bonferroni correction.

Histological Assessment of Articular Cartilage and Joint Degeneration. VEH and LPS treated *C57Bl/6J*, injured, contralateral and uninjured joints were

dissected 6 weeks post injury, free of soft tissue, fixed, dehydrated, paraffin embedded and sectioned as previously described[82] . The cartilage was visualized in sagittal 6μm paraffin serial using Safranin-O (0.1%, Sigma; S8884) and Fast Green (0.05%, Sigma; F7252) as previously described[144]. OA severity was evaluated 6 weeks post injury on sagittal sections using a modified osteoarthritis research society international (OARSI) scoring scale as previously described[145]. Starting from the synovium membrane to the articular cartilage, for each region, cartilage scoring began ~0.4 mm out from the start of synovium. Blinded slides were evaluated by seven scientists (six with and one without expertise in OA) utilizing a modified (sagittal) OARSI scoring parameters due to the severity of the phenotype due to TC loading. Modified scoring scores (0) for intact cartilage staining with strong red staining on the femoral condyle and tibia, (1) minor fibrillation without cartilage loss, (2) clefts below the superficial zone, (3) cartilage thinning on the femoral condyle and tibia, (4) lack of staining on the femoral condyle and tibia, (5) staining present on 90% of the entire femoral condyle with tibial resorption, (6) staining present on over 80% of the femoral condyle with tibial resorption, (7) staining present on 75% of the femoral condyle with tibial resorption, (8) staining present on over 50% of the femora condyle with tibial resorption, (9), staining present in 25% of the femoral condyle with tibial resorption, (10) staining present in less than 10% of the femoral condyle with tibial resorption.

Immunofluorescent Staining. Six-micrometer sections from injured samples from both treatment groups were used. Unitrieve was used as an antigen retrieval method for 30 minutes at 65ºC. Primary antibodies: Anti-F4/80 [Abcam, ab16911(1:50)], Anti-CD206 [Abcam, ab64693(1:500)], and Anti-iNOS [Abcam, ab15323(1:100)] were used and incubated overnight at room temperature in a dark humid chamber using protocol previously shown[86]. Negative control slides were incubated with secondary antibody-only. Stained slides were mounted with Prolong Gold with DAPI (Molecular Probes, Eugene, OR, USA). Slides were

imaged using a Leica DM5000 microscope. ImagePro Plus V7.0 Software and a QIClick CCD camera (QImaging, Surrey, BC, Canada) were used for imaging and photo editing.

RNA Sequencing and Data Analysis. Injured, contralateral, and uninjured samples VEH and LPS from male *C57Bl/6J* were collected 24 hours after injury (N=5). Joints were dissected and cut at the edges of the joint region with small traces of soft tissue to preserve the articular integrity. RNA was isolated and sequenced as previously described[86]. RNA-seq data quality was checked using FastQC software (version 0.11.5). Sequence reads were aligned to the mouse reference genome (mm10) using STAR (version 2.6). After read mapping, 'featureCounts' from Rsubread package (version 1.30.5) was used to perform summarization of reads mapped to RefSeq genes and gene-wise read counts were generated. RUVseq (version 1.16.0) was used to identify factors of unwanted variation. Differentially expressed genes were identified using edgeR (version 3.22.3), adjusting for unwanted variation. Genes with false discovery rate (FDR) corrected p-value less than 0.05 and fold change greater than 1.25 were considered as differentially expressed genes (DEGs). Heatmaps were generated using heatmap.2 function in R package 'gplots'.

Results

LPS Administration Causes a More Severe PTOA Phenotype

Using a tibial compression PTOA mouse model[77], we examined whether a single dose of LPS (1mg/kg) would impact OA outcomes, post injury. *C57Bl/6J* strain of mice were examined histologically at 6 weeks post injury. The male VEH uninjured joints looked similar to the female VEH uninjured with no significant changes in the OARSI score (**Fig. 1A, E**), while the VEH injured female displayed more cartilage erosion than the VEH injured male (**Fig. 1B, F**). On the medial side we observed more cartilage erosion on the VEH injured female joint

than on the VEH injured male which was statistically significant (**Fig 1b, f, arrow, asterisk**). VEH injured female joints showed increased synovitis compared to the VEH injured male joints, as noted by increased cellularization (**Fig 1bb, ff, asterisk**). While the cartilage of male LPS treated uninjured joints was relatively normal compared to male VEH treated, and sham-injured groups (**Fig. 1A, C**), significant differences were observed in the LPS treated injured joints (**Fig. 1B, D**). The biomechanical destabilization and lateral subluxation of the joint promoted significant erosion of both cartilage and bone on the femoral and tibial posterior side (**Fig. 1B, D)** of the medial compartment of the joint, in all groups, however, there was a clear reduction in the amount of subchondral bone visualized in the LPS-treated femurs relative to VEH-treated femurs (**Fig. 1B, D, F, H asterisks)**. VEH treated injured joints retained significantly more of the articular cartilage integrity throughout the joint while LPS-treated injured joints displayed significant thinning of the femoral articular cartilage (**Fig. 1b, d, f, h arrow, asterisks**). LPS-treated injured joints also displayed significantly hyperplastic synovium (**Fig. 1bb, dd, ff, hh**) indicative of synovitis and elevated inflammation occurring in LPS-treated but not VEH-treated injured joints. The PTOA phenotype was more severe in females than males treated with LPS (**Fig D, H).** Examination of the sagittal views of each joint by a modified OARSI grading scale determined that LPS-treated injured joints had a significantly more severe cartilage loss phenotype than VEH-treated injured joints, independent of sex (**Fig. 1I**). VEH uninjured males and females have significantly lower scores compared to their LPS counterparts, while the LPS uninjured females have higher OARSI scores compared to males. VEH injured males had the lowest OARSI score of all the groups followed by LPS injured males. VEH injured females had a significantly higher OARSI score than the VEH injured males and the LPS injured females. LPS injured females had significantly higher scores than all groups. These results imply that a single systemic inflammatory dose of LPS shortly prior to a non-invasive knee injury is sufficient to induce synovitis in the injured joint and contribute to a more severe PTOA phenotype.

LPS Administration Reduces Subchondral Bone and Osteophyte Volume in Injured Joints

Since several studies have shown that LPS increases bone resorption and decreases bone mass[153,154], we next examined osteoarthritic remodeling in LPS and VHL treated mice by quantifying the gain in osteophyte volume and the loss in subchondral trabecular bone at 6 weeks post injury through the use of micro-computed tomography (μCT) (**Fig. 2**). Consistent with prior results, VEH male injured femurs had significantly less subchondral bone volume by ~4% and ~6.6% when compared to uninjured and contralateral, respectively. VEH females had significantly less subchondral bone with ~3.3% less on injured relative to contralateral. LPS female injured joints had significantly less subchondral bone than the uninjured by ~2.7% and contralateral by ~3.3%; injured LPS males had ~9.3% and ~9.5% significantly less subchondral bone than uninjured and contralateral respectively. In all groups examined the percent loss of subchondral bone volume in females was significantly less than in males (**Fig. 2A**). VEH treated females had ~6.5%, ~5.2%, ~8.4% less subchondral bone than VEH males on the uninjured, injured, and contralateral joints respectively; all were statistically significant. LPS treated females had ~9.28%, ~5.22%, ~9.49% less subchondral bone than VEH males on the uninjured, injured, and contralateral joints respectively; injured and contralateral were statistically significant. However, LPS-treatment promoted a significant loss in subchondral bone volume of injured joints when compared to VEH treated joint, independent of sex. The loss between injured VEH and injured LPS was statistically significant and was ~2.8% in females and ~2.7% in males, respectively (**Fig. 2A**) the LPS-related change between sexes were not statistically significant. This suggests that LPS does not have a more catabolic effect on female joints than on male joints.

Other bone parameters were consistent with a bone loss phenotype in the distal femoral epiphysis of injured groups (**Fig. 2**). Trabecular number was significantly lower in the VEH female injured legs by ~4.2% compared to

contralateral; VEH male injured legs were significantly lower on uninjured and contralateral by ~6.3% and ~6% relative to both (**Fig. 2B**). VEH treated females had ~25.4%, ~22.1%, and ~23.5% lower trabecular number than the males on uninjured, injured, and contralateral; all were statistically significant. LPS treated females had ~24.1%, ~23.6%, and ~25.5% lower trabecular number than the corresponding uninjured, injured, and contralateral males; all were statistically significant. LPS treatment significantly reduced trabecular number on injured females by ~6%; injured LPS males had ~4.2% less trabecular number which was not statistically significant (**Fig. 2B**).

Trabecular thickness was significantly higher on VEH female uninjured compared to VEH injured by ~6.2%; trabecular thickness was significantly higher on VEH male contralateral compared to uninjured and injured by ~9.2% on each. LPS treated injured females had significantly thinner trabeculae compared to uninjured and contralateral by ~9.2% and ~7.8%; LPS treated injured males had significantly thinner trabeculae than the contralateral by ~13.6% (**Fig. 2C**). Female and male comparisons for both treatment groups only showed that VEH uninjured females had significantly higher trabecular thickness than males by ~9.2%, all other comparisons were not statistically significant but are in supplementary table 1 (**Fig. 2C**).

In females, trabecular spacing was significantly larger in VEH injured compared to the contralateral by ~4.5%; male injured had significantly larger trabecular spacing than the male uninjured and contralateral by ~4.6% and ~6.9%. LPS treated injured males had a significantly larger trabecular spacing by ~7.6% (**Fig. 2D**). VEH treated females had ~27.7%, ~23.7%, and ~26.2% significantly larger trabecular spacing than the VEH treated males; LPS treated females had significantly larger trabecular spacing by ~29.4, ~26.2, and ~29.7 than the LPS treated males (**Fig. 2D**). Differences between different treatment groups are listed inn supplementary Table 1 and *p*-values are in supplementary Table 2.

Osteophyte volume was significantly higher in male than in female VEH injured joints by ~22.7% (**Fig. 3**). LPS-administration induced a reduction in the amount of ectopic bone formed by ~21.7% in females and ~19.4% in males; this reduction was statistically significant in females only (**Fig. 3A**). While no significant differences were observed between VEH and LPS treated male joints, the trend was also in the negative direction, and μCT images showed a decrease in the osteophyte volume area in LPS treated males (**Fig. 3B**). These findings suggest that LPS treatment enhances the injury mediated catabolic activity in the subchondral bone resulting in higher subchondral bone loss, but it slightly protects the injured joint from excessive osteophyte formation, and this protection is more dramatic in females.

Cellular Infiltration by Type 1 Macrophages is Elevated in the Meniscus of LPS Treated Groups

Tissue resident macrophages are essential in providing innate immune defenses and regulating tissue and organ homeostasis. Macrophages and other inflammatory cells are recruited to tissue injury sites where they also play key roles in tissue remodeling and repair[155,156]. Macrophages can be both pro-inflammatory (M1) and anti-inflammatory (M2), and the co-action of these subtypes can promote damaged tissue repair through specific cytokine secretion. In the joint however, inactive macrophages reside that will become activated as needed, a change in the M1/M2 ratio may be critical in PTOA progression and outcomes. To determine whether LPS administration prior to ACL rupture altered the composition of M1 and M2 cells in the injured joint we used M1/M2 specific antibody markers to distinguish these subtypes by immunohistochemistry. Histological analysis showed that the anterior tibial condyle presented cellular infiltration on the LPS injured joints (**Fig. 1D, dd**). To determine whether LPS alters the composition of M1 and M2 macrophages in the injured joint we used M1/M2 specific antibody markers to distinguish these subtypes. Immunohistochemical examination with macrophage markers determined that

the increase in cellularity correlated with a larger amount of M1 macrophages present in the LPS injured joints than in the VEH injured joints, indicative of a higher level of inflammation (**Fig. 4bbb**). In contrast, we observed a slight decrease in the abundance of M2 macrophages in LPS relative to VEH injured joints, suggesting that the joints of LPS treated animals lack sufficient anti-inflammatory macrophages. The change in M1/M2 ratio in the joint may influence the repair process and modulate PTOA phenotypes towards a more severe outcome (**Fig. 4L, P**).

Characterizing Early Molecular Changes Associated with PTOA Development on LPS Treated Mice

To identify early molecular changes associated with LPS-modification of PTOA development, we examined gene expression changes in LPS treated injured joints one day post-injury (**Fig 5**). VEH Injured, LPS Sham, and LPS Injured had 429, 590, and 385 up-regulated genes relative to VEH Sham (**Fig 5A**). There were 73 genes associated with inflammation and immune responses significantly up-regulated in the LPS treated samples when compared to the control, VEH Sham. Genes associated with inflammation included transcripts such as toll like receptors 5 and 8 (*tlr5, tlr8*) [157,158(p5)]. We found that genes associated with the innate immune system, specifically monocyte infiltration, like *Ccl6* and *Ccr2* were up-regulated in the LPS treated joints[159–161]. *Cd80*, a gene associated with dendritic cell maturation and activation was also up-regulated in the LPS treated samples[162]. This shows that there is an innate immune response being activated in LPS treated joints when compared to the VEH Sham (**Fig. 5B**).

We found 452, 343, 258 genes down-regulated in VEH Injured, LPS Sham, and LPS Injured compared to VEH Sham. There were 78 down-regulated genes that were exclusive to LPS Injured when compared to every other group (**Fig. 5C**). Several genes associated with bone and cartilage formation like *Col9a1*[163], *Col10a1*[164], and *Chad*[165] were also down-regulated in LPS Injured samples (**Fig. 5D**). Genes whose lack of expression is associated with OA like

Ucma[166], and *Cytl1*[167] were also down-regulated. These early markers of lower cartilage and bone formation could be an indicator of the more severe PTOA phenotype on LPS Injured samples.

Discussion

The effects of LPS-induced systemic inflammation prior to joint injury on the development of PTOA has not been previously examined. This study provides insights into how unresolved systemic inflammation accelerates the progression to PTOA after an ACL injury in mice. We were able to show how a single LPS injection five days prior to injury can cause significant changes to PTOA phenotypes by increasing the amount of cartilage degradation, reducing the subchondral bone volume fraction and trabecular bone microstructure, and reducing osteophyte volume. These effects were significantly greater in the female LPS injured mice than in the corresponding males, although similar trends were seen in both sexes. Immunohistochemistry analysis showed the presence of activated inflammatory macrophages six weeks post-injury, this indicates that the inflammation is not resolved on LPS treated samples.

RNA sequencing data showed that systemic LPS significantly up-regulated the expression of genes associated with inflammation in the joints of uninjured mice. At six days post LPS-injection we 73 of these immune and inflammatory response genes were significantly up-regulated in both injured and uninjured LPS samples when compared to the VEH Uninjured. More striking was the discovery that members of the Toll like receptor (TLR) family of genes were activated in both LPS treated samples and in particular, *Tlr7* and *Tlr*8, two endosomal TLRs have been previously shown to be activated in the synovium and synovial fluid macrophages of rheumatoid arthritis (RA) patients[168,169]. This correlation would indicate that systemic LPS induces mild RA in the joints of uninjured mice (**Fig. 6**), and that this transient RA is sufficient to exacerbate cartilage degeneration in response to a joint injury, potentially through Tlr7 and Tlr8 expressing M1 macrophages (**Fig. 6**). Evidence in support of this correlation

is provided by an OA study in TLR7 deficient mice, where *Tlr7*$^{-/-}$ mice develop a milder form of arthritis compared to control groups in the murine collagen induced arthritis (CIA) model[157]. Furthermore, overexpression of human TLR8 (huTLR8) in mice promoted spontaneous and induced arthritis and the levels of huTLR8 correlated with proinflammatory cytokines in the joints of these animals[157]. These studies highlight the potential role for these endosomal TLRs in the maintenance of inflammation in rheumatoid arthritis. Activation of these TLR7/8 by LPS might have contributed to the enhanced PTOA phenotype observed in LPS treated animals. In healthy individuals, plasma endotoxin levels are less than 0.05 EU/ml, but a study of patients with active urinary tract infections (UTI) showed significantly higher levels of plasma endotoxins. This study concluded that patients with gram-negative bacterial UTIs present symptoms of systemic inflammatory responses due to high levels of plasma endotoxin[170], and would suggests that such individuals may be at significantly higher risk of PTOA, in the event of a joint injury.

While the histological analysis of the injured joints and the RNAseq data both point to the M1 macrophage as the source of the joint inflammation (**Fig. 6**), and our data is backed by publications showing that M1 macrophages express higher mRNA levels of *Tlr7* and *Tlr8* than M2 macrophages[171] while TLR7/TLR8 expression is significantly higher in the macrophages within synovial tissue of RA patients when compared to normal, future studies will have to also survey the contribution of other immune cell types since genes associated with monocyte activation (Ccr2), eosinophils (Ccl6), and neutrophil activation (Cd300ld)[172] were also significantly upregulated in LPS treated joints. While *Ccr2* has also been found to be upregulated in RA, most of the 73 inflammation-associated genes elevated by LPS like *Lst1*[173], *Ptger2*[174,175], *C5aR2*[176], and more[177] have not yet been investigated in the context of osteoarthritis and could represent potential candidates for PTOA research. Also, the fact that the super-healer mice *MRL/MpJ* developed PTOA after LPS-administration highlights that these mice are not resistant from inflammatory-mediated PTOA risks.

In our model system, PTOA develops in response to joint injury in both VEH and LPS treated joints, however, patients receive reconstructive surgery post ACL rupture, and only 50% of these patients develop PTOA. Future experiments will have to address two key questions: (1) Do injured individuals with high plasma endotoxin levels develop PTOA at higher frequency than individuals with normal plasma endotoxin levels? and (2) Do anti-inflammatory drugs administered immediately post joint injury lower the risk of developing PTOA? Furthermore, genes associated with bone and cartilage metabolism were significantly down-regulated in LPS injured samples relative to all other groups, suggesting that LPS+injury may have a significant bone and cartilage catabolic effect. These genes included *Comp*[178] noncollagenous extracellular matrix encoding gene; *Hapln1*[179]*, Chad, Col9a1,* and *Col10a1,* which encode cartilage matrix proteins; and *Cnmd* which promotes chondrocyte growth[180,181]. LPS alone kept the inflammatory pathways elevated while the addition of injury inhibited both bone and cartilage formation, influencing skeletal metabolism.

Our study uniquely examined how unresolved inflammation affects PTOA progression in a noninvasive ACL rupture models in mice. This noninvasive model closely mimics human ACL rupture from a single high impact event that leads to PTOA development. While we recognize that patients receive reconstructive surgery and that our model remains unstabilized throughout, the ability to track molecular and morphological changes in the joint during PTOA progression will capture unknown events that cannot be perceived in humans since most patient samples are from individuals at advanced stages of the disease. The findings that a pre-existing systemic inflammation state produces RA-like molecular phenotypes in the uninjured joint and accelerates the progression to PTOA following injury may guide future clinical risk assessments of patients. Most striking is the revelation that unresolved inflammation in individuals with a mild autoimmune disease or suffering from a gram-negative mediated infection such as UTI at the time of injury may be at significantly higher

risk of developing severe PTOA phenotypes. In future experiments, this model will allow us to study whether blocking immune-derived molecules like Tlr7 and Tlr8 immediately post injury would prevent unwarranted PTOA phenotypes such as cartilage degeneration.

Figures

Figure 1 Histological Assessment of LPS Treated Tibial Compression Injured Joints

(A-H) Histological assessment of contralateral and injured joints 6 weeks post-injury at 16 weeks of age using Safranin-O and Fast-Green staining. Joints were identified by sex, injured or contralateral, and treatment [VEH (vehicle); LPS (intraperitoneal lipopolysaccharide injection). Images were taken in 5x magnification and 20x magnification. **(I)** OARSI scoring for histological samples separated by treatment (VEH or LPS). *p<0.05

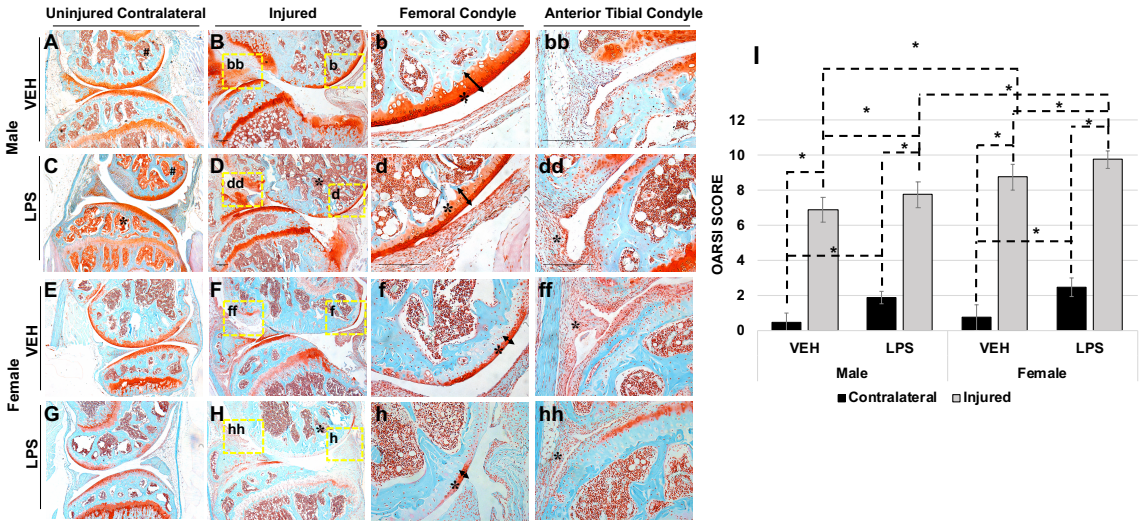

Figure 2 Bone Microstructure Assessment Using Micro-CT

(A) Subchondral bone volume is the bone volume fraction which is the ratio of the segmented bone volume to the total volume of the region of interest. **(B)** Trabecular number was measured using the average number of trabeculae per unit length. **(C)** Trabecular thickness was measured using the mean thickness of trabeculae, assessed using direct 3D methods. **(D)** Trabecular spacing was measured using the mean distance between trabeculae, assessed using direct 3D methods[141]. Statistics were performed using two-way ANOVA and Student's T-Test. *p<0.01

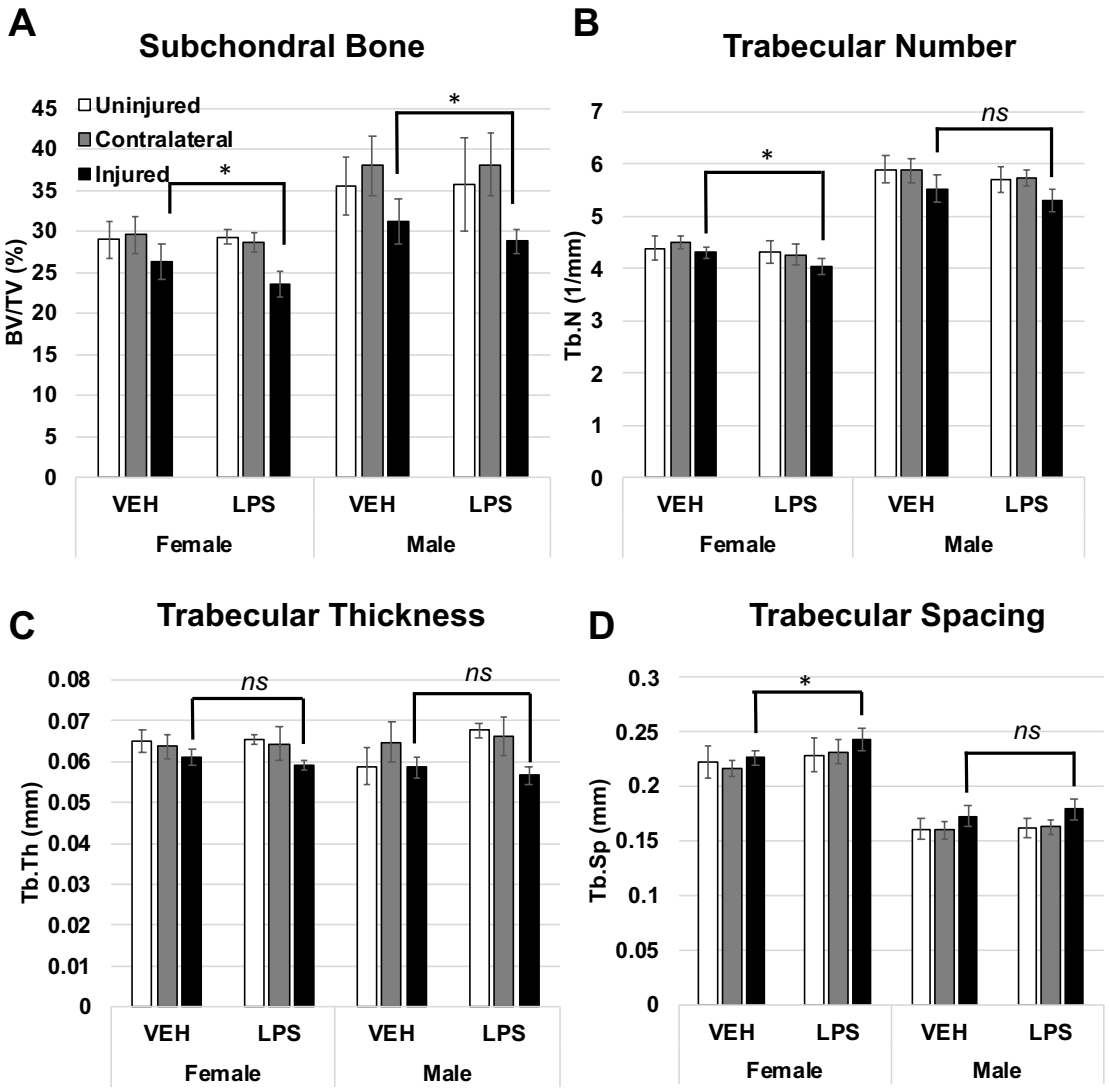

Figure 3 Osteophyte Representation Using Micro-Computed Tomography **(A)** Osteophyte volume was measured by quantification of ectopic bone around the injured joint compared to contralateral. All statistics were made using sex, injury type, and treatment [VEH (vehicle); LPS (intraperitoneal lipopolysaccharide injection)] using two-way ANOVA and Student's T-Test. *p<0.05 **(B)** Micro-Computed tomography image of the joints of all groups using data gathered during **(A)**. Dark grey regions show osteophyte growth compared to the white. Contralateral shows the normal bone.

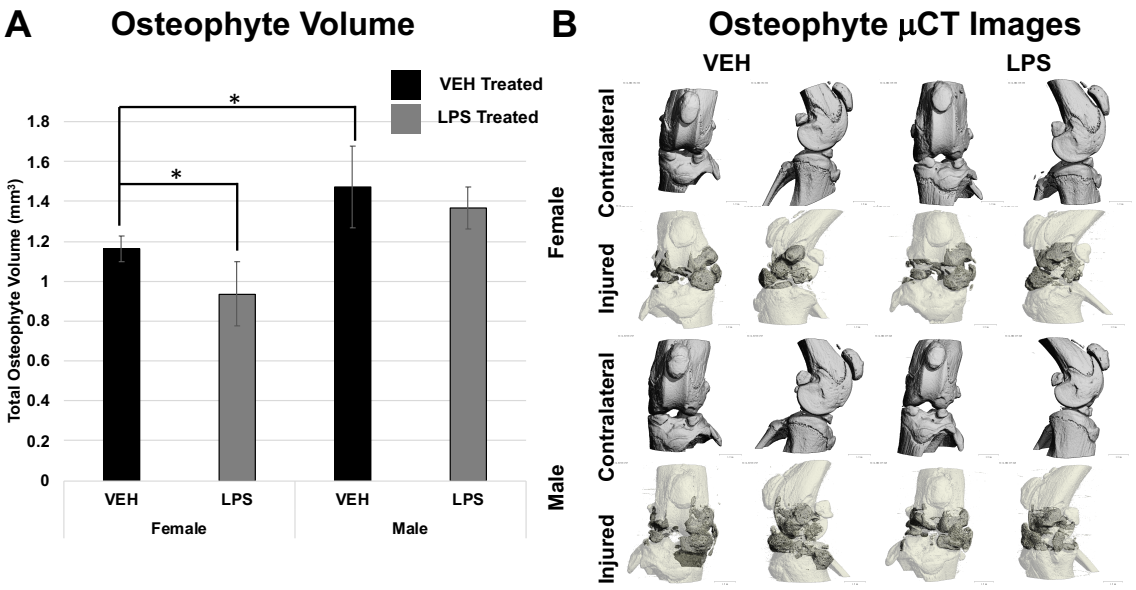

Figure 4 Fluorescent Immunohistochemistry Analysis of Injured Joints 6 Weeks Post-Injury

(A-B) Fluorescent immunohistochemistry (IHC) of macrophage type 1 markers F4/80 and iNOS. **(C-D)** Fluorescent IHC of macrophage type 2 markers F4/80 and CD205. Dashed line in white represents the surface of the anterior tibial condyle for all images.

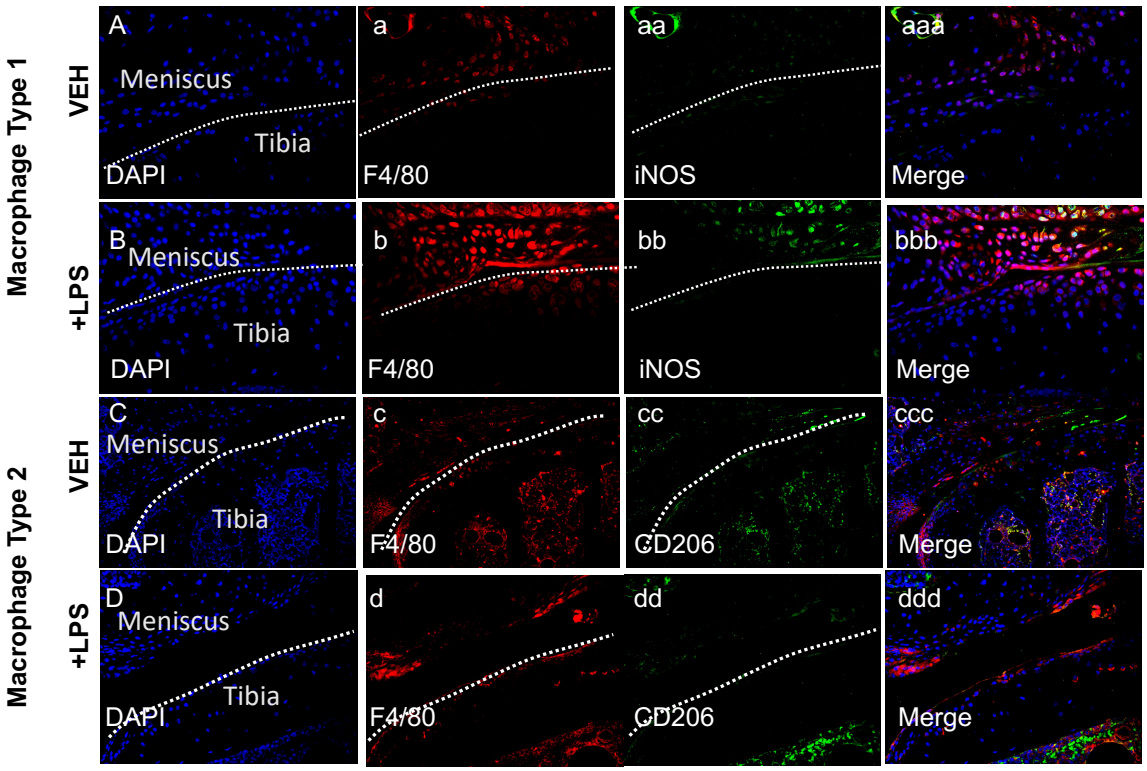

Figure 5 Gene Expression Changes Caused by LPS and Injury 24 hours Post-Injury

(A) Overlap of genes up-regulated by LPS. **(B)** Immune/inflammatory response genes up-regulated in response to LPS treatment. **(C)** Overlap of genes down-regulated by LPS treatment and injury. **(D)** Bone and cartilage formation genes down-regulated in response to LPS treatment and injury.

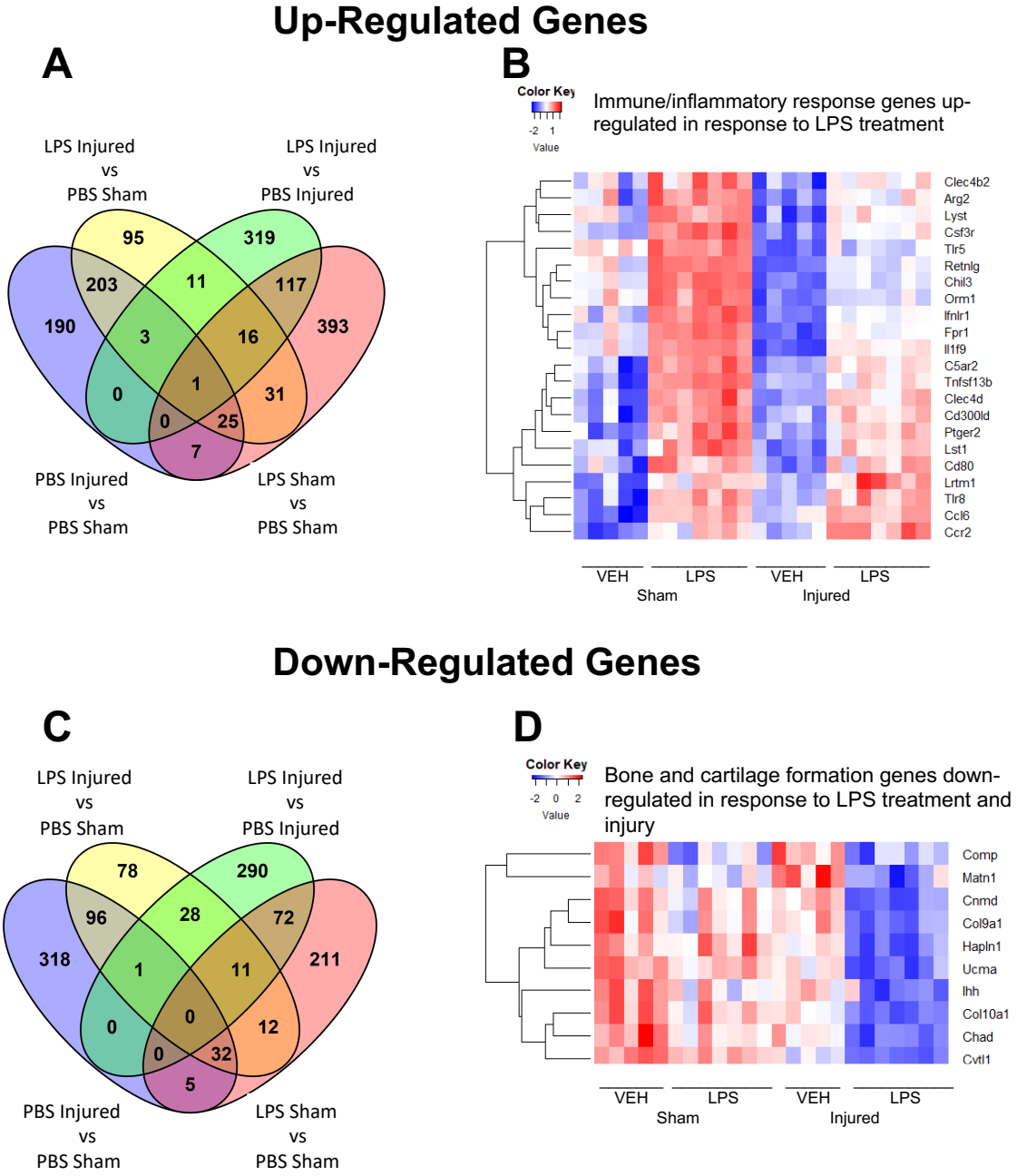

Figure 6 LPS Enhances the Vulnerability to PTOA Development

Healthy individuals exposed to systemic inflammation, like LPS, will develop symptoms similar to those of rheumatoid arthritis patients. In the joint it will cause synovitis which has an increase of macrophages type 1, eosinophils, neutrophils, and inflammatory cytokines and chemokines. If an injury happens at the time of elevated systemic inflammation will increase vulnerability and accelerate the development of PTOA.

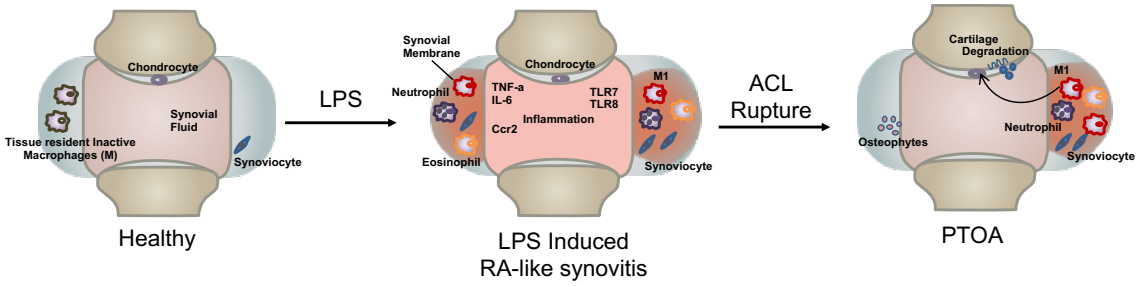

Healthy

LPS Induced RA-like synovitis

PTOA

Chapter 4: Antibiotic Treatment Prior to Injury Exacerbate the Development of Post-Traumatic Osteoarthritis on *C57Bl/6J* Mice

Introduction

The individual microbial cells that constitute the human gut microbiome outnumber our cells by a factor of 10. Most babies within the womb are free of microorganisms[182]. First exposure babies have to microbes is during birth as they move through the birth canal, hence babies born in natural birth are inoculated with some microorganisms by the mom. The gut microbiome initiates with breast feeding and builds complexity as the baby's diet evolves from milk to other types of foods[183]. It reaches dynamic stability by the age of 3, and while a person's gut biome is relatively stable, there are many genetic and environmental factors that influence its composition, in each person[184]. The microorganisms living in our gut that do not cause harm for humans are called commensals. The gut microbiome can have disruptions that change its composition and with that affect the entire system[171,185,186].

Published literature suggests that the gut microbiome has an indirect effect on bone through changes to the immune system and inflammatory cytokines[102,187]. Commensals aid in immunoregulation by releasing microbial associated molecules patterns that bind and activate toll-like receptors[103,188–190]. This activation cause an inflammatory cascade that releases inflammatory cytokines and interferons that act as transcription factors that induce naïve immune cells to mature[191–193]. The lack of a gut microbiome has led to conflicting results on bone mass but modifications to the gut microbiome can improve the PTOA phenotype on obese mice[122,194]. Studies have suggested that dysbiosis can promote aggressive bone destruction mediated by osteoclasts due to the increase of tumor necrosis factor alpha (TNF-α). TNF-α promotes osteoclastogenesis by increasing RANK-L expression in marrow cells and with that the number of osteoclast precursors[110,195–197].

In the context of arthritis *Zhang et al.* (2015) showed that patients suffering from rheumatoid arthritis (RA) had have a perturbed gut microbiome that returned to levels compared to healthy people, after RA treatment, suggesting a strong correlation between gut microbiome composition and RA symptoms[131,198]. *Maeda et al* (2017) proposed that there is an increased presence of *Prevotella copri* species in early RA cases, while the abundance of *Prevotella histicola* species suppressed the development of arthritis; this study showed a correlative link between some species of the gut microbiome and arthritis[133]. In addition, *Wu et al* (2016) suggested that treating dysbiosis could help improve the outcome of rheumatoid arthritis patients[132]. Although PTOA is not considered an inflammatory disease, it is associated with an elevation of inflammatory pathways, therefore it can be better understood by looking at factors like inflammation and immunoregulation. Recently the gut microbiome was modified in obese mice by adding oligofructose supplementation showed a decrease in the OA outcome by reducing the levels of inflammation on the colon, circulating in the serum, and on the knee[122]. However no study to date has examined how the gut microbiome through antibiotic treatment affects PTOA outcome.

Most PTOA related studies to date, examined factors likely to increase the probability of developing PTOA, if administer at the time of injury or shortly thereafter[55]. This study looked at how antibiotic treatment administered prior to injury would influence the outcomes of PTOA. Studying the effects of medication administered before an injury is of high biomedical importance, because clinically, most concerns center on side-effects due to co-administration, and no account of gut biome dysbiosis is recoded in a clinical setting to determine correlations with PTOA outcomes. In addition, antibiotics are widely prescribed to teens who may be active in sports. According to the CDC, in 2016, 64.9 million oral antibiotic prescriptions were issued to people under the age of 20, the equivalent of 790 per 1000 people, therefore gut dysbiosis may be more common than expected, in young athletes suffering a knee injury[137]. As the population of the USA ages there will be an increase in PTOA cases, studying how antibiotics

could modify the PTOA phenotypes will be helpful to find preventative treatment in the future, in both young and old patients.

Materials and Methods

Experimental Animals and ACL Injury Model. C57Bl/6J mice were purchased (Jackson Laboratory, Bar Harbor, ME, USA; Stock No: 000664) at 4 weeks of age and kept under normal cage conditions. Cohorts of mice (N=10 per group) were separated into two groups for both male and female. The antibiotic treated group (AB) received treatment [ampicillin[199,200] (1.0g/L); neomycin[201,202,203] (0.5g/L)] in drinking water starting at weaning (4 weeks of age) for six weeks; the untreated group (VEH) was left with regular drinking water. At 10 weeks of age, both groups received a non-invasive single dynamic tibial compressive load for an ACL rupture using an electromagnetic material testing machine (ElectroForce32000, TA Instruments, New Castle, DE, USA) as previously described. All animal work was conducted in accordance to the Institutional Animal Care and Use Committees at Lawrence Livermore National Laboratory and the University of California, Davis in AAALAC-accredited facilities.

Micro-Computed Tomography. Samples were collected 6-weeks post injury for female and male VEH and AB injured, contralateral, and uninjured joints. Samples were dissected and fixed for 72 hours in a 4^{o}C using 10% neutral buffer formalin. Samples were stored in 70% EtOH at 4^{o}C until scanned. Whole knees were scanned using a SCANO μCT 35 (Bassersdorf, Switzerland) according to the rodent bone structure analysis guidelines (X-ray tube potential = 55kVp, intensity = 114 μA, 10 μm isotropic nominal voxel size, integration time = 900 ms). Trabecular bone in the distal femoral epiphysis was analyzed manually drawing contours on 2D transverse slides. The distal femoral epiphysis was designated as the region of trabecular bone enclosed by the growth plate and subchondral cortical bone plate. We quantified trabecular bone volume per total

volume (BV/TV), trabecular thickness (Tb.Th), trabecular number (Tb.N), and trabecular spacing (Tb.Sp). Osteophyte volume in injured and contralateral joints was quantified by drawing contours around all heterotopic mineralized tissue attached to the distal femur and proximal tibia as well as the whole fabellae, menisci, and patella. Total mineralized osteophyte volume was then determined as the volumetric difference in mineralized tissue between injured and uninjured joints. Statistical analysis was performed using two-way ANOVA and Student's T-test with a two-tailed distribution, with two-sample equal variance (homoscedastic test). For all tests, $p<0.01$ was considered statistically significant after Bonferoni correction.

Histological Assessment of Articular Cartilage and Joint Degeneration. VEH and AB treated *C57Bl/6J*, injured, contralateral and uninjured joints were dissected 6 weeks post injury, free of soft tissue, fixed, dehydrated, paraffin embedded and sectioned as previously described[82] . The cartilage was visualized in sagittal 6μm paraffin serial using Safranin-O (0.1%, Sigma; S8884) and Fast Green (0.05%, Sigma; F7252) as previously described[144]. OA severity was evaluated 6 weeks post injury on sagittal sections using a modified osteoarthritis research society international (OARSI) scoring scale as previously described[145]. Starting from the synovium membrane to the articular cartilage, for each region, cartilage scoring began ~0.4 mm out from the start of synovium. Blinded slides were evaluated by seven scientists (six with and one without expertise in OA) utilizing a modified (sagittal) OARSI scoring parameters due to the severity of the phenotype due to TC loading. Modified scoring scores (0) for intact cartilage staining with strong red staining on the femoral condyle and tibia, (1) minor fibrillation without cartilage loss, (2) clefts below the superficial zone, (3) cartilage thinning on the femoral condyle and tibia, (4) lack of staining on the femoral condyle and tibia, (5) staining present on 90% of the entire femoral condyle with tibial resorption, (6) staining present on over 80% of the femoral condyle with tibial resorption, (7) staining present on 75% of the femoral condyle

with tibial resorption, (8) staining present on over 50% of the femora condyle with tibial resorption, (9), staining present in 25% of the femoral condyle with tibial resorption, (10) staining present in less than 10% of the femoral condyle with tibial resorption.

Immunofluorescent Staining. Six-micrometer sections from injured samples from both treatment groups were used. Unitrieve was used as an antigen retrieval method for 30 minutes at 65^{o}. Primary antibodies: Anti-F4/80 [Abcam, ab16911(1:50)], Anti-CD206 [Abcam, ab64693(1:500)], and Anti-iNOS [Abcam, ab15323(1:100)] were used and incubated overnight at room temperature in a dark humid chamber as previously described[86]. Negative control slides were incubated with secondary antibody-only. Stained slides were mounted with Prolong Gold with DAPI (Molecular Probes, Eugene, OR, USA). ImagePro Plus V7.0 Software and a QIClick CCD camera (QImaging, Surrey, BC, Canada) were used for imaging and photo editing.

Results

Antibiotic treatment prior to joint injury improves PTOA outcomes

Using a tibial compression PTOA mouse model[77], we examined whether a six weeks course of antibiotic would impact OA outcomes, post injury. *C57Bl/6J* male mice were examined histologically at 6 weeks post injury. Examining the contralateral femoral head (**Fig. 1A, C; numeral**) we observed that the VEH contralateral group displayed a slight reduction in staining while the AB contralateral group showed stronger staining throughout; this is was not statistically significant, and both groups had normal joint morphology. The injured AB treated group showed slightly less mineralized area on the femoral head when compared to the VEH injured group (**Fig. 1B, D**). The femoral condyle of the injured AB group (**Fig. 1d; arrow, asterisk**) appeared to have an increase in staining intensity as well as a thicker articular cartilage layer than the injured VEH

which suggest higher levels of proteoglycans and reduced chondrocyte apoptosis in the injured joints of AB treated animals (**Fig. 1b; arrow, asterisk**). Analyzing the meniscus (**Fig. 1bb, dd; arrow, asterisk**) injured AB joints showed a thicker hyperplastic tissue with enhanced cellular infiltration. The injured VEH showed cellular infiltration but it was less than the AB injured group. Examination of the sagittal views of the joints by a modified OARSI grading scale determined that AB-treated injured joints had a significantly lower cartilage score than VEH-treated injured joints (**Fig. 1E**). These results imply that modifying the gut microbiome using antibiotics prior to injury is sufficient to improve the cartilage phenotype subsequent to trauma.

Evaluating the Subchondral and Osteophyte Changes During the Progression to PTOA Development on Antibiotic Treated C57Bl/6J Male and Female Mice

The bone phenotypes of AB and VEH treated mice were characterized by micro-computed tomography (μCT) to quantify osteophyte volume and subchondral trabecular bone mass at 6 weeks post injury (**Fig. 2**). Consistent with prior results, VEH females had significantly less subchondral bone volume (BV/TV) female AB cohort showed ~7%, ~12.7%, and ~6.2% lower BV/TV than female VEH uninjured, injured, and contralateral; injured was statistically significant. Male AB group had ~0.2%, ~9.4%, and ~10.8% lower BV/TV than the male VEH group when comparing the uninjured, injured, and contralateral groups; injured and contralateral groups were statistically significant. Female AB had ~11.9, ~19.4, and ~17.8% less BV/TV than the male AB uninjured, injured, and contralateral; injured and contralateral were statistically significant. Since female BV/TV baseline was significantly lower than males, these differences are significantly more dramatic in females than in males.

Trabecular number (Tb.N) AB females had ~1.2%, ~5, and ~0.8% lower Tb.N than the uninjured, injured, and contralateral VEH female; . AB male group had ~0.2% and ~0.1% higher Tb.N on the uninjured and injured groups

compared to VEH; the contralateral had ~0.8% lower Tb.N on the VEH. AB females had ~24.7%, ~26%, and ~23.5% lower Tb.N than the uninjured, injured, and contralateral; injured and contralateral were statistically significant.

Trabecular thickness (Tb.Th) showed VEH female presented ~9.2, ~3.3, and ~1.5% more Tb.Th than VEH males in uninjured, injured, and contralateral; only uninjured was significant. (**Fig. 2C**). VEH females had ~5.2%, ~2.6%, and ~3.8% higher Tb.Th than the uninjured, injured, and contralateral AB females; none were significant. VEH males had ~2.9%, ~7.6%, and ~10.6 higher Tb.Th than uninjured, injured, and contralateral AB males; injured and contralateral were significant. AB females had ~11.5%, ~10.2%, and ~6.1% lower Tb.Th than the AB males; injured group was statistically significant.

When examining trabecular spacing (Tb.Sp) we observed VEH treated females had ~27.7%, ~23.7%, and ~26.2% significantly larger trabecular spacing than the VEH treated males. AB females had ~1.2%, ~6%, and ~1.5% larger Tb.Sp than the uninjured, injured, and contralateral VEH females; none were statistically significant. AB males showed ~1%, ~0.01%, and ~2.2% larger Tb.Sp than the VEH uninjured, injured, and contralateral; none were statistically significant. AB female had ~27.5%, ~28.2%, and ~25.7% higher Tb.Sp than the uninjured, injured, and contralateral AB males; injured and contralateral were both significant.

Osteophyte volume (Op.V) analysis represents the quantity of bone growth outside of the injured joint when compared to the uninjured contralateral. VEH females had ~26% lower Op.V than VEH males which was statistically significant. VEH females had ~5.8% higher Op.V than the AB females which was not significant. AB females had ~13.5% higher Op.V than AB males which was not significant. VEH males had ~39.7% significantly higher Op.V compared to the AB males.

Macrophage Analysis of Antibiotic Treated Mice

As previously described in chapter 3, tissue resident macrophages are essential in providing innate immune defenses and regulating tissue and organ homeostasis[204]. Macrophages and other inflammatory cells are recruited to tissue injury sites where they also play key roles in tissue remodeling and repair[155,156]. In the joint there is a population of inactive macrophages residing in the synovium. These cells are activated under certain conditions such as injury or inflammation. Macrophages can be both pro-inflammatory (M1) and anti-inflammatory (M2), and the co-action of these subtypes can repair damaged tissue through specific cytokine secretion. In the joint however, a change in the M1/M2 ratio may be critical in PTOA progression and development. Data indicated a hyperplastic synovium that appeared to have cellular infiltration on histological analysis (**Fig. 1dd; asterisk**), and this morphology was similar to that of LPS treated injured joints described in prior chapter. To determine whether AB treatment prior to ACL rupture altered the composition of M1 and M2 cells in the injured joint we used M1/M2 specific antibody markers to distinguish these subtypes by immunohistochemistry. On the meniscus we observed a slightly higher staining of anti iNOS antibody indicative of low level M1 macrophage infiltration the AB injured joints compared to the VEH(**Fig. 4D, H**). In contrast, we observed a higher level of anti CD206 antibody stain in AB injured joints when compared to VEH injured, indicative to higher levels of M2 macrophages present in the injured joint of AB treated animals. These results suggest that AB treated animals have an increase in anti-inflammatory macrophages which may be helping the PTOA phenotype. While morphologically LPS and AB treated injured joint looked highly similar, the source of the cellular infiltration was reversed with more M1 in LPS (**Chapter 3 Fig 4**) and more M2 macrophages in AB treated injure joints(**Fig. 4L, P**).

Discussion

The role of antibiotic treatment prior to injury on the development of PTOA has not been previously investigated. Previous such studies have focuses on bone,

showing how the gut microbiome can influence osteoclastogenesis and with that affect bone volume, but no study has looked at how antibiotics affect the development of PTOA. Although data indicated cellular infiltration in the synovium of injured AB joints, reminiscent of synovitis induced by LPS administration, AB treatment improved the cartilage phenotype as reflected by a significantly lower OARSI score in AB injured joints. A limiting factor of this experiment is the lack of female histological samples, a future direction will be to add histological analysis of females in order to understand the female cartilage phenotype.

The male cartilage phenotype improves on the AB treated group however, data indicated a decrease in the subchondral bone phenotype. AB injured joints male and female had a significant decrease in BV/TV compared to the VEH injured male and female joints respectively. The lower BV/TV indicates higher levels of femoral epiphysis bone resorption. The current literature presents conflicting evidence on how antibiotics affect bone, and these discrepancies may be highly dependent on both the diversity and abundance of microbial species that persist after antibiotic treatment[101]. Literature has shown that long-term antibiotic treatment in males at 20 weeks of age have been found to have no changes on the bone mineral density (BMD) with antibiotic treatment while females of the same age displayed BMD increases[127]. Studies with long-term antibiotic treatment at early time timepoints showed an increase in BMD at 7 weeks of age while no significant changes were observed at 11 weeks of age[136]. While a composite put in to repair fracture with antibiotics during infection promotes bone formation[205]. The decrease in BV/TV has been observed after injury in strains that are resistant to PTOA, like *MRL/MpJs* that were discussed in chapter 2. Although inflammation is resolved quicker in *MRL/MpJ* mice resorption still happens due to the presence of pro-inflammatory cytokine and slight presence of matrix metalloproteinase (MMP) that promote osteoclastogenesis and extracellular matrix degradation[206–208].

This study does not include gene expression analysis data that could be useful in determining the changes that happen during the immediate and acute phases after injury. RNA sequencing analysis could determine if the decrease in resorption of cartilage on AB *C57Bl/6J* joints like the *MRL/MpJ* are able to resolve inflammation quicker than the VEH and have the presence of MMP repressors. Future studies will include RNA sequencing analysis a day post-injury to analyze how gene expression changes might be affecting the PTOA outcome.

Future studies will perform microbiome sequencing analysis in order to determine the exact changes caused by our antibiotic treatment. The combination of ampicillin and neomycin was not intended to erase the gut microbiome completely but to modify it and cause little changes to the mouse development given that those antibiotics are poorly absorbed by the body. The changes in the gut microbiome could point at the decrease in resorption. They could answer if the cartilage resorption decrease could be caused by changes to the immune system due to a lack of naïve immune cell activation by the gut microbiome.

Our study uniquely looks at PTOA development changes caused by long-term antibiotic treatment. Prior to this study we did not know if there were any changes caused by antibiotics to PTOA. This study highlights the importance of how the body works as a system and factors prior to injury can lead to changes in the development of PTOA. This study provides a direction for studying how to delay and prevent the development of PTOA by targeting the gut microbiome.

Tables

Table 1 Bone Analysis Percentage Comparison

Results from statistical analysis comparing groups by sex, injury type, and mice strains. Percentages were established by comparing the larger to the smaller of the values. Statistical significance was established when $p < 0.05$.

Comparison	BV/TV (%)	Tb.N (%)	Tb.Th (%)	Tb.Sp (%)
VEH Female C57Bl/6J Injured to VEH Female C57Bl/6J Contralate	3.3	4.2	4.7	4.5
VEH Female C57Bl/6J Injured to VEH Female C57Bl/6J Uninjured	2.7	2.0	6.2	1.8
VEH Male C57Bl/6J Injured to VEH Male C57Bl/6J Contralateral	6.6	6.0	9.2	7.6
VEH Male C57Bl/6J Injured to VEH Male C57Bl/6J Uninjured	4.0	6.3	0.6	6.9
VEH Uninjured C57Bl/6J Female to Male	6.5	25.4	9.2	27.7
VEH Injured C57Bl/6J Female to Male	5.2	22.1	3.3	23.7
VEH Contralateral C57Bl/6J Femalel to Male	8.4	23.5	1.5	26.2
AB Female C57Bl/6 Uninjured AB to C57Bl/6J Injured	26.4	8.0	13.3	8.8
AB Female C57Bl/6 Contralateral AB to C57Bl/6J Injured	17.6	8.2	8.5	8.8
AB Male AB Injured to AB Uninjured	7.1	6.4	0.5	7.5
AB Male AB Injured to AB Contralateral	5.4	5.1	9.4	5.1
Female VEH Uninjured to AB Uninjured	7.0	1.2	5.2	1.2
Female VEH Injured to AB Injured	12.7	5.0	2.6	6.0
Female VEH Contralteral to AB Contralateral	6.2	0.8	3.8	1.5
Male VEH Uninjured to AB Uninjured	0.1	0.2	2.9	1.0
Male VEH Injured to AB Injured	3.0	0.1	7.6	0.01
Male VEH Contralteral to AB Contralateral	4.1	0.8	10.6	2.2
AB Uninjured C57Bl/6J Female to Male	11.9	24.7	11.5	27.5
AB Injured C57Bl/6J Female to Male	19.4	26.0	10.2	28.2
AB Contralateral C57Bl/6J Femalel to Male	17.8	23.5	6.1	25.7

Figures

Figure 1 Histological Assessment of PTOA Severity Depending on Treatment Post-Tibial Compression Injured Joints

(A-H) Histological assessment of contralateral and injured joints 6 weeks post-injury at 16 weeks of age using Safranin-O and Fast-Green staining. Joints were identified by sex, injured or contralateral, and treatment [ampicillin (1000mg. Images were taken in 5x magnification and 20x magnification. **(I)** OARSI scoring for histological samples separated by strain. *p<0.05

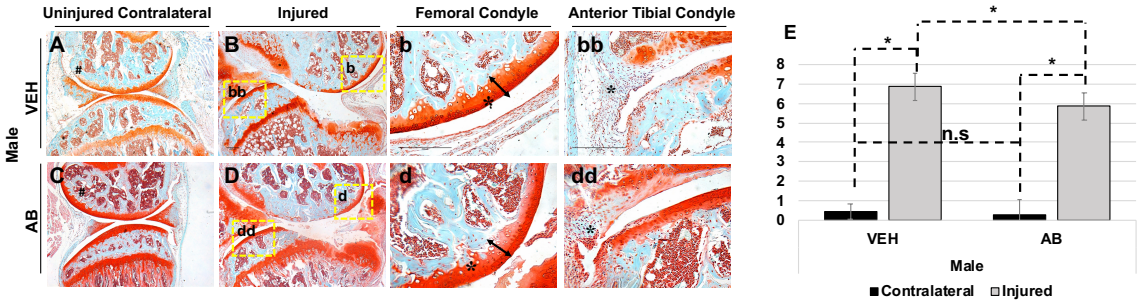

Figure 2 Bone Microstructure Assessment Using Micro-Computed Tomography of Multiple Strains

(A) Subchondral bone is the bone volume fraction which is the ratio of the segmented bone volume to the total volume of the region of interest. **(B)** Trabecular number was measured using the average number of trabeculae per unit length. **(C)** Trabecular thickness was measured using the mean thickness of trabeculae, assessed using direct 3D methods. **(D)** Trabecular spacing was measured using the mean distance between trabeculae, assessed using direct 3D methods (PMID 20533309). All statistics were made using sex, injury type, and strain using two-way ANOVA and Student's T-Test. *p<0.05

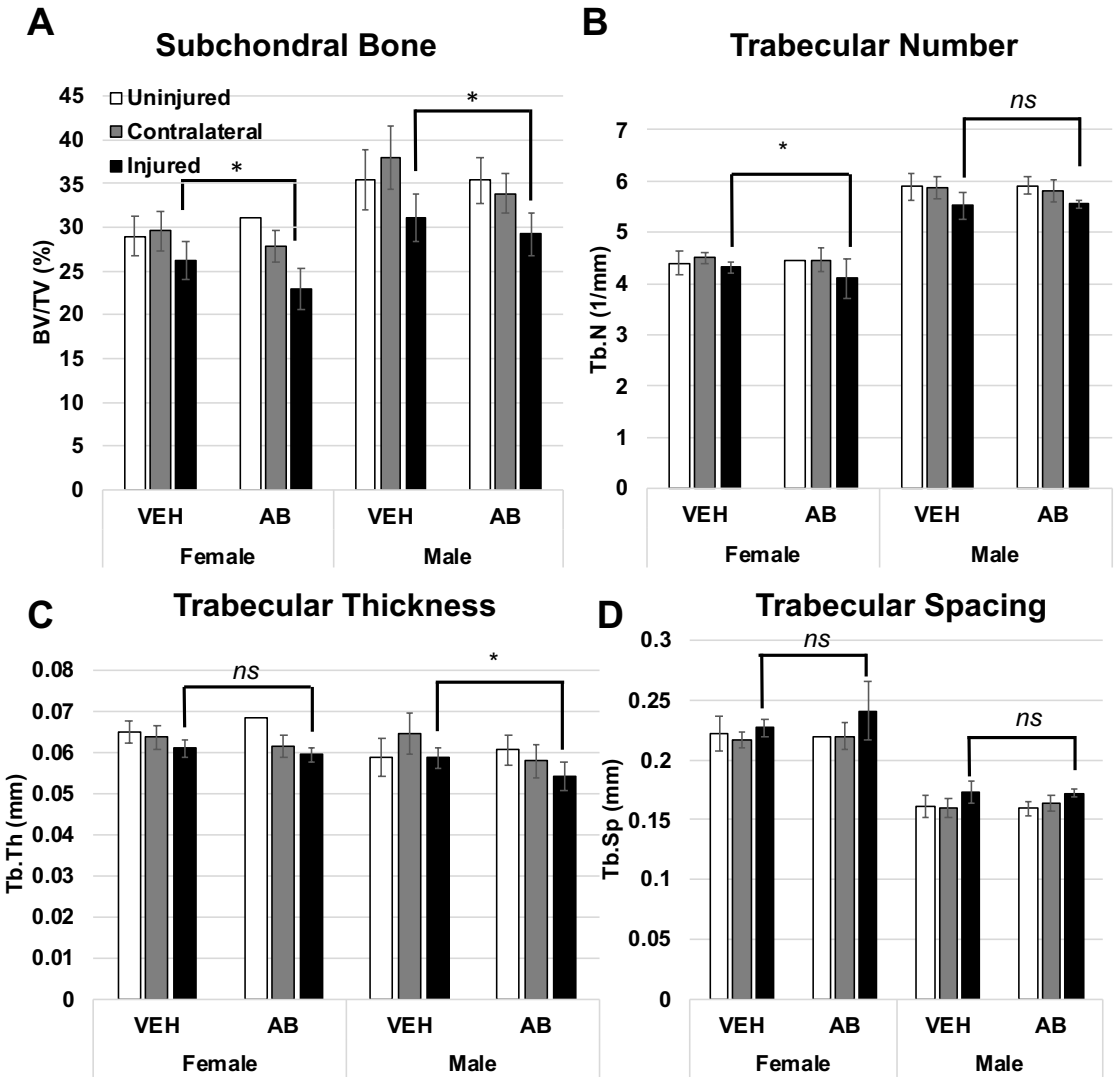

Figure 3 Osteophyte Representation Using Micro-Computed Tomography
(A) Osteophyte volume was measured by quantification of ectopic bone around the injured joint compared to contralateral. All statistics were made using sex, injury type, and treatment using two-way ANOVA and Student's T-Test. *p<0.05
(B) Micro-Computed tomorgraphy image of the joints of all groups using data gathered during **(A)**. Dark grey regions show osteophyte growth compared to the white. Contralateral shows the normal bone.

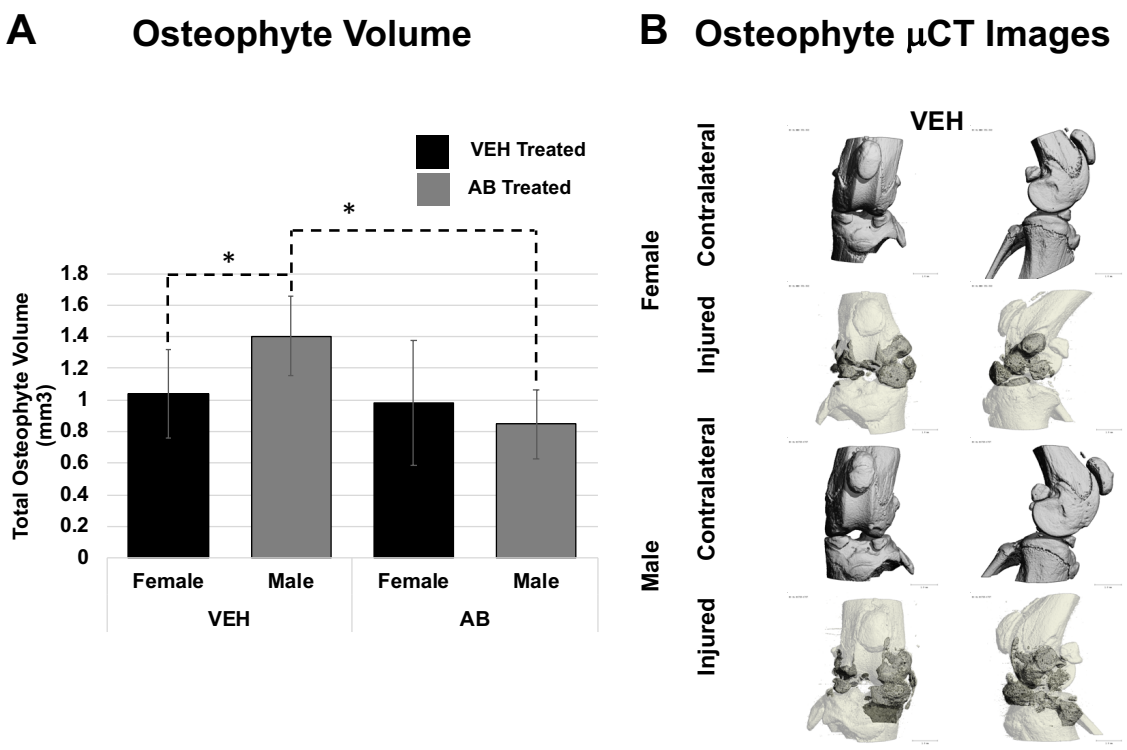

Figure 4 Fluorescent Immunohistochemistry Analysis of Injured Joints 6 Weeks Post-Injury

(A-B) Fluorescent immunohistochemistry (IHC) of macrophage type 1 markers F4/80 and iNOS. **(C-D)** Fluorescent IHC of macrophage tye 2 markers F4/80 and CD205. Dashed line in white represents the surface of the anterior tibial condyle for all images.

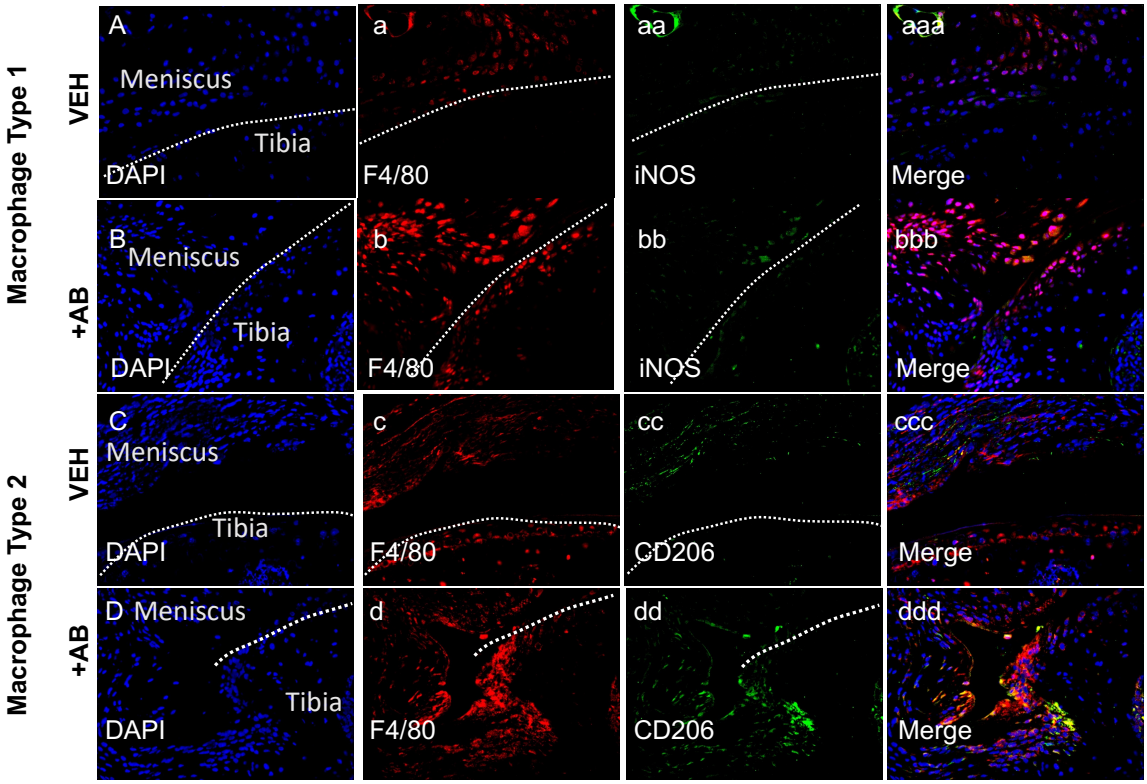

Chapter 5: LPS Induced Inflammation and Antibiotic Treatment Prior to Injury Modify the Development of Post-Traumatic Osteoarthritis on *C57Bl/6J, MRL/MpJ*, and *STR/ort* Mice

Introduction

Inflammatory diseases, genetics, repeated injury, and bone volume affect the susceptibility of inbred strains to post-traumatic osteoarthritis (PTOA). *C57Bl/6J* male mice have been previously shown to be susceptible to PTOA and their phenotypes are considered moderate, therefore we use this strain as our baseline for the disease progression to reference the other stains to. Murphy Roths Large (*MRL/MpJ)* male mice have been previously shown to be resistant to PTOA on the tibial plateau fracture[88], destabilization of the medial meniscus[90], and tibial compression overload[86] due to their ability to resolve inflammation faster than male *C57Bl/6J* post-injury and their ability to repair damaged cartilage; these two factors are likely to contribute to *MRL/MpJ*'s perceived resistance to PTOA. *C3H/HeJ* mice have a higher bone mass than *C57Bl/6J* strain, and carry a defect in the toll-like receptor 4 (TLR4) which makes them insensitive to activation by the gram-negative released LPS endotoxin[94–96]. *STR/ort* male mice have a higher bone mass than the *C57Bl/6J* strain, to develop OA spontaneously due to elevated levels of circulating pro-inflammatory cytokines and chemokines. Additionally, *STR/ort* mice have altered articular cartilage chondrocytes with lower succinate dehydrogenase and lactate activities, with changes in the monoamine oxidase on the articular cartilage that later presents OA[89].

People are constantly exposed to factors that could potentially affect the probability of developing PTOA post injury, and antibiotic use could be such a factor. The CDC reported that there were 793 prescriptions dispensed per 1000 people in the United States in 2017; the prevalence of antibiotics could significantly influence OA outcomes, following joint trauma[137]. With the direction

of more leniency to FDA regulations there have been reported more cases of gram-negative bacteria infections. Understanding how these factors are going to be modifying the PTOA development is key in order to treat the growing prevalence of the disease. No study to date has examined the impact of antibiotic administration and how it may affect the predisposition to PTOA. PTOA develops in ~50% of patients who suffer a severe articular injury, understanding factors influencing PTOA outcomes like genetic predisposition and inflammatory diseases, and developing strategies to improve the phenotype of pre-disposed strains will help identify new avenues for treating the disease.

Materials and Methods

Experimental Animals and ACL Injury Model. *STR/ort* and *MRL/MpJ* strains were bred in house. *C57Bl/6J* and *C3H/HeJ* mice were purchased (Jackson Laboratory, Bar Harbor, ME, USA; Stock No: 000664, 000659). At 4 weeks of age mice were allocated to four treatment groups: control (VEH), lipopolysaccharide treated (LPS), antibiotic treatment (AB), and antibiotic plus LPS treatment (AB+LPS). Cohorts of mice (n=4 for female *STR/ort* and *MRL/MpJ*, n=5 male *STR/ort*, male *MRL/MpJ*, and female *C3H/HeJ*, n=10 male *C3H/HeJ*, male *C57Bl/6J*, and female *C57Bl/6J* per group) included male and female groups. AB and AB+LPS groups received an antibiotic cocktail [ampicillin (1.0g/L); neomycin (0.5g/L)] in drinking water starting at weaning (4 weeks of age) while VEH and LPS groups received regular drinking water for six weeks. Five days prior to injury, LPS and AB+LPS groups received an LPS intraperitoneal injection (1mg/kg) in the abdominal area, while VEH and AB received a saline IP injection of equivalent volume. At 10 weeks of age, 50% of animals from all groups received a non-invasive single dynamic tibial compressive load for an ACL rupture using an electromagnetic material testing machine (ElectroForce32000, TA Instruments, New Castle, DE, USA) as previously described[76,82,86,144] . All animal work was conducted on approved

protocols in accordance to the Institutional Animal Care and Use Committees at Lawrence Livermore National Laboratory and the University of California, Davis in AAALAC-accredited facilities and conform to the Guide for the care and use of laboratory animals.

Micro-Computed Tomography. Samples were collected 6-weeks post injury for female and male VEH, LPS, AB, and AB+LPS injured, contralateral, and uninjured joints. Samples were dissected and fixed for 72 hours at 4^{o}C using 10% neutral buffer formalin. Samples were stored in 70% EtOH at 4^{o}C until scanned. Whole knees were scanned using a SCANO μCT 35 (Bassersdorf, Switzerland) according to the rodent bone structure analysis guidelines (X-ray tube potential = 55kVp, intensity = 114 μA, 10 μm isotropic nominal voxel size, integration time = 900 ms). Trabecular bone in the distal femoral epiphysis was analyzed manually drawing contours on 2D transverse slides. The distal femoral epiphysis was designated as the region of trabecular bone enclosed by the growth plate and subchondral cortical bone plate. We quantified trabecular bone volume per total volume (BV/TV), trabecular thickness (Tb.Th), trabecular number (Tb.N), and trabecular spacing (Tb.Sp). Osteophyte volume in injured and contralateral joints was quantified by drawing contours around all heterotopic mineralized tissue attached to the distal femur and proximal tibia as well as the whole fabellae, menisci, and patella. Total mineralized osteophyte volume was then determined as the volumetric difference in mineralized tissue between injured and uninjured joints.

Statistics. Statistical analysis was performed using two-way ANOVA and Student's T-test with a two-tailed distribution, with two-sample equal variance (homoscedastic test). $p<0.01$ was considered statistically significant after a Bonferroni correction when comparing within strains and $p<0.00081$ between strains.

Histological Assessment of Articular Cartilage and Joint Degeneration. Joint samples were dissected 6 weeks post injury, free of soft tissue, fixed, dehydrated, paraffin embedded and sectioned as previously described[1,2]. The cartilage was visualized in sagittal 6μm paraffin serial sections using Safranin-O (0.1%, Sigma; S8884) and Fast Green (0.05%, Sigma; F7252) as previously described[1,2]. OA severity was evaluated using a modified osteoarthritis research society international (OARSI) scoring scale as previously described[6]. Starting from the synovium membrane to the articular cartilage, for each region, cartilage scoring began ~0.4 mm out from the start of synovium. Blinded slides were evaluated by seven scientists (six with and one without expertise in OA) utilizing a modified (sagittal) OARSI scoring parameters due to the severity of the phenotype due to TC loading[(19)]. Modified scoring scores (0) for intact cartilage staining with strong red staining on the femoral condyle and tibia, (1) minor fibrillation without cartilage loss, (2) clefts below the superficial zone, (3) cartilage thinning on the femoral condyle and tibia, (4) lack of staining on the femoral condyle and tibia, (5) staining present on 90% of the entire femoral condyle with tibial resorption, (6) staining present on over 80% of the femoral condyle with tibial resorption, (7) staining present on 75% of the femoral condyle with tibial resorption, (8) staining present on over 50% of the femora condyle with tibial resorption, (9), staining present in 25% of the femoral condyle with tibial resorption, (10) staining present in less than 10% of the femoral condyle with tibial resorption.

Results

Combination of Treatments Restores the PTOA Cartilage Phenotype in *C57Bl/6J* Mice

Using a tibia compression PTOA mouse model we examined what changes the inbred mouse strain would have on the OA outcome, and whether a treatment of antibiotics, a single dose of LPS, or a combination of both have a synergistic

impact on the PTOA outcome. This chapter will focus on the changes on groups not previously discussed on this dissertation. For VEH see chapter 2, for LPS *C57Bl/6J* see chapter 3, and for AB *C57Bl/6J* see chapter 4.

The AB+LPS *C57Bl/6J* uninjured showed staining throughout the entire femoral condyle highly similar to that observed for the uninjured VEH *C57Bl/6J* (**Fig. 1A, F**). Whereas LPS treatment produced a significant change in the cartilage of uninjured joints by showing proteoglycan degradation and lack of staining on the femoral condyle (**Fig 1A, C; numeral**); there was no significant difference in OARSI scores between the uninjured VEH *C57Bl/6J* and the uninjured AB+LPS *C57Bl/6J* (**Fig. 1AB**). VEH and AB+LPS *C57Bl/6J* injured samples were also similar, showing a reduction in staining from the corresponding uninjured (**Fig. 1A, F, AA, FF**), but the effects of LPS on injured joints were blunted by the AB treatment. VEH and AB+LPS *C57Bl/6J* anterior condyle showed similar cellular infiltration (**Fig. 1aa, ff**). There was no significant difference in OARSI scoring between the injured VEH *C57Bl/6J* and the injured AB+LPS *C57Bl/6J* (**Fig. 1AB**), suggesting that AB treatment rescued the LPS-mediated PTOA phenotype.

AB Treatment Has Similar Effects on the Bone of Injured Joints as the LPS Treatment

Comparisons of the combined effects of AB and LPS treatment prior to injury has never been studied in relationship to the development of PTOA. We next examined osteoarthritic remodeling in VEH, LPS, AB, and the AB+LPS treated mice by quantifying the loss in subchondral trabecular bone at 6 weeks post injury by micro-computed tomography (μCT). Comparisons will be shown for groups not discussed on previous chapters.

There were no significant changes in the subchondral bone volume (BV/TV) of the injured male or female *C57Bl/6J* LPS compared to the corresponding AB (**Fig. 2A**). BV/TV was significantly lower in *C57Bl/6J* injured AB females than the *MRL/MpJ* and *STR/ort* injured AB females. BV/TV in

C57Bl/6J injured LPS was significantly lower than the injured LPS male *MRL/MpJ* and *STR/ort*. Comparing AB injured males the BV/TV was significantly lower in *C57Bl/6J* compared to the *STR/ort*.

Data did not indicate any significant differences in the trabecular number (Tb.N) when comparing the AB and LPS groups for *C57Bl/6J* (**Fig. 2B**). Tb.N was significantly lower in injured male LPS and AB *C57Bl/6J* than the corresponding *C3H/HeJ*. Tb.N of *C57Bl/6J* injured AB male was significantly lower than corresponding *STR/ort*.

Trabecular thickness (Tb.Th) analysis of injured male had no differences between the AB and the LPS of *C57Bl/6J* (**Fig. 2C**). Female *C57Bl/5J* injured AB was significantly lower Tb.Th than the female AB injured *STR/ort*. Male *C57Bl/6J* injured LPS and AB presented significantly lower Tb.Th than the corresponding *C3H/HeJ* and *STR/ort*.

Trabecular spacing (Tb.Sp) did not show any differences between the LPS and the AB groups in the *C57Bl/6J* (**Fig. 2D**). Male *C57Bl/6J* injured AB and LPS had lower Tb.Sp than the *C3H/HeJ* injured males. Injured male *C57Bl/6J* showed lower Tb.Sp than the injured male *STR/ort*.

LPS Increases the Severity of PTOA in *MRL/MpJ* Mice

The uninjured VEH *MRL/MpJ* males showed more staining than the uninjured LPS and AB *MRL/MpJ* but were more similar to the AB+LPS *MRL/MpJ* uninjured (**Fig. 3G, O, K, M**). Uninjured VEH *MRL/MpJ* male joints did not show a statistically difference between the OARSI scores when compared to the uninjured LPS, AB, or AB+LPS *MRL/MpJ* male joint (**Fig. 3GH**). Injured LPS and AB+LPS *MRL/MpJ* males had thinning of the femoral condyle cartilage and clefts compared to the VEH (**Fig. 3g, i, k; arrow, asterisk**). There was a lack of staining in the LPS and AB+LPS injured *MRL/MpJ* males on the anterior tibial condyle (**Fig. 3ii, kk**). The OARSI score showed that there was a significant difference between the VEH and both the LPS and AB+LPS injured joints, both of which had a significantly higher OARSI score (**Fig. 3GH**). The AB injured

MRL/MpJ staining was stronger than the VEH *MRL/MpJ* males (**Fig. 3g, gg, m, mm**), but it was not significantly different comparing the OARSI scores (**Fig. 3GH**).

The uninjured *MRL/MpJ* female VEH, LPS, and AB+LPS showed similar staining while the AB group showed thinning of cartilage and less staining (**Fig. 3H, J, L, N**). Unlike the males the VEH injured *MRL/MpJ* females (**Fig. 3HH**) showed a thinning of the femoral condyle (**Fig. 3h; arrow, asterisk**), and a reduction in staining on the anterior tibial condyle (**Fig. 3hh**). The OARSI score was significantly higher for the VEH injured *MLR/MpJ* females compared to the contralateral VEH *MRL/MpJ* females (**Fig. 3GH**). The LPS injured *MRL/MpJ* female (**Fig. 3JJ**) also showed a thinning of the femoral condyle cartilage compared to VEH (**Fig. 3h, j; arrow, asterisk**) and a hyperplastic synovium (**Fig. 3jj; asterisk**). The OARSI score was significantly higher when comparing the injured female *MLR/MpJ* VEH to the LPS (**Fig. 3GH**). LPS had a catabolic effect on the cartilage of both female and male *MRL/MpJ* injured joints, but the phenotype was more severe in females than in males.

Contrary to results obtained for the C57Bl6 strain (**Fig. 2B, bb; arrow, asterisk**), the injured AB treated *MRL/MpJ* females showed even more thinning of the cartilage on the femoral condyle (**Fig. 3l; arrow, asterisk**) and reduced staining on the anterior tibial condyle but no cellular infiltration (**Fig. 3ll; asterisk**). OARSI score was significantly higher in the injured AB *MRL/MpJ* females than the VEH injured *MRL/MpJ* females (**Fig. 3GH**). The injured AB+LPS *MRL/MpJ* (**Fig. 3NN**) showed the most aggressive of the phenotypes with practically no staining on the femoral condyle (**Fig. 3n; arrow, asterisk**), reduced staining in the anterior tibial condyle, and a slight increase of cellularity than the AB treated injured female *MRL/MpJ* joints (**Fig. 3ll, nn; asterisk**). OARSI score for the injured VEH *MRL/MpJ* females was significantly lower than the AB+LPS injured *MLR/MpJ* females (**Fig. 3GH**). Unlike *C57Bl6* males where AB treatment rescued the LPS phenotype, in this strain, the combined LPS/AB

treatment exacerbated the PTOA cartilate phenotype, in both male and female *MRL/MpJ*.

AB Rescues the PTOA Phenotype of the Female *MRL/MpJ*

BV/TV analysis did not show any differences when comparing VEH, LPS, AB, and AB+LPS treatment groups for both sexes on *MRL/MpJ MRL/MpJ.* LPS and AB+LPS injured female had lower BV/TV compared to the injured *MRL/MpJ* LPS and AB+LPS males (**Fig. 4A**). AB alone is not enough to change the phenotype of the male Injured *MRL/MpJ* males had lower BV/TV than the *STR/ort* injured males when comparing the VEH, LPS, AB, and AB+LPS groups.

Tb.N analysis did not show any differences when comparing VEH, LPS, AB, and AB+LPS treatment groups for both sexes on injured *MRL/MpJ. MRL/MpJ* injured female VEH, LPS, AB, AB+LPS Tb.N was significantly lower than injured male *MRL/MpJ* (**Fig. 4B**). Injured male *MRL/MpJ* VEH, LPS, AB, and AB+LPS Tb.N was significantly higher than the corresponding *C3H/HeJ* injured males.

Tb.Th analysis did not show any differences when comparing between VEH, LPS, AB, and AB+LPS for male and female *MRL/MpJ* (**Fig. 4C**). AB *MRL/MpJ* female injured had lower Tb.Th than the AB injured female *STR/ort*. LPS, AB, and AB+LPS *MRL/MpJ* injured males presented significantly lower Tb.Th than the corresponding male injured *STR/ort*. Tb.Th was significantly lower on injured male *MRL/MpJ* AB and AB+LPS than corresponding male injured *C3H/HeJ*.

Tb.Sp did not show any differences between the VEH, LPS, AB, and AB+LPS groups for either sexes in *MRL/MpJ* (**Fig 4D**). Tb.Sp was significantly larger on the injured female *MRL/MpJ* for the LPS, AB, and AB+LPS compared to the injured male *MRL/MpJ* (**Fig 4D**). Tb.Sp was significantly lower than *MRL/MpJ* injured LPS, AB, and AB+LPS male compared to the male injured corresponding *C3H/HeJ* strain.

AB Treatment Improves the PTOA Severity of *C3H/HeJ* Mice

The uninjured *C3H/HeJ* male VEH and LPS (**Fig. 5O, Q**) were similar while the *C3H/HeJ* uninjured male AB and AB+LPS (**Fig. 5S, T**) had slightly less cartilage staining that was not found to be significant when comparing the OARSI scores (**Fig. 5OP**). The VEH injured, LPS, and AB+LPS (**Fig. 5OO, QQ, TT**) all showed similar thinning of the femoral condyle cartilage (**Fig. 5o, q, t; arrow, asterisk**) but the VEH and AB+LPS showed more cellularity than the LPS (**Fig. 5oo, ss, tt; asterisk**) although they all showed a similar lack of staining on the anterior tibial condyle. The LPS and AB+LPS injured *C3H/HeJ* male mice were not statistically significantly different comparing the OARSI score to than the VEH injured *C3H/HeJ* male mice (**Fig. 5OP**). The AB treated injured *C3H/HeJ* (**Fig. 5SS**) males showed slightly thicker cartilage staining on the femoral condyle (**Fig. 5s; arrow, asterisk**) but lower cellularity than the VEH and more staining of the anterior tibial condyle (**Fig. 5ss; asterisk**). The AB injured *C3H/HeJ* males showed a significantly lower OARSI score than the VEH injured *C3H/HeJ* males (**Fig. 5OP**).

In *C3H/HeJ* females, both the uninjured VEH and LPS (**Fig. 5P, R**) joint lacked cartilage staining of the femoral condyle. The injured *C3H/HeJ* VEH and LPS (**Fig. 5PP, RR**) showed similar stain on the femoral condyle (**Fig. 5p, r; arrow, asterisk**). Both samples showed similar lack of staining on the tibial anterior condyle but no cellularity (**Fig. 5pp, rr**). Similar to the males, the injured VEH and LPS samples were virtually similar, which is why they had no difference between the OARSI scores (**Fig. 5OP**).

LPS Treatment Does Not Affect PTOA in *C3H/HeJ* Male Mice

C3H/HeJ LPS females were not analyzed.*C3H/HeJ* injured males did not show any differences in BV/TV, Tb.N, Tb.Th, and Tb.Sp between the treatment groups when compared to each other (**Fig. 6A, B, C, D**). Male injured *C3H/HeJ* had lower BV/TV in the VEH, AB, and AB+LPS than the corresponding male injured *STR/ort*. Tb.N and Tb.Sp in *C3H/HeJ* injured males was significantly lower than

the *STR/ort* injured males when comparing the VEH, LPS, AB, and AB+LPS. Tb.Th was significantly lower on *C3H/HeJ* injured males AB+LPS group compared to the *STR/ort* injured males.

AB Treatment Improves PTOA Severity in *STR/ort* Mice

The uninjured *STR/ort* male VEH (**Fig. 7U**) had more staining than the LPS (**Fig. 7W**); VEH uninjured *STR/ort* had a significantly lower OARSI score than the LPS uninjured *STR/ort*. The uninjured *STR/ort* male AB (**Fig. 7X**) had less staining than the VEH, reflected by a significantly higher OARSI score than the VEH uninjured *STR/ort* males (**Fig. 7UV**). The uninjured *STR/ort* male AB+LPS had fibrillations and clefts around the entire femur (**Fig. 7Z**), OARSI score is significantly higher than the VEH uninjured *STR/ort* males (**Fig. 7UV**).

The injured VEH *STR/ort* male had thicker staining than the injured LPS (**Fig. 7UU, WW**), which had no staining on the femoral condyle (**Fig. 7w; arrow, asterisk**) but the anterior tibial condyle was similar (**Fig. 7ww**). The OARSI score was significantly higher in the LPS injured *STR/ort* males compared to the VEH injured *STR/ort* males (**Fig. 7UV**). The AB injured *STR/ort* males however (**Fig. 7XX**) showed thicker cartilage than the VEH injured on the femoral condyle (**Fig. 7u, x; arrow, asterisk**), and there was stronger staining of the anterior tibial condyle than the VEH (**Fig. 7uu, xx**). AB injured *STR/ort* males had a lower OARSI score compared to the VEH *STR/ort* injured males (**Fig. 7UV**). The AB+LPS injured *STR/ort* (**Fig. 7ZZ**) had a similar femoral condyle than VEH (**Fig. 7u, z; arrow, asterisk**), but more staining on the synovium (**Fig. 7uu, zz; asterisk**). OARSI score for VEH and AB+LPS injured *STR/ort* males was not significantly different (**Fig. 7UV**).

The uninjured *STR/ort* female VEH showed a lack of staining while the AB showed stronger staining (**Fig. 7V, Y**), indicative of an improved cartilage phenotype which was reflected by a lower OARSI score (**Fig. 7UV**). The injured *STR/ort* VEH showed less staining than the corresponding AB (**Fig. 7VV, YY**), the femoral condyle had a thinner cartilage layer in the VEH than the AB (**Fig. 7v,**

y; arrow, asterisk) treated joints. Both samples showed similar lack of staining on the tibial anterior condyle but no greater cellularity (**Fig. 7vv, yy; asterisk**). OARSI score of the injured AB *STR/ort* females was lower than the injured VEH *STR/ort* females (**Fig. 7UV**).

AB and AB+LPS Treatment Improves the Subchondral Bone Phenotype of the *STR/ort* Male Mice

STR/ort injured female did not show differences on BV/TV between the VEH and AB treatment. *STR/ort* injured males had significantly higher BV/TV in AB and AB+LPS than the VEH *STR/ort* injured males (**Fig. 8A**). *STR/ort* injured female did not have differences when comparing the VEH and AB, and injured males on VEH, LPS, AB, and AB+LPS groups when comparing the Tb.N, Tb.Th, and Tb.Sp (**Fig. 8B, C, D**).

Antibiotic Treated *STR/ort* Mice Have a Decrease in Osteophyte Volume

Osteophyte volume (Op.V) analysis shows that there was a significant reduction in osteophytes in the AB treated males compared to the VEH males of the *C57Bl/6J* strain (**Fig 7**). There were no significant differences on the Op.V of the *C57Bl/6J* LPS to the AB. There were no differences in either the female or the male *MRL/MpJ* in any of the treatment groups. There was a significant reduction of Op.V on the AB+LPS treated *C3H/HeJ* male samples compared to the VEH *C3H/HeJ* males. There was significantly less Op.V in the *STR/ort* AB females than the *STR/ort* VEH females. There was a significant decrease in Op.V of the AB treated and the AB+ LPS *STR/ort* males compared to the VEH *STR/ort* males.

Discussion

This study looks at how the combination of antibiotics and inflammation prior to injury affect the inbred strains with varying susceptibilities to PTOA. LPS treatment was shown to have a negative effect on the cartilage of the injured joint

in every strain except for the *C3H/HeJ* male and females. *C3H/HeJ* mice are resistant to the endotoxin which justifies why there is no effect on the cartilage of the injured samples of this strain. In contrast, we observed that even in the MRL/MpJ strain, which is known to be resistant to PTOA, a spike in inflammation five days prior to injury was sufficient to modify PTOA outcomes and generate a more severe PTOA phenotype.

Overall, antibiotic treatment improved the cartilage phenotype of all strains susceptible to PTOA. The only strain that did not follow this trend was *MRL/MpJ*. We expected MRLs to be unaffected by AB treatment and persist as resistant to PTOA, however, AB treatment produced a mild, but significant PTOA phenotype in both male and female *MRL/MpJ* mice. The uninjured AB treated *MRL/MpJ* females also had a significantly higher OARSI score than the uninjured *MRL/MpJ* female VEH Antibiotic treatment worsened the PTOA phenotype for the *MRL/MpJ* mice, suggesting that this strain responds dramatically different to AB treatment than all other strains.

A combination of AB and LPS did not affect the cartilage phenotype of most strains relative to VEH, but AB treatment rescued the negative effects of LPS administration alone. We observed no significant differences in the injured joints of AB+LPS from the *C57Bl/6J, MRL/MpJ C3H/HeJ*, and *STR/ort* male mice joints, relative to VEH injured joints from each strain. There was however, a negative effect observed in the *MRL/MpJ* female joints when exposed to the treatment combination. In order to determine if it is sex dependent, future directions will include the female cohorts on the AB+LPS treatment.

The BV/TV of the injured *MRL/MpJ* male VEH compared to the injured *C57Bl/6J* VEH was not statistically significant, and although data indicated that inside the strain LPS did not have a large change, the comparison between the LPS treated male injured *MRL/MpJ* and the LPS injured male *C57Bl/6J* became statistically significant. This could be due to the *MRL/MpJ* potentially resolving inflammation faster than the *C57Bl/6J*. Future directions would look at gene

expression analysis in specific immune populations present in the injured joint, in order to understand how *MRL/MpJ* effectively resolves inflammation.

The subchondral bone of *C3H/HeJ* and *STR/ort* LPS males was unaffected by injury, where injured and uninjured groups had similar bone mineral density parameters. This was in contrast to the other 2 strains, which had a significant reduction in the BV/TV of injured legs. This could be that inflammation prior to injury caused contralateral to be affected as well. *C3H/HeJ* LPS males had thicker trabeculae than VEH. The error bars for these groups were large and the volume per group was low, which could be the reason for showing no statistical significance.

C3H/HeJ AB males and *STR/ort* AB females had large error bars for the bone analysis due to a smaller number of mice in the cohort. This could be affecting the results. Future directions could sample larger groups in order to achieve statistical significance, given that *STR/ort* AB mice gained BV/TV and lost Tb.Sp compared to the corresponding VEH mice it could add more statistical power to the treated groups. Similar to the LPS treated the differences between the injury groups was no longer present on the AB treated mice which could be due to the combination of the number of samples per group and the AB treatment.

STR/ort AB+LPS injured showed a decrease in bone mineral density compared to the VEH injured group, meaning the combined treatment had a negative effect on bone. However, AB+LPS *C3H/HeJ* and *STR/ort* did not show differences between the uninjured, injured, and contralateral joints. The lack of changes of the uninjured, injured, and contralateral is inconsistent with the trend observed amount VEH groups, suggesting that the effect of the treatment changes the bone response to injury.

BV/TV was significant in the uninjured VEH males of those strains and not in the uninjured LPS comparing the *C57Bl/6J* to the *STR/ort*. Injured BV/TV group was significant on the VEH which is no longer significant after LPS treatment for the *C3H/HeJ*. LPS alone does not significantly change the bone

phenotype for the *MRL/MpJ* mice even though it is enough to show lack of staining on the cartilage.

Antibiotic treatment caused a loss of subchondral bone in the uninjured joints of *MRL/MpJ* males that was not observed in VEH groups. The rest of the results were consistent to those seen in the VEH treated joints. The comparison between the VEH *STR/ort* groups to the *STR/ort* AB BV/TV results were not significant. The injured VEH *STR/ort* groups had statistically significant change on the Tb.Th between sexes which was not significant in the corresponding AB groups. The VEH *STR/ort* group had significantly higher Op.V than the AB treated *STR/ort* on both male and female mice. Male *STR/ort* mice showed that the AB treatment was enough to reduce Op.V even on the AB+LPS when the LPS alone increased Op.V in a not statistically significant way.

The AB+LPS treatment statistically significantly reduces the Op.V on C3H/HeJ males and on the *STR/ort* males; on the *C3H/HeJ*, the AB treatment alone did not significantly reduce the Op.V, but it did reduce it. We believe that AB treatment is enough to reduce the Op.V, on *C57Bl/6J, C3H/HeJ*, and *STR/ort*, independent of the LPS treatment or not. We will be adding to the group number of *C3H/HeJ* it will increase statistical power, reducing the error bars and giving a statistically significant reduction of Op.V on the AB *C3H/HeJ* male mice. It is interesting to note that the LPS treatment on *STR/ort* males increases osteophyte number the antibiotic treatment is sufficient to reduce the osteophyte formation, indicating that gut microbiome modifications can reduce external bone growth formation.

The results shown on this study provide an insight into how PTOA development can be related back to external factors. LPS treatment mimics a spike in bacterial inflammation, which is enough to cause a more severe PTOA phenotype on every strain susceptible to LPS. The mutation on *C3H/HeJ* causes it to become insensitive to LPS and therefore cause no changes between the LPS and the VEH groups. *C57Bl/6J* which shows our baseline and our control group show a reduction on bone mass and a reduction on cartilage staining on

male and female mice. *MRL/MpJ* showed that there are no changes to the bone phenotype but there is an increase in cartilage resorption on mice that are thought to be resistant to the development of PTOA. *STR/ort* mice have elevated levels of circulating inflammatory chemokines and cytokines that could be compared to people suffering from inflammatory diseases; the bone has no significant changes while the cartilage resorption increases. The results we got are significant due to the study of inflammation prior to injury, which as previously mentioned inflammation has only been studied after injury. We can conclude from this that the exposure to higher levels of inflammation days prior to injury is enough to cause a more severe PTOA phenotype.

Ampicillin and neomycin treatment are poorly absorbed in the small intestine and therefore are going to only change the gut microbiome. The antibiotic cocktail we administered was not enough to wipe the gut microbiome, but it was enough to heavily modify it. The results from ampicillin and neomycin treatment are a decrease in diversity of the gut microbiome and an increase on bacteria that already populate the gut microbiome like *Firmicutes* and *Bacteroidetes*. This change to the gut microbiome is going to modify PTOA by reducing the levels of cartilage resorption found on every strain except for *MRL/MpJ* females. *MRL/MpJ* show that there are no significant changes on the bone phenotype. Male *MRL/MpJ* show stronger staining on the AB treated injured joints while the females show a decrease in staining. This result is not surprising given that we previously saw that the *MRL/MpJ* females behave differently than the males by being susceptible to PTOA on VEH groups. The changes between the male and female *MRL/MpJ* could be due to how the response to inflammation changes depending on the sex. *C57Bl/6J* male mice showed an improvement on the cartilage staining, but showed a significant decrease on bone mass, and a significant decrease on the Op.V. The bone mass decrease was significant on the AB female *C57Bl/6J* but the Op.V changes were not significant on the same group. Given that PTOA is a disease that is marked by the degradation of cartilage, this means that the phenotype improves in the

C57Bl/6J treated with antibiotics. The AB *C3H/HeJ* male mice showed a decrease in the OARSI score compared to VEH, but no changes in the bone phenotypes. *STR/ort* mice showed an improvement on the injured joints by having lower OARSI scores in the AB treated joints for both sexes. There was an improvement on the BV/TV in AB treated *STR/ort* males. Both sexes of AB *STR/ort* had a lowering in the Op.V compared to the VEH.

The LPS treatment can blunt the positive benefits of the AB treatment on the *C57Bl/6J, C3H/HeJ*, and *STR/ort*. Op.V is significantly lower on the AB+LPS compared to VEH for the *C3H/HeJ* and the *STR/ort*. In the future, we will analyze the AB+LPS strain in order to see the bone phenotype changes happening due to that treatment for *C57Bl/6J*. These strains showered no changes on the cartilage phenotype compared to the VEH. AB *MRL/MpJ* male and female both showed a higher OARSI score than the VEH. There are no changes between the This could allow us to conclude that for *MRL/MpJ* strain the LPS treatment is enough to be able to eliminate the resistance to PTOA for males and to worsen the female phenotype. We can also conclude that resistance to PTOA for male *MRL/MpJ* is sex dependent and could be caused by different mechanisms of inflammation resolution on males compared to females.

Future studies will perform RNA sequencing analysis on the samples from different strains and treatments in order to determine how gene expression changes during the immediate and acute phase after injury. We will be performing immunohistochemistry to study the cellularity present on the anterior tibial condyle side of the medial compartment of the injured joints; this will allow us to determine the localized immune cell changes on the joint. We will be performing FACS on the infrapatellar fat pad in order to determine immune population changes due to treatment, strain, and injury type.

Figures

Figure 1. *C57Bl/6J* Histological Assessment of PTOA Severity Depending on Strains and Treatment Post-Tibial Compression Injured Joints

(A-ff) Histological assessment of contralateral and injured joints 6 weeks post-injury at 16 weeks of age using Safranin-O and Fast-Green staining. Joints were identified by sex, injured or contralateral, and strain. Images were taken in 5x magnification and 20x magnification. **(AB)** OARSI scoring for histological samples separated by strain. Independently graded by seven scientists on two samples per condition. *p<0.05

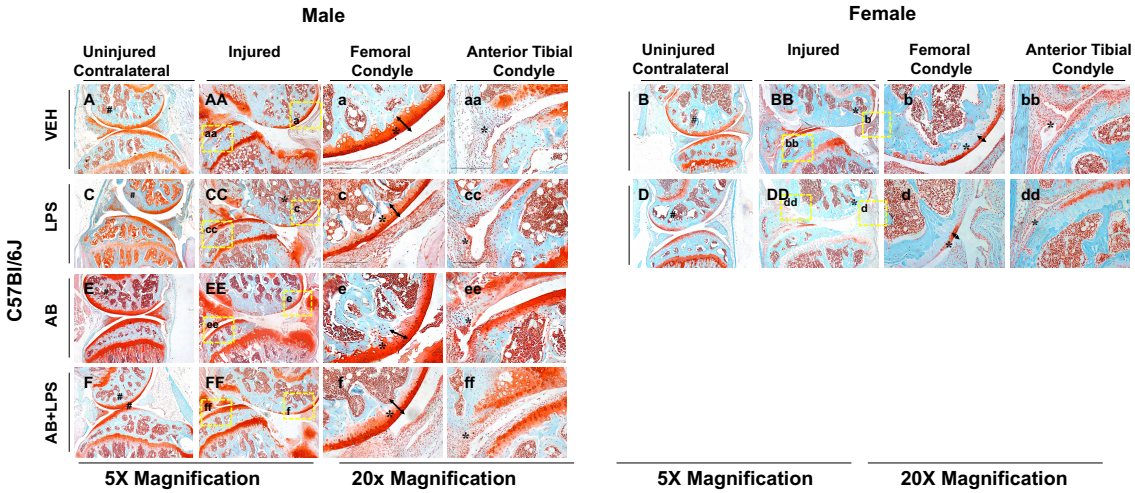

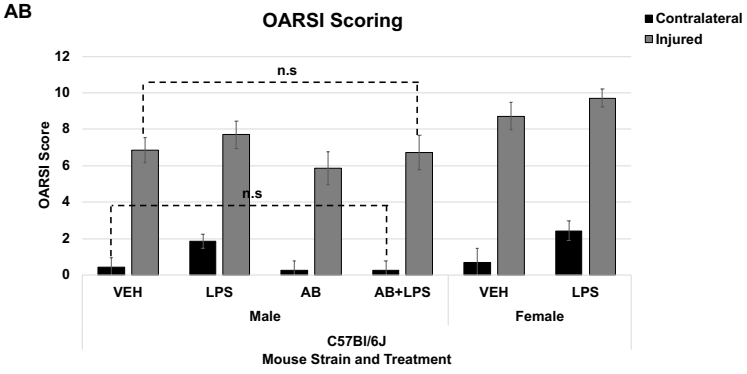

Figure 2. *C57Bl/6J* Bone Microstructure Assessment Using Micro-CT
(A) Subchondral bone volume is the bone volume fraction which is the ratio of the segmented bone volume to the total volume of the region of interest. **(B)** Trabecular number was measured using the average number of trabeculae per unit length. **(C)** Trabecular thickness was measured using the mean thickness of trabeculae, assessed using direct 3D methods. **(D)** Trabecular spacing was measured using the mean distance between trabeculae, assessed using direct 3D methods[141]. Statistics were performed using two-way ANOVA and Student's T-Test with a Bonferroni correction. *p<0.01

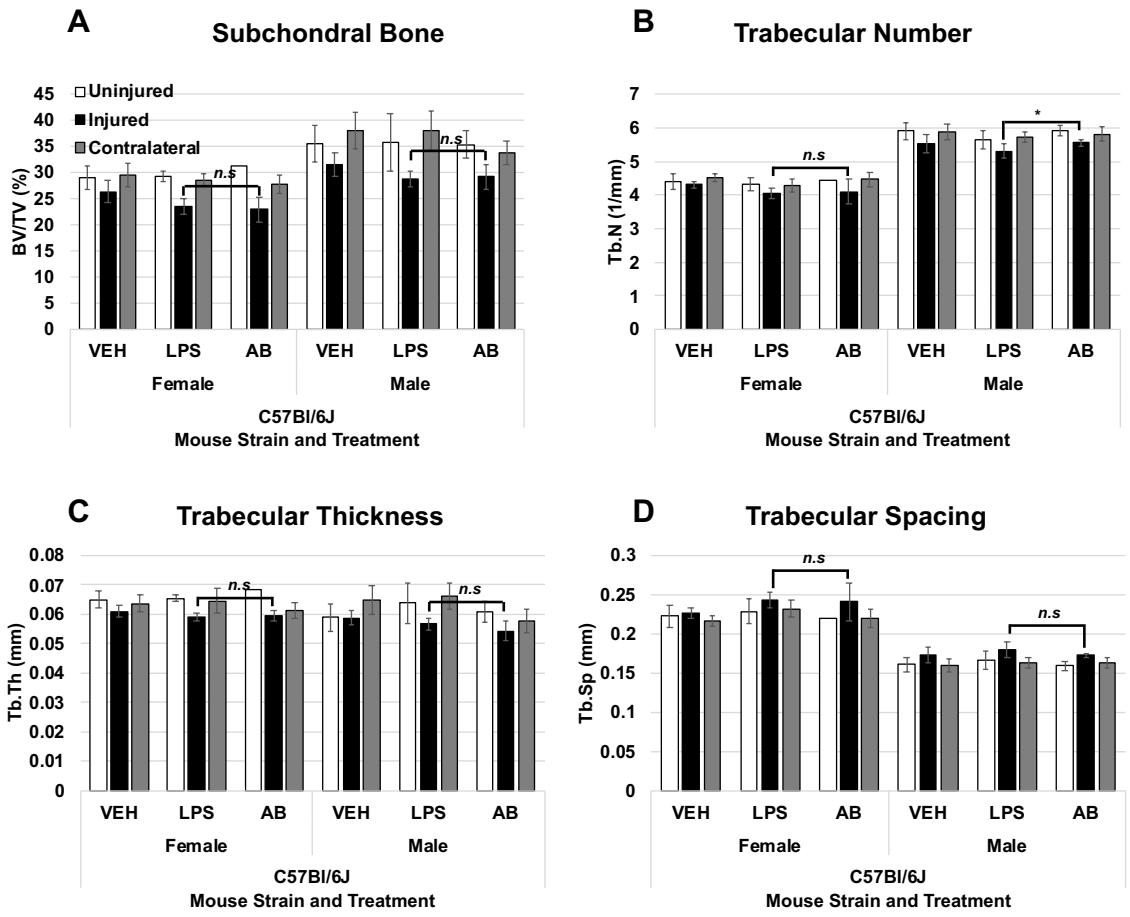

Figure 3. *MRL/MpJ* Histological Assessment of PTOA Severity Depending on Strains and Treatment Post-Tibial Compression Injured Joints

(G-nn) Histological assessment of contralateral and injured joints 6 weeks post-injury at 16 weeks of age using Safranin-O and Fast-Green staining. Joints were identified by sex, injured or contralateral, and strain. Images were taken in 5x magnification and 20x magnification. **(GH)** OARSI scoring for histological samples separated by strain. Independently graded by seven scientists on two samples per condition. *$p<0.05$

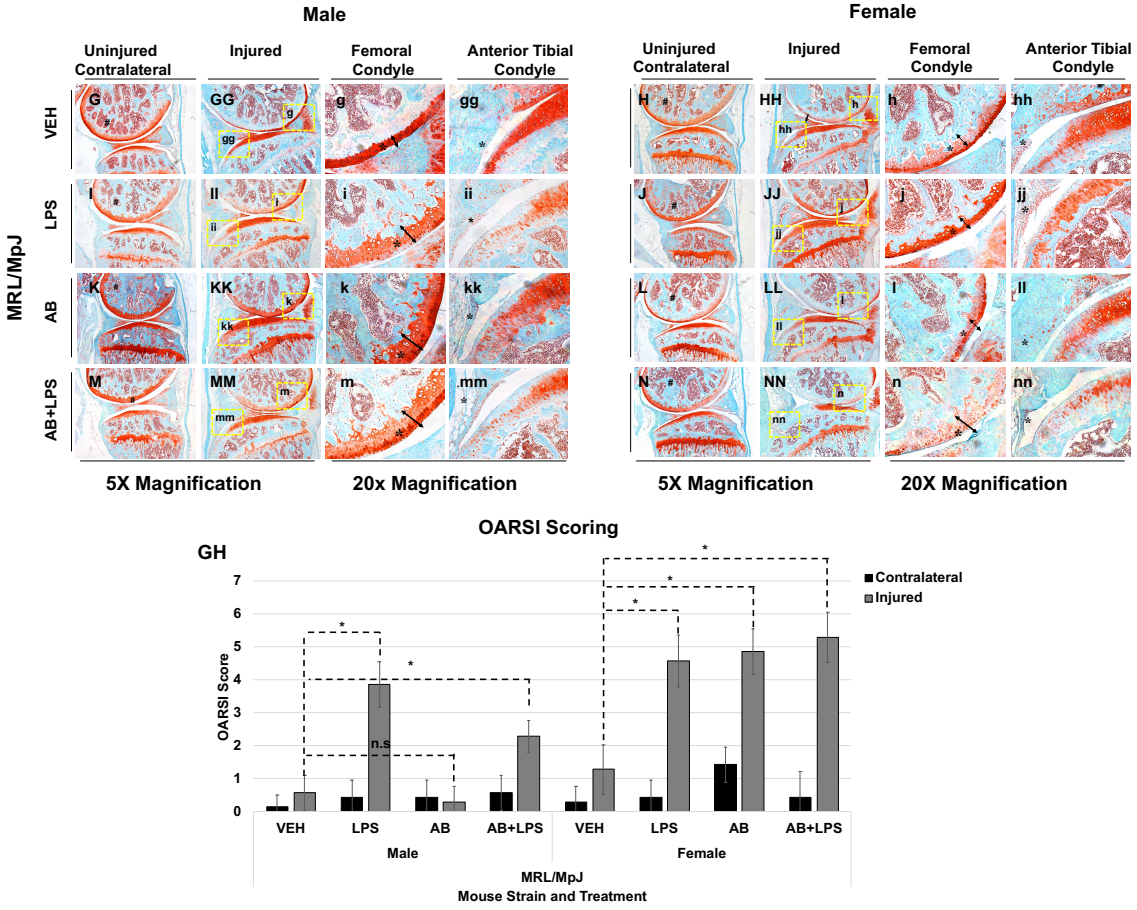

Figure 4. *MRL/MpJ* Bone Microstructure Assessment Using Micro-CT
(A) Subchondral bone volume is the bone volume fraction which is the ratio of the segmented bone volume to the total volume of the region of interest. **(B)** Trabecular number was measured using the average number of trabeculae per unit length. **(C)** Trabecular thickness was measured using the mean thickness of trabeculae, assessed using direct 3D methods. **(D)** Trabecular spacing was measured using the mean distance between trabeculae, assessed using direct 3D methods[141]. Statistics were performed using two-way ANOVA and Student's T-Test with a Bonferroni correction. *p<0.01

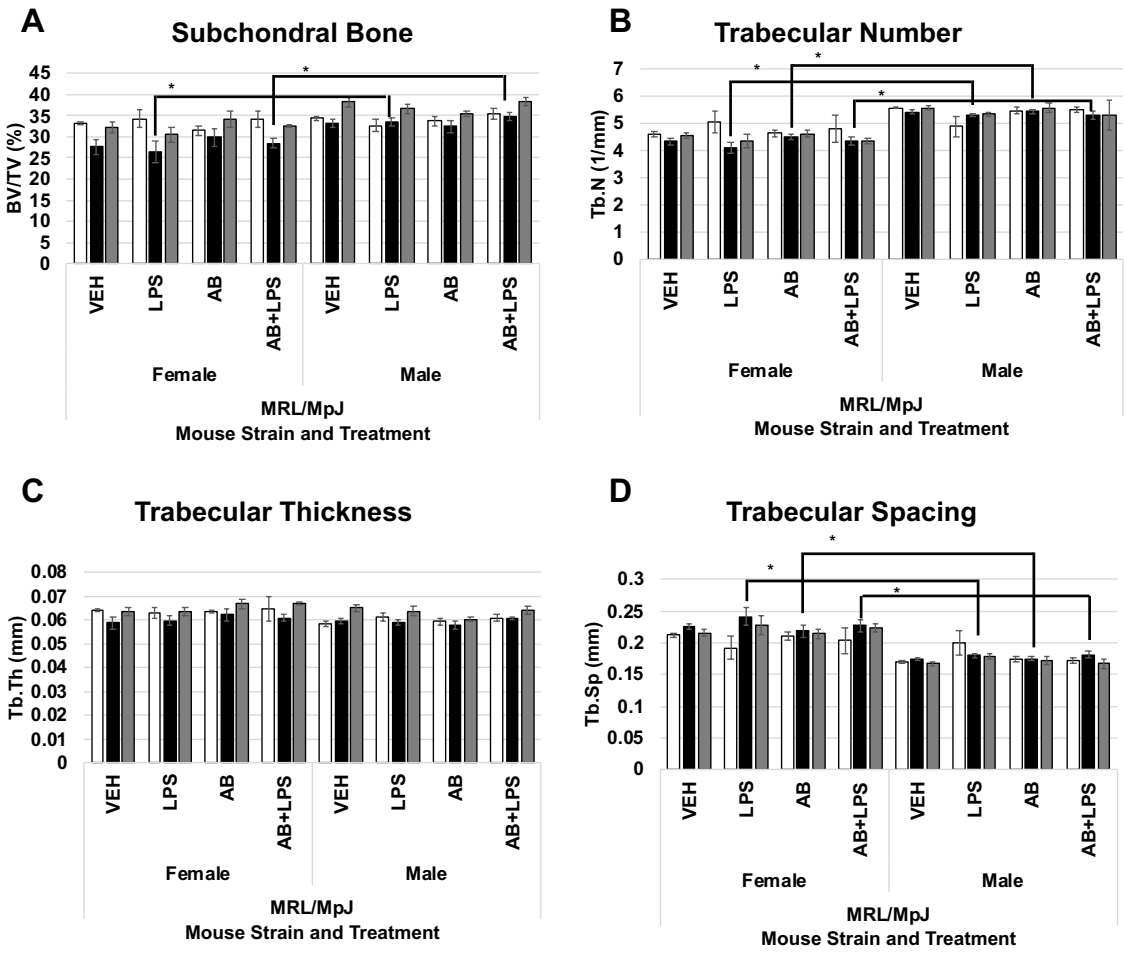

Figure 5. *C3H/HeJ* Histological Assessment of PTOA Severity Depending on Strains and Treatment Post-Tibial Compression Injured Joints

(O-tt) Histological assessment of contralateral and injured joints 6 weeks post-injury at 16 weeks of age using Safranin-O and Fast-Green staining. Joints were identified by sex, injured or contralateral, and strain. Images were taken in 5x magnification and 20x magnification. **(OP)** OARSI scoring for histological samples separated by strain. Independently graded by seven scientists on two samples per condition. *p<0.05

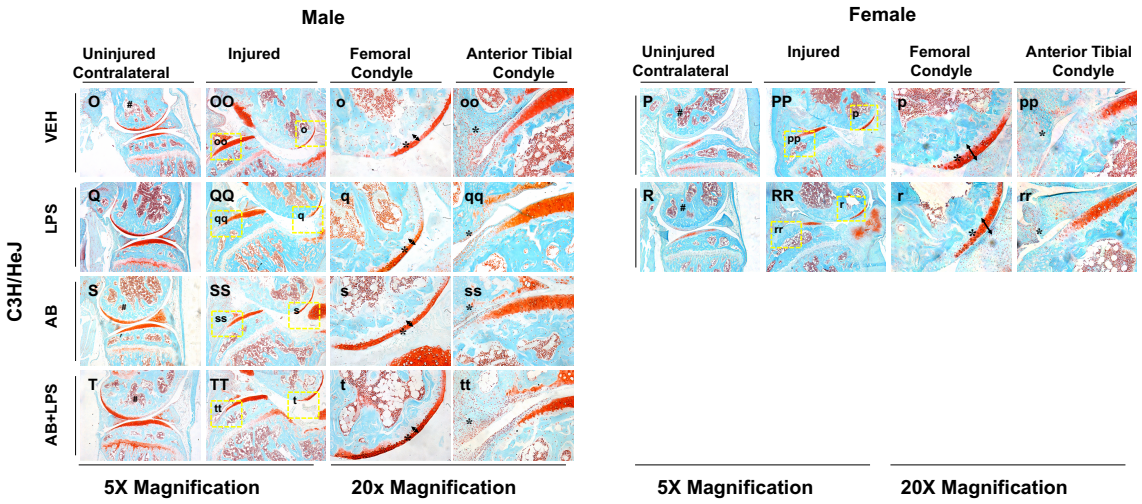

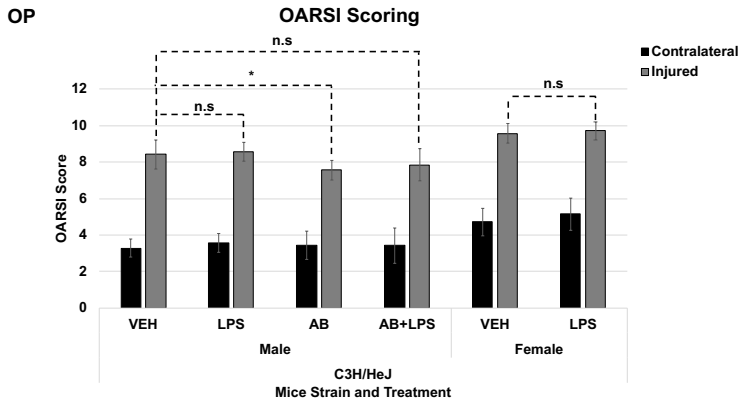

Figure 6. *C3H/HeJ* Bone Microstructure Assessment Using Micro-CT
(A) Subchondral bone volume is the bone volume fraction which is the ratio of the segmented bone volume to the total volume of the region of interest. **(B)** Trabecular number was measured using the average number of trabeculae per unit length. **(C)** Trabecular thickness was measured using the mean thickness of trabeculae, assessed using direct 3D methods. **(D)** Trabecular spacing was measured using the mean distance between trabeculae, assessed using direct 3D methods[141]. Statistics were performed using two-way ANOVA and Student's T-Test with a Bonferroni correction. *p<0.01.

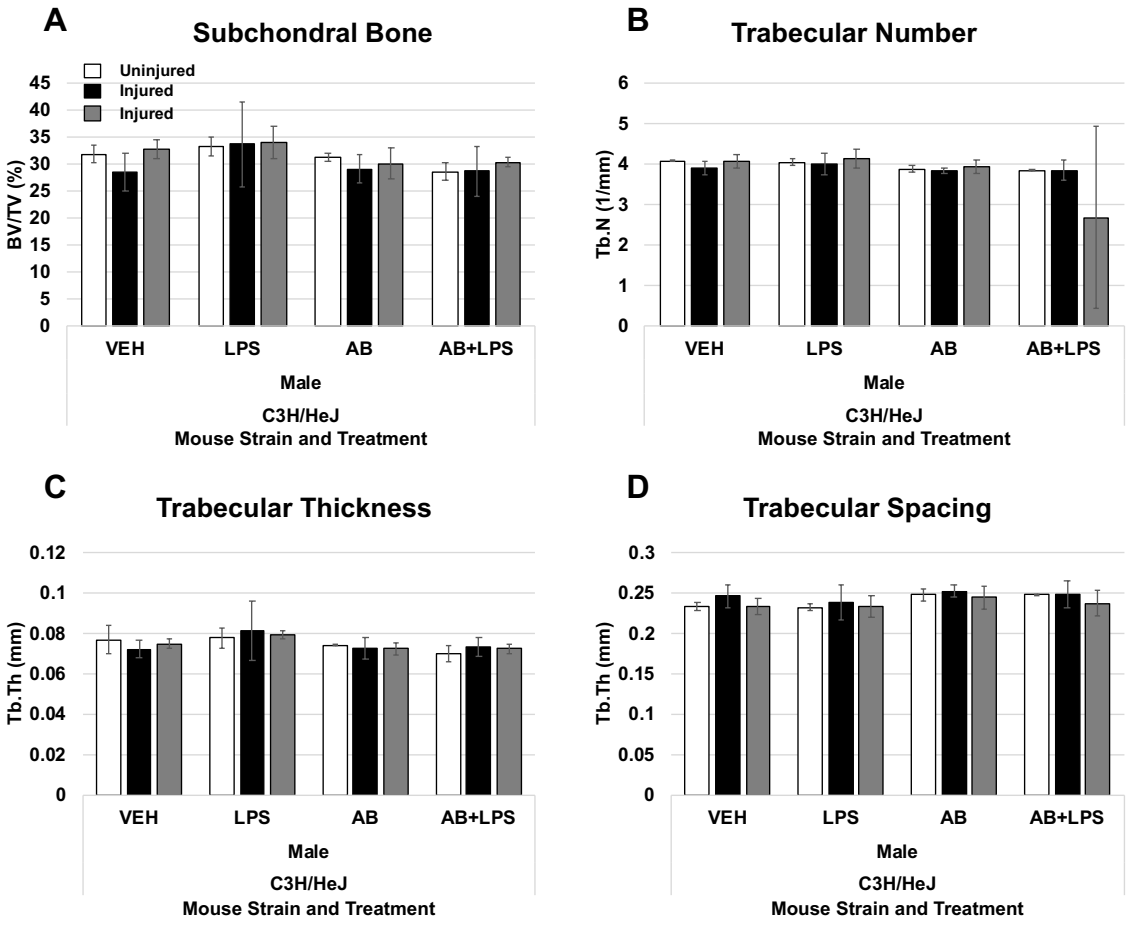

Figure 7. *STR/ort* Histological Assessment of PTOA Severity Depending on Strains and Treatment Post-Tibial Compression Injured Joints

(U-zz) Histological assessment of contralateral and injured joints 6 weeks post-injury at 16 weeks of age using Safranin-O and Fast-Green staining. Joints were identified by sex, injured or contralateral, and strain. Images were taken in 5x magnification and 20x magnification. **(UV)** OARSI scoring for histological samples separated by strain. Independently graded by seven scientists on two samples per condition. *p<0.05

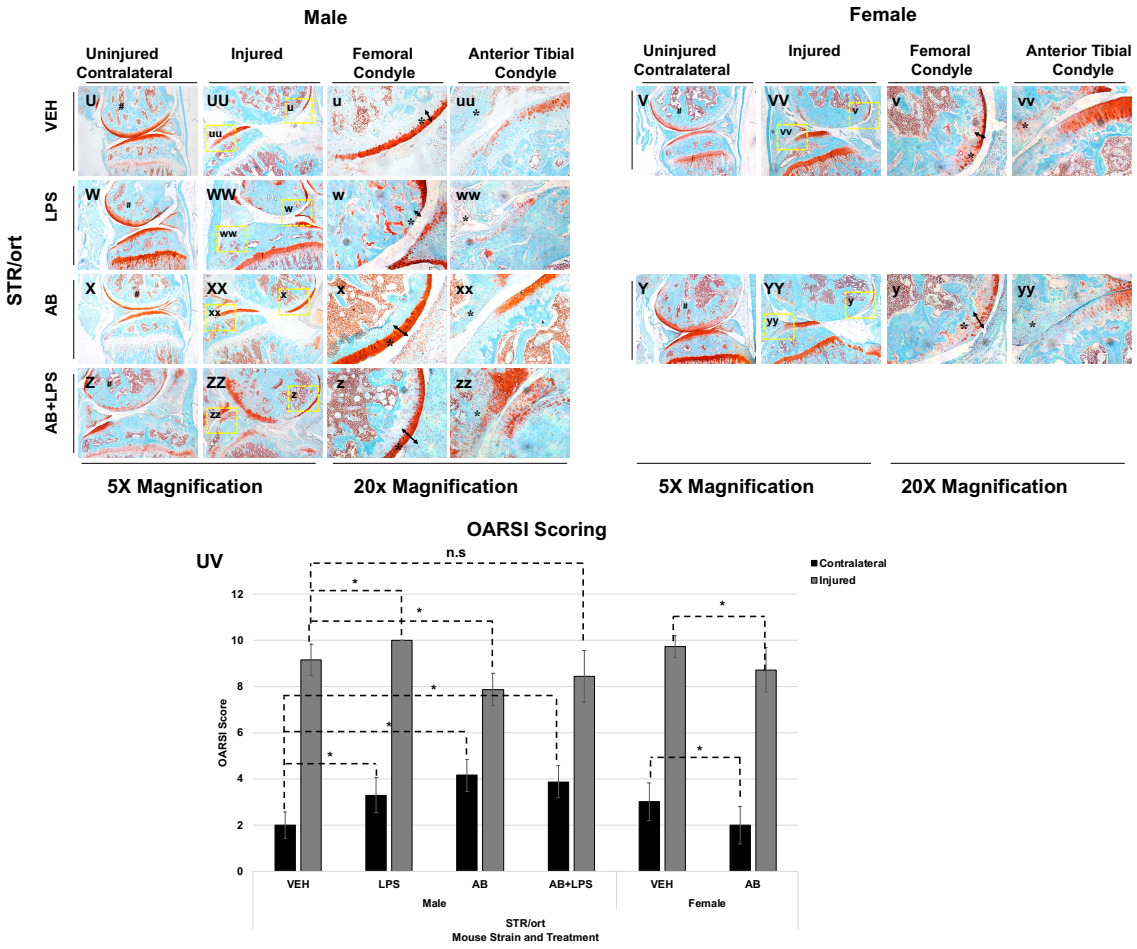

Figure 8. *STR/ort* Bone Microstructure Assessment Using Micro-CT
(A) Subchondral bone volume is the bone volume fraction which is the ratio of the segmented bone volume to the total volume of the region of interest. **(B)** Trabecular number was measured using the average number of trabeculae per unit length. **(C)** Trabecular thickness was measured using the mean thickness of trabeculae, assessed using direct 3D methods. **(D)** Trabecular spacing was measured using the mean distance between trabeculae, assessed using direct 3D methods[141]. Statistics were performed using two-way ANOVA and Student's T-Test with a Bonferroni correction. *p<0.01.

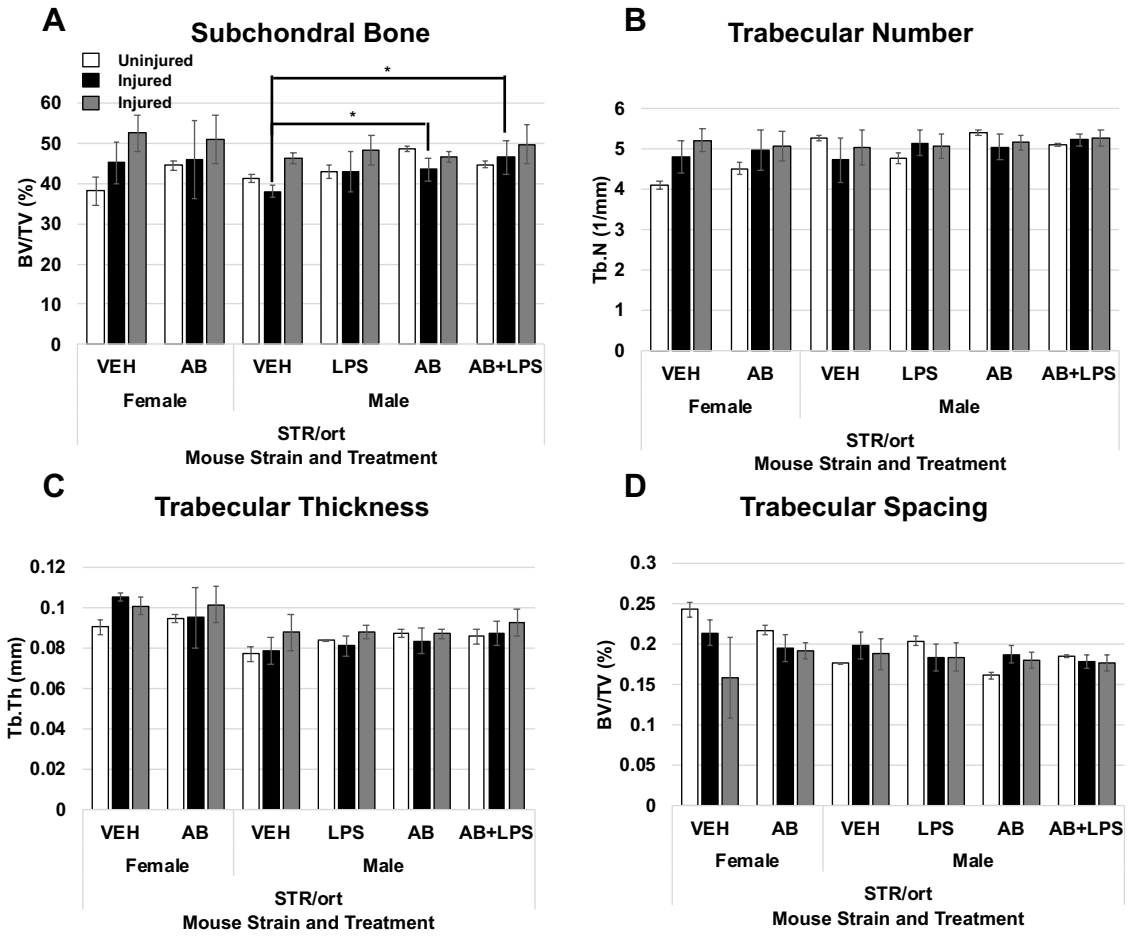

Figure 9. Osteophyte Representation Using Micro-Computed Tomography **(A)** Osteophyte volume was measured by quantification of ectopic bone around the injured joint compared to contralateral. All statistics were made using strain, sex, injury type, and treatment using two-way ANOVA and Student's T-Test. **p*<0.01 **(B)** Micro-Computed tomography image of the joints of all groups using data gathered during **(A)**. Dark grey regions show osteophyte growth compared to the white. Contralateral shows the normal bone.

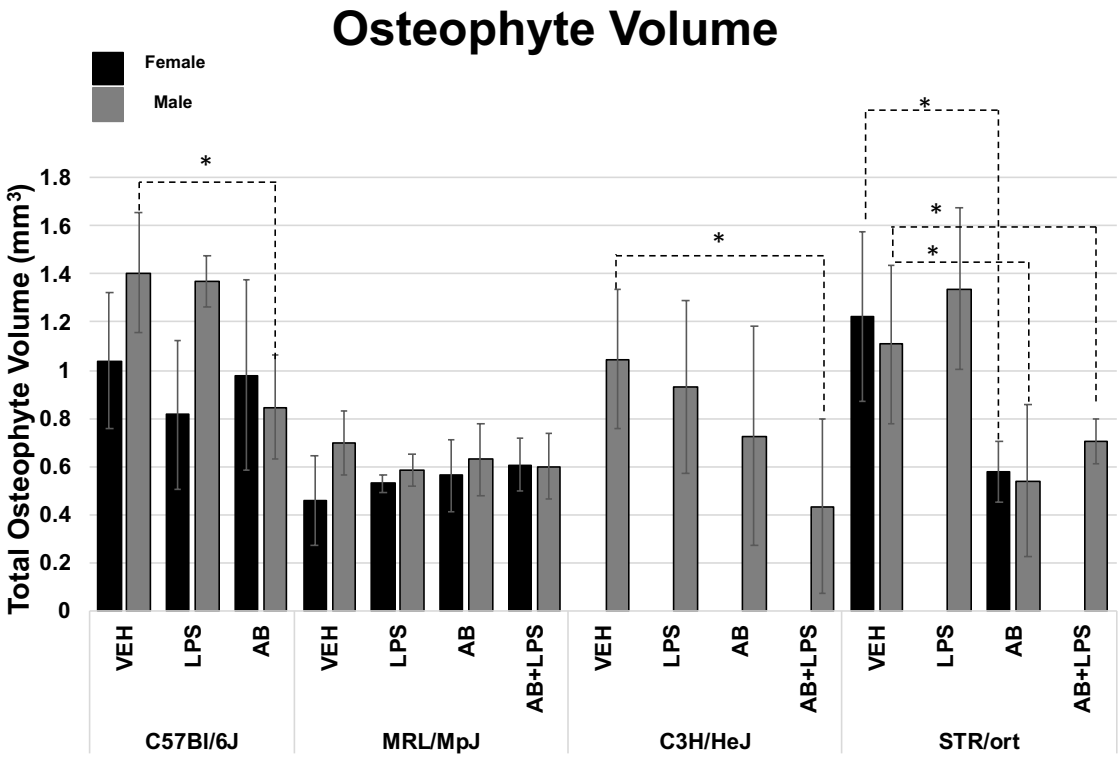

Chapter 6: Conclusions and Future Directions

The studies discussed in this dissertation have led to a better understanding of how PTOA mediated by an anterior cruciate ligament (ACL) injury can be influenced by inflammation and antibiotics administration shortly prior to the injury. Our studies have led to the following overall conclusions:

1. *Female mice are more susceptible to cartilage degradation than the males of the same strain*. Prior work from our lab, described the PTOA phenotype of *C57Bl/6J*, *MRL/MpJ* and *STR/ort* male mice at 12 weeks post injury, and showed that *MRL/MpJ* males were resistant to PTOA while *STR/ort* males were more susceptible to PTOA relative to the *C57Bl/6J* strain[86]. In this study, we examined the phenotype at an earlier time point, six weeks post-injury, and included female cohorts. Unlike males, the *MRL/MpJ* female mice exhibited a PTOA phenotype, but this phenotype was significantly milder than both *C57Bl/6J* injured male and female joints. Both *C3H/HeJ* and *STR/ort* strains exhibited OA phenotypes independent of injury and independent of sex, but females were had significantly more cartilage loss than the males. Upon injury, animals of both these strains developed very severe PTOA, but the phenotypes of these animals were equally severe in male and female mice, such that no statistically significant differences were observed between sexes or these two strains. Interestingly, *C57Bl/6J* injured females developed more severe PTOA phenotypes than the *C57Bl/6J* injured males, and the phenotypes in *C57Bl/6J* females were as severe as those observed for the *C3H/HeJ* and *STR/ort* strains, suggesting that only *C57Bl/6J* males develop moderate PTOA phenotypes in the TC injury model.
2. *LPS induced inflammation prior to injury exacerbates the development of post-traumatic osteoarthritis in C57Bl/6J mice*. Our inflammation study revealed that the residual effects of a single dose of LPS induced

inflammation are still present five days post-treatment and can significantly modify PTOA outcomes in response to joint injury. Gene expression changes 24 hours post injury showed a significant down-regulation of genes associated with bone and cartilage matrix formation. The most striking phenotype we observed in this study was that *MRL/MpJ* males, which are normally resistant to PTOA, now develop mild PTOA phenotypes. With the exception of the *C3H/HeJ* strain which is insensitive to LPS, all other injured strains, both males and females, had more severe OA phenotypes in the LPS treated groups when compared to the VEH groups. This is a very significant result and it may in part explain why 50% of people who suffer an ACL injury go on to develop PTOA while 50% spontaneously resolve the injury. In future experiments we hope to identify ways to identify these patients at higher risk, as well as block this negative immune effect, to alleviate the unwarranted risk of PTOA in this high-risk group.

3. *Antibiotic treatment prior to injury rescues the cartilage phenotype of post-traumatic osteoarthritis on C57BL/6J mice*. The cartilage phenotype for every strain and sex treated with antibiotics improves six weeks after injury. We see that there is a decrease in the OARSI scoring, indicating a better PTOA outcome for those treated with OA. This is significant since it suggests that modifications to the gut microbiome can improve the PTOA outcome.
4. *LPS induced inflammation blunts the positive effect of AB in C57Bl/6J, C3H/HeJ, and STR/ort while worsening the PTOA outcome on MRL/MpJ. C57Bl/6J, C3H/HeJ*, and *STR/ort* mice all show that there is no significant difference between the VEH and the AB+LPS treated mice. This suggests that a single LPS injection is enough to worsen the phenotype even after treatment with AB for 6 weeks. *MRL/MpJ* mice show that there is an increase on the OARSI score of the mice treated with AB+LPS compared to the VEH. Suggesting that LPS has a

negative effect on the cartilage phenotype of *MRL/MpJ* even with the combination of AB treatment.

5. *Antibiotics increase the bone resorption in C57Bl/6J.* Our antibiotic study revealed that the effects of a modification of the gut microbiome through antibiotic usage would increase the resorption of bone while increasing cartilage staining. The AB-treated injured male joints show a decrease in trabecular thickness that is significant compared to the VEH joints. This suggests that there is going to be higher bone resorption associated with AB treatment. Antibiotic treated injured joints show subchondral bone loss compared to the untreated injured joints. This allows us to conclude that prolonged AB treatment during bone development after weaning is enough to lower bone mass density independent of it continuing later in life.

These studies heavily relied on the use of histological analysis in order to identify changes to the PTOA phenotype and study the immune changes happening within the synovium. Histology provides a visualization of the bone and cartilage in order to compare how the joint will look after injury. Histological analysis is based on researchers recognizing joint landmarks and cell morphology in order to establish the area of interest. Although histology provides a view into the joint damage caused by an ACL injury it is a qualitative study that can be subjective due to it being open for interpretation. We combat this by using blind scoring by multiple observers to assure blind assessment of the joints. Future work should include a quantitative approach using an algorithm to provide a more unbiased histological analysis.

Immune profiling heavily relied on immunohistochemistry for these experiments. In future directions should use the infrapatellar fat pad and compare it to the population of the rest of the joint to, in order to describe the changes in the inactive macrophage populations that circulate in the synovium[209]. This is significant due to results from previous experiments using the whole joint at

various timepoints did not show significant changes between the immune cells, we believe a more concentrated effort will show the changes in the immune populations of the different strains, treatments, and sex. Future investigation should focus on dissecting the fat pad which we have seen in previous experiments to be much larger due to inflammation and cellular infiltration on the injured joints or LPS treated joints compared to the VEH and uninjured joints (**Fig 1**). Then use FACS to analyze the immune profile of the fat pads to see how immune cell infiltration changes depending on injury and treatment. This should provide insights into the immune population activity depending on the strain susceptibility to PTOA. In clinical studies they could apply this by applying immune-profiling that could allow for screening of high risk patients and using personalized medicine to decrease the risk and prolong the time prior to joint replacement surgery.

Our findings revealed that PTOA severity might be sex-linked. PTOA phenotype was more severe for every female strain, even in the resistant *MRL/MpJ* data indicates that there are changes to the females that were not present in the males. The females of each strain seem to be more severely affected by PTOA and even the spontaneous development of OA on the *C3H/HeJ* female uninjured contralateral joints. Analyzing gene expression data for females could provide valuable insight into how inflammation and bone and cartilage formation could be negatively affected on females compared to males. This could aid in understanding how female patients could have exacerbated phenotypes compared to male patients in the clinic.

This study showed that a state of inflammation prior to injury is more harmful to PTOA outcomes and increases the severity of the disease than the state of inflammation during or shortly after the injury. For example, for a set of inflammatory markers we see that LPS alone upregulates these transcripts in the joint, which the injury itself in VEH treated animals does not produce this effect. In contrast, these up-regulates inflammatory markers emerged in the LPS injured joints, but interesting injured joints in animals challenged with LPS seem to

actually have a slight reduction in the levels of some inflammatory markers relative to the uninjured sham joints. For example, the toll-like receptor 5 (TLR5), is actually down-regulated in LPS injured joints relative to LPS uninjured joints. TLR5 expression levels have recently been linked to RA, where elevated levels of TLR5 were identified in macrophages within the synovial fluid of RA patients[107,158,208]. This is novel due to LPS being a toll-like receptor 4 (TLR4) activator and having no previous relationship to the activation of TLR5 and we can see that the RA-like synovitis activated by LPS in our uninjured samples similarly activates this pathway.

In future experiments we should survey synovial macrophages and determine whether high levels of TLR5 persist in LPS injured mice compared to VEH injured groups. If this molecular phenotype persists, we can explore the use of TLR5 blocking molecules for the prevention of PTOA in injured joints. Persistently elevated levels of inflammation after injury cause a more severe PTOA phenotype[71,211]. Our study demonstrates that with a single spike in inflammation days prior to injury has an exacerbated effect on bone and cartilage resorption. This leads to question relating to how unresolved inflammation can have a negative effect on the ECM and causes gene expression changes that hinder the joint's ability to heal. Compared to *C57Bl/6J* inflammation is able to be quickly resolved on *MRL/MpJ* mice since they have virtually no changes on the bone phenotype but the inflammation effect on *C57Bl/6J* is so severe that the bone volume that was not significant on the untreated becomes significantly less when exposed to inflammation. In female *MRL/MpJ* mice, LPS exposure significantly alters the resorption of cartilage in the injured joint.

To date only two studies have explored the relationship between the gut biome and osteoarthritis development, but both studies were carried out in the context of obesity[211]. Conflicting results have come from studying how antibiotic treatment and the gut microbiome affects bone, but no studies have examined the effects of gut biome depletion through antibiotic administration on cartilage with and without injury. We found that AB treatment prior to injury had an overall

positive effect on PTOA outcomes. We observed significant improvement in cartilage morphology in the majority of the treated joints, including the *STR/ort* joint which exhibited the most severe PTOA phenotype of all the VEH treated strains. Interestingly the was a strong negative correlation between BV/TV percent loss post injury and cartilage integrity, such that a larger percent of subchondral bone loss correlated with less cartilage loss.

AB treatment also significantly influenced the formation of osteophytes, such that AB groups had significantly less external bone growths in the *C57Bl/6J* male mice and the *STR/ort* male and female mice. The finding that the *STR/ort* mouse cartilage phenotype could be improve is a very valuable insight, since these mice are genetically prone to OA, and provides new avenues for exploring how to prevent damage and potentially even build new cartilage, in individuals in early stages of the disease. Lastly, we found that the combination of both AB+LPS treatments was not very significant on most strains, except for *MRL/MpJ* which have already been shown to resolve inflammation differently. This data indicates that either treatment can have an effect on disease development, but likely through different pathways.

In conclusion, our findings provide insights into new factors that should be taken into account in order to determine the progression to PTOA. In chapter 2 and 4 we found that females are susceptible to a more severe form of PTOA. In chapter 3 we observed that a single spike in inflammation that does not show outwardly appearance of affecting the system is enough to cause a dramatically more severe PTOA phenotype. In chapter 4 we look at how long-term antibiotic treatment can negatively affect bone while positively affecting the cartilage during development of PTOA. Chapter 5 shows that inflammation is capable of changing the susceptibility to PTOA to the most resistant inbred mice strains and antibiotics can help strains that are extremely susceptible.

Our future studies will aim to look at the female groups that did not receive treatment, increase the group size in order to establish statistical significance for the groups that did not have. We will analyze gene expression changes at

multiple time points and on multiple strains in order to compare how the bone and cartilage matrix formation is affected by the treatment. Last, we will perform the fat pad flow cytometry analysis in order to characterize the cellularity that we observed on our joints.

Through this study we were able to pinpoint aspects that could relate back to patients in the clinic. Early inflammation resolution similar to that of *MRL/MpJ* could indicate a better outcome and a lower risk for PTOA, this could be compromised by residual inflammation coming from an infection. Obesity, chronic inflammation like RA or Crohn's disease, and an elevation of inflammation inducing commensals would indicate an accelerated PTOA outcome. Screening of inflammatory cytokines could provide an insight into higher risk individuals. These patients should be more closely monitored to prolong the chronic phase of PTOA and delay full-joint replacement surgery. As a long-term goal we should create pharmaceutical intervention to reduce levels of inflammation during the immediate and acute phases of PTOA like TLR blockers. However, during the short-term treatment with NSAIDs immediately after injury should be given as a standard and probiotic treatment with inflammation reducing probiotics. The results presented in this study provide a better understanding of factors that affect the development of PTOA, they provide a guideline for studying the mechanisms that are influencing the severity and PTOA outcome of ~50% of people who suffered a severe articular injury, and will eventually help us prevent it, possibly.

Figures

Figure 1. Infrapatellar Fat Pad on Uninjured and Injured Joints

Infrapatellar fat pad of injured joints has been observed to be larger. Literature states that has cellular infiltration. We will characterize the cellular infiltration in future experiments.

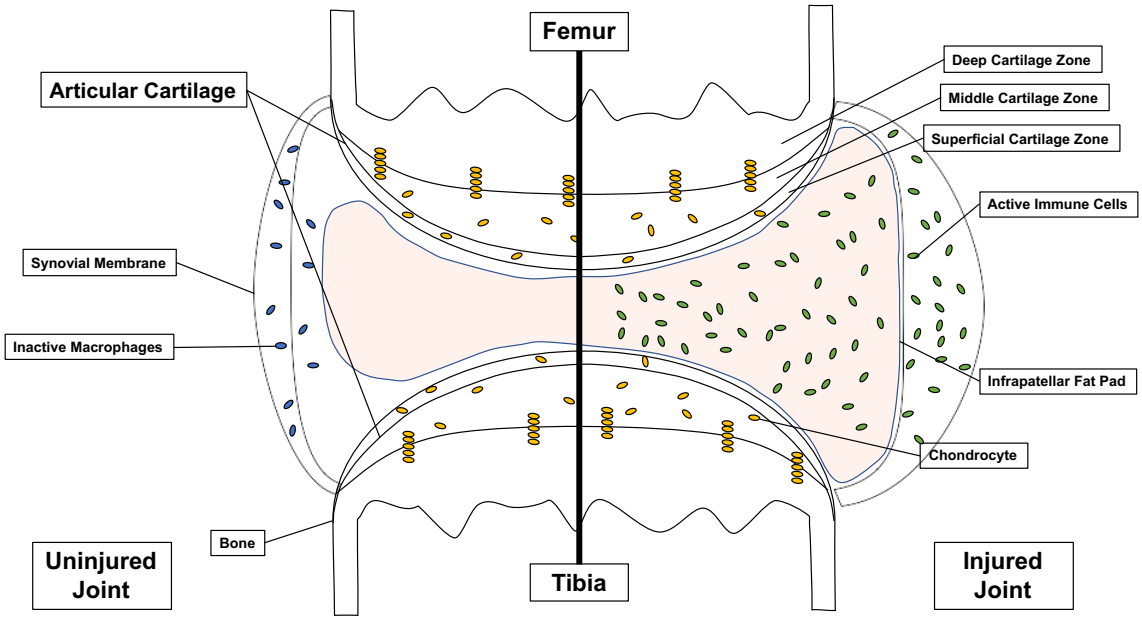

References

1. Su N, Yang J, Xie Y, et al. Bone function, dysfunction and its role in diseases including critical illness. *Int J Biol Sci*. 2019;15(4):776-787. doi:10.7150/ijbs.27063

2. Sommerfeldt DW, Rubin CT. Biology of bone and how it orchestrates the form and function of the skeleton. *Eur Spine J Off Publ Eur Spine Soc Eur Spinal Deform Soc Eur Sect Cerv Spine Res Soc*. 2001;10 Suppl 2:S86-95. doi:10.1007/s005860100283

3. Frassica FJ, Inoue N, Virolainen P, Chao EY. Skeletal system: biomechanical concepts and relationships to normal and abnormal conditions. *Semin Nucl Med*. 1997;27(4):321-327. doi:10.1016/s0001-2998(97)80004-9

4. *Office of the Surgeon General (US). Bone Health and Osteoporosis: A Report of the Surgeon General*. Office of the Surgeon General; 2004. https://www.ncbi.nlm.nih.gov/books/NBK45504/.

5. Marieb EN, Hoehn K. *Human Anatomy & Physiology*. Eleventh edition. Hoboken, New Jersey: Pearson; 2018.

6. Mader SS, Windelspecht M. *Human Biology*. 13th ed. New York, NY: McGraw-Hill; 2014.

7. Clarke B. Normal bone anatomy and physiology. *Clin J Am Soc Nephrol CJASN*. 2008;3 Suppl 3:S131-139. doi:10.2215/CJN.04151206

8. Toogood PA, Skalak A, Cooperman DR. Proximal femoral anatomy in the normal human population. *Clin Orthop*. 2009;467(4):876-885. doi:10.1007/s11999-008-0473-3

9. Khan IM, Redman SN, Williams R, Dowthwaite GP, Oldfield SF, Archer CW. The Development of Synovial Joints. In: *Current Topics in Developmental Biology*. Vol 79. Elsevier; 2007:1-36. doi:10.1016/S0070-2153(06)79001-9

10. Makris EA, Hadidi P, Athanasiou KA. The knee meniscus: structure-function, pathophysiology, current repair techniques, and prospects for regeneration. *Biomaterials*. 2011;32(30):7411-7431. doi:10.1016/j.biomaterials.2011.06.037

11. Fox AJS, Bedi A, Rodeo SA. The basic science of human knee menisci: structure, composition, and function. *Sports Health*. 2012;4(4):340-351. doi:10.1177/1941738111429419

12. Eyre DR, Wu JJ. Collagen of fibrocartilage: a distinctive molecular phenotype in bovine meniscus. *FEBS Lett*. 1983;158(2):265-270. doi:10.1016/0014-5793(83)80592-4

13. Lowe J, Almarza AJ. A review of in-vitro fibrocartilage tissue engineered therapies with a focus on the temporomandibular joint. *Arch Oral Biol*. 2017;83:193-201. doi:10.1016/j.archoralbio.2017.07.013

14. Juneja P, Hubbard JB. *Anatomy, Joints*. StatPearls Publishing; 2018. https://www.ncbi.nlm.nih.gov/books/NBK507893/.

15. Murphy MK, Masters TE, Hu JC, Athanasiou KA. Engineering a fibrocartilage spectrum through modulation of aggregate redifferentiation. *Cell Transplant*. 2015;24(2):235-245. doi:10.3727/096368913X676204

16. Thomopoulos S, Das R, Birman V, et al. Fibrocartilage tissue engineering: the role of the stress environment on cell morphology and matrix expression. *Tissue Eng Part A*. 2011;17(7-8):1039-1053. doi:10.1089/ten.TEA.2009.0499

17. Benjamin M, Evans EJ. Fibrocartilage. *J Anat*. 1990;171:1-15.

18. Benjamin M, Ralphs JR. Fibrocartilage in tendons and ligaments--an adaptation to compressive load. *J Anat*. 1998;193 (Pt 4):481-494. doi:10.1046/j.1469-7580.1998.19340481.x

19. Benjamin M, Ralphs JR. Biology of fibrocartilage cells. *Int Rev Cytol*. 2004;233:1-45. doi:10.1016/S0074-7696(04)33001-9

20. Kariyama Y. Effect of Jump Direction on Joint Kinetics of Take-Off Legs in Double-Leg Rebound Jumps. *Sports Basel Switz*. 2019;7(8). doi:10.3390/sports7080183

21. Ritzmann R, Freyler K, Kümmel J, et al. High Intensity Jump Exercise Preserves Posture Control, Gait, and Functional Mobility During 60 Days of Bed-Rest: An RCT Including 90 Days of Follow-Up. *Front Physiol*. 2018;9:1713. doi:10.3389/fphys.2018.01713

22. Luo Y, Sinkeviciute D, He Y, et al. The minor collagens in articular cartilage. *Protein Cell*. 2017;8(8):560-572. doi:10.1007/s13238-017-0377-7

23. Sophia Fox AJ, Bedi A, Rodeo SA. The basic science of articular cartilage: structure, composition, and function. *Sports Health*. 2009;1(6):461-468. doi:10.1177/1941738109350438

24. Yoon T-H, Jung M, Choi C-H, et al. Arthroscopic gel-type autologous chondrocyte implantation presents histologic evidence of regenerating hyaline-like cartilage in the knee with articular cartilage defect. *Knee Surg*

Sports Traumatol Arthrosc Off J ESSKA. June 2019. doi:10.1007/s00167-019-05572-6

25. Mahbub SB, Guller A, Campbell JM, et al. Non-Invasive Monitoring of Functional State of Articular Cartilage Tissue with Label-Free Unsupervised Hyperspectral Imaging. *Sci Rep*. 2019;9(1):4398. doi:10.1038/s41598-019-40942-7

26. Alberton P, Dugonitsch HC, Hartmann B, et al. Aggrecan Hypomorphism Compromises Articular Cartilage Biomechanical Properties and Is Associated with Increased Incidence of Spontaneous Osteoarthritis. *Int J Mol Sci*. 2019;20(5). doi:10.3390/ijms20051008

27. Nebelung S, Post M, Knobe M, et al. Detection of Early-Stage Degeneration in Human Articular Cartilage by Multiparametric MR Imaging Mapping of Tissue Functionality. *Sci Rep*. 2019;9(1):5895. doi:10.1038/s41598-019-42543-w

28. Raggatt LJ, Partridge NC. Cellular and molecular mechanisms of bone remodeling. *J Biol Chem*. 2010;285(33):25103-25108. doi:10.1074/jbc.R109.041087

29. Chocholata P, Kulda V, Babuska V. Fabrication of Scaffolds for Bone-Tissue Regeneration. *Mater Basel Switz*. 2019;12(4). doi:10.3390/ma12040568

30. Tang KC, Pan W, Doschak MR, Alexander RT. Increased FoxO3a expression prevents osteoblast differentiation and matrix calcification. *Bone Rep*. 2019;10:100206. doi:10.1016/j.bonr.2019.100206

31. Patel JJ, Bourne LE, Davies BK, et al. Differing calcification processes in cultured vascular smooth muscle cells and osteoblasts. *Exp Cell Res*. 2019;380(1):100-113. doi:10.1016/j.yexcr.2019.04.020

32. Buckwalter JA. Articular cartilage: injuries and potential for healing. *J Orthop Sports Phys Ther*. 1998;28(4):192-202. doi:10.2519/jospt.1998.28.4.192

33. Clark D, Nakamura M, Miclau T, Marcucio R. Effects of Aging on Fracture Healing. *Curr Osteoporos Rep*. 2017;15(6):601-608. doi:10.1007/s11914-017-0413-9

34. Tanaka Y, Nakayamada S, Okada Y. Osteoblasts and osteoclasts in bone remodeling and inflammation. *Curr Drug Targets Inflamm Allergy*. 2005;4(3):325-328.

35. Akizuki S, Mow VC, Müller F, Pita JC, Howell DS, Manicourt DH. Tensile properties of human knee joint cartilage: I. Influence of ionic conditions, weight bearing, and fibrillation on the tensile modulus. *J Orthop Res Off Publ Orthop Res Soc*. 1986;4(4):379-392. doi:10.1002/jor.1100040401

36. Kiapour AM, Sieker JT, Proffen BL, Lam TT, Fleming BC, Murray MM. Synovial fluid proteome changes in ACL injury-induced posttraumatic osteoarthritis: Proteomics analysis of porcine knee synovial fluid. *PloS One*. 2019;14(3):e0212662. doi:10.1371/journal.pone.0212662

37. Clair AJ, Kingery MT, Anil U, Kenny L, Kirsch T, Strauss EJ. Alterations in Synovial Fluid Biomarker Levels in Knees With Meniscal Injury as Compared With Asymptomatic Contralateral Knees. *Am J Sports Med*. 2019;47(4):847-856. doi:10.1177/0363546519825498

38. Warnecke D, Meßemer M, de Roy L, et al. Articular cartilage and meniscus reveal higher friction in swing phase than in stance phase under dynamic gait conditions. *Sci Rep*. 2019;9(1):5785. doi:10.1038/s41598-019-42254-2

39. Cox CF, Bordoni B. Anatomy, Bony Pelvis and Lower Limb, Knee Posterior Cruciate Ligament. In: *StatPearls*. Treasure Island (FL): StatPearls Publishing; 2019. http://www.ncbi.nlm.nih.gov/books/NBK535416/. Accessed August 26, 2019.

40. Krause M, Freudenthaler F, Frosch K-H, Achtnich A, Petersen W, Akoto R. Operative Versus Conservative Treatment of Anterior Cruciate Ligament Rupture. *Dtsch Arzteblatt Int*. 2018;115(51-52):855-862. doi:10.3238/arztebl.2018.0855

41. Evans J, Nielson J I. Anterior Cruciate Ligament (ACL) Knee Injuries. In: *StatPearls*. Treasure Island (FL): StatPearls Publishing; 2019. http://www.ncbi.nlm.nih.gov/books/NBK499848/. Accessed August 26, 2019.

42. Raj MA, Varacallo M. Posterior Cruciate Ligament (PCL) Knee Injuries. In: *StatPearls*. Treasure Island (FL): StatPearls Publishing; 2019. http://www.ncbi.nlm.nih.gov/books/NBK430726/. Accessed August 26, 2019.

43. Elkin JL, Zamora E, Gallo RA. Combined Anterior Cruciate Ligament and Medial Collateral Ligament Knee Injuries: Anatomy, Diagnosis, Management Recommendations, and Return to Sport. *Curr Rev Musculoskelet Med*. 2019;12(2):239-244. doi:10.1007/s12178-019-09549-3

44. Usker Naqvi, Sherman AI. *Medial Collateral Ligament (MCL) Knee Injuries*. StatPearls Publishing; 2019. https://www.ncbi.nlm.nih.gov/books/NBK431095/.

45. Shea KG, Cannamela PC, Fabricant PD, et al. Lateral Radiographic Landmarks for ACL and LCL Footprint Origins During All-Epiphyseal Femoral Drilling in Skeletally Immature Knees. *J Bone Joint Surg Am*. 2017;99(6):506-511. doi:10.2106/JBJS.16.00641

46. Elsaid KA, Fleming BC, Oksendahl HL, et al. Decreased lubricin concentrations and markers of joint inflammation in the synovial fluid of patients with anterior cruciate ligament injury. *Arthritis Rheum*. 2008;58(6):1707-1715. doi:10.1002/art.23495

47. Lombardi G, Ziemann E, Banfi G. Physical Activity and Bone Health: What Is the Role of Immune System? A Narrative Review of the Third Way. *Front Endocrinol*. 2019;10:60. doi:10.3389/fendo.2019.00060

48. Stannus O, Jones G, Cicuttini F, et al. Circulating levels of IL-6 and TNF-α are associated with knee radiographic osteoarthritis and knee cartilage loss in older adults. *Osteoarthritis Cartilage*. 2010;18(11):1441-1447. doi:10.1016/j.joca.2010.08.016

49. Yuan G-H, Tanaka M, Masuko-Hongo K, et al. Characterization of cells from pannus-like tissue over articular cartilage of advanced osteoarthritis. *Osteoarthritis Cartilage*. 2004;12(1):38-45.

50. Mehana E-SE, Khafaga AF, El-Blehi SS. The role of matrix metalloproteinases in osteoarthritis pathogenesis: An updated review. *Life Sci*. 2019;234:116786. doi:10.1016/j.lfs.2019.116786

51. Adamopoulos IE. Inflammation in bone physiology and pathology. *Curr Opin Rheumatol*. 2018;30(1):59-64. doi:10.1097/BOR.0000000000000449

52. Stolina M, Schett G, Dwyer D, et al. RANKL inhibition by osteoprotegerin prevents bone loss without affecting local or systemic inflammation parameters in two rat arthritis models: comparison with anti-TNFalpha or anti-IL-1 therapies. *Arthritis Res Ther*. 2009;11(6):R187. doi:10.1186/ar2879

53. van der Kraan PM. The Interaction between Joint Inflammation and Cartilage Repair. *Tissue Eng Regen Med*. 2019;16(4):327-334. doi:10.1007/s13770-019-00204-z

54. Sellam J, Berenbaum F. The role of synovitis in pathophysiology and clinical symptoms of osteoarthritis. *Nat Rev Rheumatol*. 2010;6(11):625-635. doi:10.1038/nrrheum.2010.159

55. Carbone A, Rodeo S. Review of current understanding of post-traumatic osteoarthritis resulting from sports injuries. *J Orthop Res Off Publ Orthop Res Soc*. 2017;35(3):397-405. doi:10.1002/jor.23341

56. Hsu H, Siwiec RM. Knee Osteoarthritis. In: *StatPearls*. Treasure Island (FL): StatPearls Publishing; 2019. http://www.ncbi.nlm.nih.gov/books/NBK507884/. Accessed August 27, 2019.

57. Shane Anderson A, Loeser RF. Why is osteoarthritis an age-related disease? *Best Pract Res Clin Rheumatol*. 2010;24(1):15-26. doi:10.1016/j.berh.2009.08.006

58. Loeser RF. The Role of Aging in the Development of Osteoarthritis. *Trans Am Clin Climatol Assoc*. 2017;128:44-54.

59. Feng JE, Novikov D, Anoushiravani AA, Schwarzkopf R. Total knee arthroplasty: improving outcomes with a multidisciplinary approach. *J Multidiscip Healthc*. 2018;11:63-73. doi:10.2147/JMDH.S140550

60. Weber M, Renkawitz T, Voellner F, et al. Revision Surgery in Total Joint Replacement Is Cost-Intensive. *BioMed Res Int*. 2018;2018:8987104. doi:10.1155/2018/8987104

61. Bliddal H, Leeds AR, Christensen R. Osteoarthritis, obesity and weight loss: evidence, hypotheses and horizons - a scoping review. *Obes Rev Off J Int Assoc Study Obes*. 2014;15(7):578-586. doi:10.1111/obr.12173

62. Messier SP. Obesity and osteoarthritis: disease genesis and nonpharmacologic weight management. *Rheum Dis Clin North Am*. 2008;34(3):713-729. doi:10.1016/j.rdc.2008.04.007

63. Steinmeyer J, Bock F, Stöve J, Jerosch J, Flechtenmacher J. Pharmacological treatment of knee osteoarthritis: Special considerations of the new German guideline. *Orthop Rev*. 2018;10(4):7782. doi:10.4081/or.2018.7782

64. Watt FE, Gulati M. New Drug Treatments for Osteoarthritis: What is on the Horizon? *Eur Med J Rheumatol*. 2017;2(1):50-58.

65. Wu Y, Goh EL, Wang D, Ma S. Novel treatments for osteoarthritis: an update. *Open Access Rheumatol Res Rev*. 2018;10:135-140. doi:10.2147/OARRR.S176666

66. Hermann W, Lambova S, Muller-Ladner U. Current Treatment Options for Osteoarthritis. *Curr Rheumatol Rev*. 2018;14(2):108-116. doi:10.2174/1573397113666170829155149

67. Yu SP, Hunter DJ. Managing osteoarthritis. *Aust Prescr*. 2015;38(4):115-119.

68. Harkey MS, Luc BA, Golightly YM, et al. Osteoarthritis-related biomarkers following anterior cruciate ligament injury and reconstruction: a systematic review. *Osteoarthritis Cartilage*. 2015;23(1):1-12. doi:10.1016/j.joca.2014.09.004

69. Godziuk K, Prado CM, Woodhouse LJ, Forhan M. The impact of sarcopenic obesity on knee and hip osteoarthritis: a scoping review. *BMC Musculoskelet Disord*. 2018;19(1):271. doi:10.1186/s12891-018-2175-7

70. Daniel DM, Stone ML, Dobson BE, Fithian DC, Rossman DJ, Kaufman KR. Fate of the ACL-injured patient. A prospective outcome study. *Am J Sports Med*. 1994;22(5):632-644. doi:10.1177/036354659402200511

71. Lieberthal J, Sambamurthy N, Scanzello CR. Inflammation in joint injury and post-traumatic osteoarthritis. *Osteoarthritis Cartilage*. 2015;23(11):1825-1834. doi:10.1016/j.joca.2015.08.015

72. Punzi L, Galozzi P, Luisetto R, et al. Post-traumatic arthritis: overview on pathogenic mechanisms and role of inflammation. *RMD Open*. 2016;2(2):e000279. doi:10.1136/rmdopen-2016-000279

73. Lotz MK, Kraus VB. New developments in osteoarthritis. Posttraumatic osteoarthritis: pathogenesis and pharmacological treatment options. *Arthritis Res Ther*. 2010;12(3):211. doi:10.1186/ar3046

74. Bigoni M, Sacerdote P, Turati M, et al. Acute and late changes in intraarticular cytokine levels following anterior cruciate ligament injury. *J Orthop Res Off Publ Orthop Res Soc*. 2013;31(2):315-321. doi:10.1002/jor.22208

75. Sun AR, Wu X, Liu B, et al. Pro-resolving lipid mediator ameliorates obesity induced osteoarthritis by regulating synovial macrophage polarisation. *Sci Rep*. 2019;9(1):426. doi:10.1038/s41598-018-36909-9

76. Christiansen BA, Guilak F, Lockwood KA, et al. Non-invasive mouse models of post-traumatic osteoarthritis. *Osteoarthritis Cartilage*. 2015;23(10):1627-1638. doi:10.1016/j.joca.2015.05.009

77. Christiansen BA, Anderson MJ, Lee CA, Williams JC, Yik JHN, Haudenschild DR. Musculoskeletal changes following non-invasive knee injury using a novel mouse model of post-traumatic osteoarthritis. *Osteoarthritis Cartilage*. 2012;20(7):773-782. doi:10.1016/j.joca.2012.04.014

78. Staines KA, Poulet B, Wentworth DN, Pitsillides AA. The STR/ort mouse model of spontaneous osteoarthritis - an update. *Osteoarthritis Cartilage*. 2017;25(6):802-808. doi:10.1016/j.joca.2016.12.014

79. de Hooge ASK, van de Loo FAJ, Bennink MB, Arntz OJ, de Hooge P, van den Berg WB. Male IL-6 gene knock out mice developed more advanced osteoarthritis upon aging. *Osteoarthritis Cartilage*. 2005;13(1):66-73. doi:10.1016/j.joca.2004.09.011

80. Rushton MD, Reynard LN, Young DA, et al. Methylation quantitative trait locus analysis of osteoarthritis links epigenetics with genetic risk. *Hum Mol Genet*. 2015;24(25):7432-7444. doi:10.1093/hmg/ddv433

81. Bapat S, Hubbard D, Munjal A, Hunter M, Fulzele S. Pros and cons of mouse models for studying osteoarthritis. *Clin Transl Med*. 2018;7(1):36. doi:10.1186/s40169-018-0215-4

82. Chang JC, Sebastian A, Murugesh DK, et al. Global molecular changes in a tibial compression induced ACL rupture model of post-traumatic osteoarthritis: GLOBAL MOLECULAR CHANGES AFTER ACL INJURY. *J Orthop Res*. 2017;35(3):474-485. doi:10.1002/jor.23263

83. Schenker ML, Mauck RL, Ahn J, Mehta S. Pathogenesis and prevention of posttraumatic osteoarthritis after intra-articular fracture. *J Am Acad Orthop Surg*. 2014;22(1):20-28. doi:10.5435/JAAOS-22-01-20

84. Ko FC, Dragomir C, Plumb DA, et al. In vivo cyclic compression causes cartilage degeneration and subchondral bone changes in mouse tibiae. *Arthritis Rheum*. 2013;65(6):1569-1578. doi:10.1002/art.37906

85. Kuyinu EL, Narayanan G, Nair LS, Laurencin CT. Animal models of osteoarthritis: classification, update, and measurement of outcomes. *J Orthop Surg*. 2016;11:19. doi:10.1186/s13018-016-0346-5

86. Sebastian A, Chang JC, Mendez ME, et al. Comparative Transcriptomics Identifies Novel Genes and Pathways Involved in Post-Traumatic Osteoarthritis Development and Progression. *Int J Mol Sci*. 2018;19(9). doi:10.3390/ijms19092657

87. Ward BD, Furman BD, Huebner JL, Kraus VB, Guilak F, Olson SA. Absence of posttraumatic arthritis following intraarticular fracture in the MRL/MpJ mouse. *Arthritis Rheum*. 2008;58(3):744-753. doi:10.1002/art.23288

88. Furman BD, Huebner JL, Seifer DR, Kraus VB, Guilak F, Olson SA. MRL/MpJ Mouse Shows Reduced Intra-Articular and Systemic Inflammation Following Articular Fracture. In: Las Vegas, NV; 2009:1120.

89. Altman FP. A metabolic dysfunction in early murine osteoarthritis. *Ann Rheum Dis*. 1981;40(3):303-306. doi:10.1136/ard.40.3.303

90. Deng Z, Gao X, Sun X, et al. Characterization of articular cartilage homeostasis and the mechanism of superior cartilage regeneration of MRL/MpJ mice. *FASEB J Off Publ Fed Am Soc Exp Biol*. 2019;33(8):8809-8821. doi:10.1096/fj.201802132RR

91. Kyostio-Moore S, Nambiar B, Hutto E, et al. STR/ort mice, a model for spontaneous osteoarthritis, exhibit elevated levels of both local and systemic inflammatory markers. *Comp Med*. 2011;61(4):346-355.

92. Mason RM, Chambers MG, Flannelly J, Gaffen JD, Dudhia J, Bayliss MT. The STR/ort mouse and its use as a model of osteoarthritis. *Osteoarthritis Cartilage*. 2001;9(2):85-91. doi:10.1053/joca.2000.0363

93. Botter SM, van Osch GJVM, Waarsing JH, et al. Cartilage damage pattern in relation to subchondral plate thickness in a collagenase-induced model of osteoarthritis. *Osteoarthritis Cartilage*. 2008;16(4):506-514. doi:10.1016/j.joca.2007.08.005

94. Chen C, Kalu DN. Strain differences in bone density and calcium metabolism between C3H/HeJ and C57BL/6J mice. *Bone*. 1999;25(4):413-420. doi:10.1016/s8756-3282(99)00185-4

95. Sheng MH-C, Baylink DJ, Beamer WG, et al. Histomorphometric studies show that bone formation and bone mineral apposition rates are greater in C3H/HeJ (high-density) than C57BL/6J (low-density) mice during growth. *Bone*. 1999;25(4):421-429. doi:10.1016/S8756-3282(99)00184-2

96. Vogel SN, Johnson D, Perera P-Y, et al. Cutting Edge: Functional Characterization of the Effect of the C3H/HeJ Defect in Mice that Lack an Lpsⁿ Gene: In Vivo Evidence for a Dominant Negative Mutation. *J Immunol*. 1999;162(10):5666.

97. Hoshino K, Takeuchi O, Kawai T, et al. Cutting Edge: Toll-Like Receptor 4 (TLR4)-Deficient Mice Are Hyporesponsive to Lipopolysaccharide: Evidence for TLR4 as the Lps Gene Product. *J Immunol*. 1999;162(7):3749.

98. Lockwood KA, Chu BT, Anderson MJ, Haudenschild DR, Christiansen BA. Comparison of loading rate-dependent injury modes in a murine model of post-traumatic osteoarthritis. *J Orthop Res Off Publ Orthop Res Soc*. 2014;32(1):79-88. doi:10.1002/jor.22480

99. Hashimoto S, Creighton-Achermann L, Takahashi K, Amiel D, Coutts RD, Lotz M. Development and regulation of osteophyte formation during experimental osteoarthritis. *Osteoarthritis Cartilage*. 2002;10(3):180-187. doi:10.1053/joca.2001.0505

100. van der Kraan PM, van den Berg WB. Osteophytes: relevance and biology. *Osteoarthritis Cartilage*. 2007;15(3):237-244. doi:10.1016/j.joca.2006.11.006

101. Hernandez CJ, Guss JD, Luna M, Goldring SR. Links Between the Microbiome and Bone. *J Bone Miner Res Off J Am Soc Bone Miner Res*. 2016;31(9):1638-1646. doi:10.1002/jbmr.2887

102. McAleer JP, Vella AT. Understanding how lipopolysaccharide impacts CD4 T-cell immunity. *Crit Rev Immunol*. 2008;28(4):281-299.

103. Soares J-B, Pimentel-Nunes P, Roncon-Albuquerque R, Leite-Moreira A. The role of lipopolysaccharide/toll-like receptor 4 signaling in chronic liver diseases. *Hepatol Int*. 2010;4(4):659-672. doi:10.1007/s12072-010-9219-x

104. Cen X, Liu S, Cheng K. The Role of Toll-Like Receptor in Inflammation and Tumor Immunity. *Front Pharmacol*. 2018;9:878. doi:10.3389/fphar.2018.00878

105. Zeytun A, Chaudhary A, Pardington P, Cary R, Gupta G. Induction of cytokines and chemokines by Toll-like receptor signaling: strategies for control of inflammation. *Crit Rev Immunol*. 2010;30(1):53-67.

106. Takeda K, Akira S. Regulation of innate immune responses by Toll-like receptors. *Jpn J Infect Dis*. 2001;54(6):209-219.

107. Azam S, Jakaria M, Kim I-S, Kim J, Haque ME, Choi D-K. Regulation of Toll-Like Receptor (TLR) Signaling Pathway by Polyphenols in the Treatment of Age-Linked Neurodegenerative Diseases: Focus on TLR4 Signaling. *Front Immunol*. 2019;10:1000. doi:10.3389/fimmu.2019.01000

108. Fischer CR, Mikami M, Minematsu H, et al. Calreticulin inhibits inflammation-induced osteoclastogenesis and bone resorption. *J Orthop Res Off Publ Orthop Res Soc*. 2017;35(12):2658-2666. doi:10.1002/jor.23587

109. Behrends DA, Hui D, Gao C, et al. Defective Bone Repair in C57Bl6 Mice With Acute Systemic Inflammation. *Clin Orthop*. 2017;475(3):906-916. doi:10.1007/s11999-016-5159-7

110. Iqbal J, Yuen T, Sun L, Zaidi M. From the gut to the strut: where inflammation reigns, bone abstains. *J Clin Invest*. 2016;126(6):2045-2048. doi:10.1172/JCI87430

111. Wada T, Nakashima T, Hiroshi N, Penninger JM. RANKL-RANK signaling in osteoclastogenesis and bone disease. *Trends Mol Med*. 2006;12(1):17-25. doi:10.1016/j.molmed.2005.11.007

112. Steffen U, Schett G, Bozec A. How Autoantibodies Regulate Osteoclast Induced Bone Loss in Rheumatoid Arthritis. *Front Immunol*. 2019;10:1483. doi:10.3389/fimmu.2019.01483

113. Stagakis I, Bertsias G, Karvounaris S, et al. Anti-tumor necrosis factor therapy improves insulin resistance, beta cell function and insulin signaling in active rheumatoid arthritis patients with high insulin resistance. *Arthritis Res Ther*. 2012;14(3):R141. doi:10.1186/ar3874

114. Monfoulet L, Rabier B, Chassande O, Fricain J-C. Drilled hole defects in mouse femur as models of intramembranous cortical and cancellous bone regeneration. *Calcif Tissue Int*. 2010;86(1):72-81. doi:10.1007/s00223-009-9314-y

115. Todhunter PG, Kincaid SA, Todhunter RJ, et al. Immunohistochemical analysis of an equine model of synovitis-induced arthritis. *Am J Vet Res*. 1996;57(7):1080-1093.

116. Firth EC, Wensing T, Seuren F. An induced synovitis disease model in ponies. *Cornell Vet*. 1987;77(2):107-118.

117. Palmer JL, Bertone AL. Experimentally-induced synovitis as a model for acute synovitis in the horse. *Equine Vet J*. 1994;26(6):492-495. doi:10.1111/j.2042-3306.1994.tb04056.x

118. Hawkins DL, MacKay RJ, Gum GG, Colahan PT, Meyer JC. Effects of intra-articularly administered endotoxin on clinical signs of disease and synovial fluid tumor necrosis factor, interleukin 6, and prostaglandin E2 values in horses. *Am J Vet Res*. 1993;54(3):379-386.

119. Marks PH, Donaldson MLC. Inflammatory cytokine profiles associated with chondral damage in the anterior cruciate ligament-deficient knee. *Arthrosc J Arthrosc Relat Surg Off Publ Arthrosc Assoc N Am Int Arthrosc Assoc*. 2005;21(11):1342-1347. doi:10.1016/j.arthro.2005.08.034

120. Helmark IC, Mikkelsen UR, Børglum J, et al. Exercise increases interleukin-10 levels both intraarticularly and peri-synovially in patients with knee osteoarthritis: a randomized controlled trial. *Arthritis Res Ther*. 2010;12(4):R126. doi:10.1186/ar3064

121. Shen P-C, Wu C-L, Jou I-M, et al. T helper cells promote disease progression of osteoarthritis by inducing macrophage inflammatory protein-1γ. *Osteoarthritis Cartilage*. 2011;19(6):728-736. doi:10.1016/j.joca.2011.02.014

122. Schott EM, Farnsworth CW, Grier A, et al. Targeting the gut microbiome to treat the osteoarthritis of obesity. *JCI Insight*. 2018;3(8). doi:10.1172/jci.insight.95997

123. Bull MJ, Plummer NT. Part 1: The Human Gut Microbiome in Health and Disease. *Integr Med Encinitas Calif*. 2014;13(6):17-22.

124. Lozupone CA, Stombaugh JI, Gordon JI, Jansson JK, Knight R. Diversity, stability and resilience of the human gut microbiota. *Nature*. 2012;489(7415):220-230. doi:10.1038/nature11550

125. Shreiner AB, Kao JY, Young VB. The gut microbiome in health and in disease. *Curr Opin Gastroenterol*. 2015;31(1):69-75. doi:10.1097/MOG.0000000000000139

126. Kostic AD, Xavier RJ, Gevers D. The microbiome in inflammatory bowel disease: current status and the future ahead. *Gastroenterology*. 2014;146(6):1489-1499. doi:10.1053/j.gastro.2014.02.009

127. Cox LM, Yamanishi S, Sohn J, et al. Altering the intestinal microbiota during a critical developmental window has lasting metabolic consequences. *Cell*. 2014;158(4):705-721. doi:10.1016/j.cell.2014.05.052

128. Kane AV, Dinh DM, Ward HD. Childhood malnutrition and the intestinal microbiome. *Pediatr Res*. 2015;77(1-2):256-262. doi:10.1038/pr.2014.179

129. Chassaing B, Aitken JD, Gewirtz AT, Vijay-Kumar M. Gut microbiota drives metabolic disease in immunologically altered mice. *Adv Immunol*. 2012;116:93-112. doi:10.1016/B978-0-12-394300-2.00003-X

130. Tang WHW, Hazen SL. The contributory role of gut microbiota in cardiovascular disease. *J Clin Invest*. 2014;124(10):4204-4211. doi:10.1172/JCI72331

131. Zhang X, Zhang D, Jia H, et al. The oral and gut microbiomes are perturbed in rheumatoid arthritis and partly normalized after treatment. *Nat Med*. 2015;21(8):895-905. doi:10.1038/nm.3914

132. Wu X, He B, Liu J, et al. Molecular Insight into Gut Microbiota and Rheumatoid Arthritis. *Int J Mol Sci*. 2016;17(3):431. doi:10.3390/ijms17030431

133. Maeda Y, Takeda K. Role of Gut Microbiota in Rheumatoid Arthritis. *J Clin Med*. 2017;6(6). doi:10.3390/jcm6060060

134. Sjögren K, Engdahl C, Henning P, et al. The gut microbiota regulates bone mass in mice. *J Bone Miner Res Off J Am Soc Bone Miner Res*. 2012;27(6):1357-1367. doi:10.1002/jbmr.1588

135. Li J-Y, Chassaing B, Tyagi AM, et al. Sex steroid deficiency-associated bone loss is microbiota dependent and prevented by probiotics. *J Clin Invest*. 2016;126(6):2049-2063. doi:10.1172/JCI86062

136. Cho I, Yamanishi S, Cox L, et al. Antibiotics in early life alter the murine colonic microbiome and adiposity. *Nature*. 2012;488(7413):621-626. doi:10.1038/nature11400

137. *Outpatient Antibiotic Prescriptions — United States, 2017*. Center for Disease Control and Prevention; 2017. https://www.cdc.gov/antibiotic-use/community/programs-measurement/state-local-activities/outpatient-antibiotic-prescriptions-US-2017.html.

138. Anderson DD, Chubinskaya S, Guilak F, et al. Post-traumatic osteoarthritis: improved understanding and opportunities for early intervention. *J Orthop Res Off Publ Orthop Res Soc*. 2011;29(6):802-809. doi:10.1002/jor.21359

139. Yucesoy B, Charles LE, Baker B, Burchfiel CM. Occupational and genetic risk factors for osteoarthritis: a review. *Work Read Mass*. 2015;50(2):261-273. doi:10.3233/WOR-131739

140. Fernández-Moreno M, Rego I, Carreira-Garcia V, Blanco FJ. Genetics in osteoarthritis. *Curr Genomics*. 2008;9(8):542-547. doi:10.2174/138920208786847953

141. Bouxsein ML, Boyd SK, Christiansen BA, Guldberg RE, Jepsen KJ, Müller R. Guidelines for assessment of bone microstructure in rodents using micro-computed tomography. *J Bone Miner Res Off J Am Soc Bone Miner Res*. 2010;25(7):1468-1486. doi:10.1002/jbmr.141

142. Kim H-Y. Analysis of variance (ANOVA) comparing means of more than two groups. *Restor Dent Endod*. 2014;39(1):74-77. doi:10.5395/rde.2014.39.1.74

143. Kim TK. T test as a parametric statistic. *Korean J Anesthesiol*. 2015;68(6):540-546. doi:10.4097/kjae.2015.68.6.540

144. Chang JC, Christiansen BA, Murugesh DK, et al. SOST/Sclerostin Improves Posttraumatic Osteoarthritis and Inhibits MMP2/3 Expression After Injury: SOST OVEREXPRESSION IMPROVES PTOA OUTCOMES. *J Bone Miner Res*. 2018;33(6):1105-1113. doi:10.1002/jbmr.3397

145. Glasson SS, Chambers MG, Van Den Berg WB, Little CB. The OARSI histopathology initiative - recommendations for histological assessments of osteoarthritis in the mouse. *Osteoarthritis Cartilage*. 2010;18 Suppl 3:S17-23. doi:10.1016/j.joca.2010.05.025

146. Kessler MA, Behrend H, Henz S, Stutz G, Rukavina A, Kuster MS. Function, osteoarthritis and activity after ACL-rupture: 11 years follow-up results of conservative versus reconstructive treatment. *Knee Surg Sports Traumatol Arthrosc Off J ESSKA*. 2008;16(5):442-448. doi:10.1007/s00167-008-0498-x

147. Brestoff JR, Artis D. Commensal bacteria at the interface of host metabolism and the immune system. *Nat Immunol*. 2013;14(7):676-684. doi:10.1038/ni.2640

148. Goel PN, Egol AJ, Moharrer Y, Brandfield-Harvey B, Ahn J, Ashley JW. Notch signaling inhibition protects against LPS mediated osteolysis. *Biochem Biophys Res Commun*. 2019;515(4):538-543. doi:10.1016/j.bbrc.2019.05.166

149. Hardy R, Cooper MS. Bone loss in inflammatory disorders. *J Endocrinol*. 2009;201(3):309-320. doi:10.1677/JOE-08-0568

150. Lorenzo J, Horowitz M, Choi Y. Osteoimmunology: interactions of the bone and immune system. *Endocr Rev*. 2008;29(4):403-440. doi:10.1210/er.2007-0038

151. Redlich K, Smolen JS. Inflammatory bone loss: pathogenesis and therapeutic intervention. *Nat Rev Drug Discov*. 2012;11(3):234-250. doi:10.1038/nrd3669

152. Santos LCP, de Moraes AN, Saito ME. Effects of intraarticular ropivacaine and morphine on lipopolysaccharide-induced synovitis in horses. *Vet Anaesth Analg*. 2009;36(3):280-286. doi:10.1111/j.1467-2995.2009.00452.x

153. Teramachi J, Inagaki Y, Shinohara H, et al. PKR regulates LPS-induced osteoclast formation and bone destruction in vitro and in vivo. *Oral Dis*. 2017;23(2):181-188. doi:10.1111/odi.12592

154. Souza PPC, Lerner UH. The role of cytokines in inflammatory bone loss. *Immunol Invest*. 2013;42(7):555-622. doi:10.3109/08820139.2013.822766

155. Fairweather D, Cihakova D. Alternatively activated macrophages in infection and autoimmunity. *J Autoimmun*. 2009;33(3-4):222-230. doi:10.1016/j.jaut.2009.09.012

156. Wynn TA, Barron L, Thompson RW, et al. Quantitative Assessment of Macrophage Functions in Repair and Fibrosis. In: Coligan JE, Bierer BE,

Margulies DH, Shevach EM, Strober W, eds. *Current Protocols in Immunology*. Hoboken, NJ, USA: John Wiley & Sons, Inc.; 2011:im1422s93. doi:10.1002/0471142735.im1422s93

157. Guiducci C, Gong M, Cepika A-M, et al. RNA recognition by human TLR8 can lead to autoimmune inflammation. *J Exp Med*. 2013;210(13):2903-2919. doi:10.1084/jem.20131044

158. Kim S-J, Chen Z, Chamberlain ND, et al. Ligation of TLR5 promotes myeloid cell infiltration and differentiation into mature osteoclasts in rheumatoid arthritis and experimental arthritis. *J Immunol Baltim Md 1950*. 2014;193(8):3902-3913. doi:10.4049/jimmunol.1302998

159. Coelho AL, Schaller MA, Benjamim CF, Orlofsky AZ, Hogaboam CM, Kunkel SL. The chemokine CCL6 promotes innate immunity via immune cell activation and recruitment. *J Immunol Baltim Md 1950*. 2007;179(8):5474-5482. doi:10.4049/jimmunol.179.8.5474

160. Zhang Y, Khairallah C, Sheridan BS, van der Velden AWM, Bliska JB. CCR2+ Inflammatory Monocytes Are Recruited to Yersinia pseudotuberculosis Pyogranulomas and Dictate Adaptive Responses at the Expense of Innate Immunity during Oral Infection. *Infect Immun*. 2018;86(3). doi:10.1128/IAI.00782-17

161. LaFleur AM, Lukacs NW, Kunkel SL, Matsukawa A. Role of CC chemokine CCL6/C10 as a monocyte chemoattractant in a murine acute peritonitis. *Mediators Inflamm*. 2004;13(5-6):349-355. doi:10.1080/09629350400014172

162. Podojil JR, Kohm AP, Miller SD. CD4+ T cell expressed CD80 regulates central nervous system effector function and survival during experimental autoimmune encephalomyelitis. *J Immunol Baltim Md 1950*. 2006;177(5):2948-2958. doi:10.4049/jimmunol.177.5.2948

163. Dreier R, Opolka A, Grifka J, Bruckner P, Grässel S. Collagen IX-deficiency seriously compromises growth cartilage development in mice. *Matrix Biol J Int Soc Matrix Biol*. 2008;27(4):319-329. doi:10.1016/j.matbio.2008.01.006

164. Gu J, Lu Y, Li F, et al. Identification and characterization of the novel Col10a1 regulatory mechanism during chondrocyte hypertrophic differentiation. *Cell Death Dis*. 2014;5:e1469. doi:10.1038/cddis.2014.444

165. Batista MA, Nia HT, Önnerfjord P, et al. Nanomechanical phenotype of chondroadherin-null murine articular cartilage. *Matrix Biol J Int Soc Matrix Biol*. 2014;38:84-90. doi:10.1016/j.matbio.2014.05.008

166. Viegas CSB, Costa RM, Santos L, et al. Gla-rich protein function as an anti-inflammatory agent in monocytes/macrophages: Implications for calcification-related chronic inflammatory diseases. *PloS One*. 2017;12(5):e0177829. doi:10.1371/journal.pone.0177829

167. Jeon J, Oh H, Lee G, et al. Cytokine-like 1 knock-out mice (Cytl1-/-) show normal cartilage and bone development but exhibit augmented osteoarthritic cartilage destruction. *J Biol Chem*. 2011;286(31):27206-27213. doi:10.1074/jbc.M111.218065

168. Chamberlain ND, Kim S, Vila OM, et al. Ligation of TLR7 by rheumatoid arthritis synovial fluid single strand RNA induces transcription of TNFα in monocytes. *Ann Rheum Dis*. 2013;72(3):418-426. doi:10.1136/annrheumdis-2011-201203

169. Culemann S, Grüneboom A, Nicolás-Ávila JÁ, et al. Locally renewing resident synovial macrophages provide a protective barrier for the joint. *Nature*. 2019;572(7771):670-675. doi:10.1038/s41586-019-1471-1

170. Goto T, Makinose S, Ohi Y. Plasma endotoxin concentrations in patients with urinary tract infections. *Int J Urol Off J Jpn Urol Assoc*. 1995;2(4):238-242. doi:10.1111/j.1442-2042.1995.tb00464.x

171. Liang D, Leung RK-K, Guan W, Au WW. Involvement of gut microbiome in human health and disease: brief overview, knowledge gaps and research opportunities. *Gut Pathog*. 2018;10:3. doi:10.1186/s13099-018-0230-4

172. Nakano T, Tahara-Hanaoka S, Nakahashi C, et al. Activation of neutrophils by a novel triggering immunoglobulin-like receptor MAIR-IV. *Mol Immunol*. 2008;45(1):289-294. doi:10.1016/j.molimm.2007.04.011

173. Leist SR, Kollmus H, Hatesuer B, Lambertz RLO, Schughart K. Lst1 deficiency has a minor impact on course and outcome of the host response to influenza A H1N1 infections in mice. *Virol J*. 2016;13:17. doi:10.1186/s12985-016-0471-0

174. Yousif NM, de Oliveira ACP, Brioschi S, Huell M, Biber K, Fiebich BL. Activation of EP2 receptor suppresses poly(I: C) and LPS-mediated inflammation in primary microglia and organotypic hippocampal slice cultures: Contributing role for MAPKs. *Glia*. 2018;66(4):708-724. doi:10.1002/glia.23276

175. Park B-L, Park S-M, Park J-S, et al. Association of PTGER gene family polymorphisms with aspirin intolerant asthma in Korean asthmatics. *BMB Rep*. 2010;43(6):445-449. doi:10.5483/bmbrep.2010.43.6.445

176. Zhang T, Garstka MA, Li K. The Controversial C5a Receptor C5aR2: Its Role in Health and Disease. *J Immunol Res*. 2017;2017:8193932. doi:10.1155/2017/8193932

177. Omachi S, Fujii W, Azuma N, et al. B-cell activating factor deficiency suppresses splenomegaly during Leishmania donovani infection. *Biochem Biophys Res Commun*. 2017;489(4):528-533. doi:10.1016/j.bbrc.2017.06.005

178. Sengul A, Mohan S, Kesavan C. Bone response to loading in mice with targeted disruption of the cartilage oligomeric matrix protein gene. *Physiol Res*. 2012;61(6):637-641.

179. Urano T, Narusawa K, Shiraki M, et al. Single-nucleotide polymorphism in the hyaluronan and proteoglycan link protein 1 (HAPLN1) gene is associated with spinal osteophyte formation and disc degeneration in Japanese women. *Eur Spine J Off Publ Eur Spine Soc Eur Spinal Deform Soc Eur Sect Cerv Spine Res Soc*. 2011;20(4):572-577. doi:10.1007/s00586-010-1598-0

180. Kanbe K, Yang X, Wei L, Sun C, Chen Q. Pericellular matrilins regulate activation of chondrocytes by cyclic load-induced matrix deformation. *J Bone Miner Res Off J Am Soc Bone Miner Res*. 2007;22(2):318-328. doi:10.1359/jbmr.061104

181. Amano K, Densmore MJ, Lanske B. Conditional Deletion of Indian Hedgehog in Limb Mesenchyme Results in Complete Loss of Growth Plate Formation but Allows Mature Osteoblast Differentiation. *J Bone Miner Res Off J Am Soc Bone Miner Res*. 2015;30(12):2262-2272. doi:10.1002/jbmr.2582

182. Sender R, Fuchs S, Milo R. Revised Estimates for the Number of Human and Bacteria Cells in the Body. *PLoS Biol*. 2016;14(8):e1002533. doi:10.1371/journal.pbio.1002533

183. van den Elsen LWJ, Garssen J, Burcelin R, Verhasselt V. Shaping the Gut Microbiota by Breastfeeding: The Gateway to Allergy Prevention? *Front Pediatr*. 2019;7:47. doi:10.3389/fped.2019.00047

184. Tanaka M, Nakayama J. Development of the gut microbiota in infancy and its impact on health in later life. *Allergol Int*. 2017;66(4):515-522. doi:10.1016/j.alit.2017.07.010

185. Clemente JC, Ursell LK, Parfrey LW, Knight R. The impact of the gut microbiota on human health: an integrative view. *Cell*. 2012;148(6):1258-1270. doi:10.1016/j.cell.2012.01.035

186. Mohajeri MH, Brummer RJM, Rastall RA, et al. The role of the microbiome for human health: from basic science to clinical applications. *Eur J Nutr*. 2018;57(Suppl 1):1-14. doi:10.1007/s00394-018-1703-4

187. Bahar B, O'Doherty JV, Vigors S, Sweeney T. Activation of inflammatory immune gene cascades by lipopolysaccharide (LPS) in the porcine colonic tissue ex-vivo model. *Clin Exp Immunol*. 2016;186(2):266-276. doi:10.1111/cei.12839

188. Calil IL, Zarpelon AC, Guerrero ATG, et al. Lipopolysaccharide induces inflammatory hyperalgesia triggering a TLR4/MyD88-dependent cytokine cascade in the mice paw. *PloS One*. 2014;9(3):e90013. doi:10.1371/journal.pone.0090013

189. Mogensen TH. Pathogen recognition and inflammatory signaling in innate immune defenses. *Clin Microbiol Rev*. 2009;22(2):240-273, Table of Contents. doi:10.1128/CMR.00046-08

190. Maslanik T, Tannura K, Mahaffey L, et al. Commensal bacteria and MAMPs are necessary for stress-induced increases in IL-1β and IL-18 but not IL-6, IL-10 or MCP-1. *PloS One*. 2012;7(12):e50636. doi:10.1371/journal.pone.0050636

191. Chen Y, Haines CJ, Gutcher I, et al. Foxp3(+) regulatory T cells promote T helper 17 cell development in vivo through regulation of interleukin-2. *Immunity*. 2011;34(3):409-421. doi:10.1016/j.immuni.2011.02.011

192. Chu H, Mazmanian SK. Innate immune recognition of the microbiota promotes host-microbial symbiosis. *Nat Immunol*. 2013;14(7):668-675. doi:10.1038/ni.2635

193. Kim CH. Host and microbial factors in regulation of T cells in the intestine. *Front Immunol*. 2013;4:141. doi:10.3389/fimmu.2013.00141

194. Szychlinska MA, Di Rosa M, Castorina A, Mobasheri A, Musumeci G. A correlation between intestinal microbiota dysbiosis and osteoarthritis. *Heliyon*. 2019;5(1):e01134. doi:10.1016/j.heliyon.2019.e01134

195. Charles JF, Ermann J, Aliprantis AO. The intestinal microbiome and skeletal fitness: Connecting bugs and bones. *Clin Immunol Orlando Fla*. 2015;159(2):163-169. doi:10.1016/j.clim.2015.03.019

196. Collins FL, Schepper JD, Rios-Arce ND, et al. Immunology of Gut-Bone Signaling. *Adv Exp Med Biol*. 2017;1033:59-94. doi:10.1007/978-3-319-66653-2_5

197. Schepper JD, Collins FL, Rios-Arce ND, et al. Probiotic Lactobacillus reuteri Prevents Postantibiotic Bone Loss by Reducing Intestinal Dysbiosis and Preventing Barrier Disruption. *J Bone Miner Res Off J Am Soc Bone Miner Res*. 2019;34(4):681-698. doi:10.1002/jbmr.3635

198. Pan H, Guo R, Ju Y, et al. A single bacterium restores the microbiome dysbiosis to protect bones from destruction in a rat model of rheumatoid arthritis. *Microbiome*. 2019;7(1):107. doi:10.1186/s40168-019-0719-1

199. Kaushik D, Mohan M, Borade DM, Swami OC. Ampicillin: rise fall and resurgence. *J Clin Diagn Res JCDR*. 2014;8(5):ME01-03. doi:10.7860/JCDR/2014/8777.4356

200. Chudobova D, Dostalova S, Blazkova I, et al. Effect of ampicillin, streptomycin, penicillin and tetracycline on metal resistant and non-resistant Staphylococcus aureus. *Int J Environ Res Public Health*. 2014;11(3):3233-3255. doi:10.3390/ijerph110303233

201. Waksman SA, Lechevalier HA, Harris DA. NEOMYCIN-PRODUCTION AND ANTIBIOTIC PROPERTIES. *J Clin Invest*. 1949;28(5 Pt 1):934-939. doi:10.1172/JCI102182

202. Masur H, Whelton PK, Whelton A. Neomycin toxicity revisited. *Arch Surg Chic Ill 1960*. 1976;111(7):822-825. doi:10.1001/archsurg.1976.01360250098021

203. Macdonald RH, Beck M. Neomycin: a review with particular reference to dermatological usage. *Clin Exp Dermatol*. 1983;8(3):249-258. doi:10.1111/j.1365-2230.1983.tb01777.x

204. Klar AS, Michalak-Mićka K, Biedermann T, Simmen-Meuli C, Reichmann E, Meuli M. Characterization of M1 and M2 polarization of macrophages in vascularized human dermo-epidermal skin substitutes in vivo. *Pediatr Surg Int*. 2018;34(2):129-135. doi:10.1007/s00383-017-4179-z

205. Boyle KK, Sosa B, Osagie L, Turajane K, Bostrom MPG, Yang X. Vancomycin-laden calcium phosphate-calcium sulfate composite allows bone formation in a rat infection model. *PloS One*. 2019;14(9):e0222034. doi:10.1371/journal.pone.0222034

206. Paiva KBS, Granjeiro JM. Bone tissue remodeling and development: focus on matrix metalloproteinase functions. *Arch Biochem Biophys*. 2014;561:74-87. doi:10.1016/j.abb.2014.07.034

207. Nakatani T, Chen T, Partridge NC. MMP-13 is one of the critical mediators of the effect of HDAC4 deletion on the skeleton. *Bone*. 2016;90:142-151. doi:10.1016/j.bone.2016.06.010

208. Klein T, Bischoff R. Physiology and pathophysiology of matrix metalloproteases. *Amino Acids*. 2011;41(2):271-290. doi:10.1007/s00726-010-0689-x

209. Barboza E, Hudson J, Chang W-P, et al. Profibrotic Infrapatellar Fat Pad Remodeling Without M1 Macrophage Polarization Precedes Knee Osteoarthritis in Mice With Diet-Induced Obesity. *Arthritis Rheumatol Hoboken NJ*. 2017;69(6):1221-1232. doi:10.1002/art.40056

210. Chamberlain ND, Vila OM, Volin MV, et al. TLR5, a novel and unidentified inflammatory mediator in rheumatoid arthritis that correlates with disease activity score and joint TNF-α levels. *J Immunol Baltim Md 1950*. 2012;189(1):475-483. doi:10.4049/jimmunol.1102977

211. Collins KH, Paul HA, Reimer RA, Seerattan RA, Hart DA, Herzog W. Relationship between inflammation, the gut microbiota, and metabolic osteoarthritis development: studies in a rat model. *Osteoarthritis Cartilage*. 2015;23(11):1989-1998. doi:10.1016/j.joca.2015.03.014